Acknowledgements

I would like to express my gratitude to those that provided guidance, mentoring, and support throughout the process of developing this body of work. And to those that made contributions and provided helpful advice.

Dr. Eran Pichersky
Dr. Laura Olsen
Dr. John Schiefelbein
Dr. David Sherman
Dr. Mwafaq Ibdah
Dr. Takao Koeduka
Dr. Tariq Ahktar
Dr. Robert Last
Dr. Dan Jones
Dr. Anthony Schillmiller
Dr. David Gang
Dr. Eric McDowell
Ms. Jeongwoon Kim
Mr. Chao Li

Table of Contents

List of Figures

List of Tables

ABSTRACT

Specialized metabolites and related biosynthetic enzymes in tomato glandular trichomes: Defining biological functions of specific gland types.

by

Adam J. Schmidt

Chair: Eran Pichersky

Trichomes are tiny appendages that grow out from the surfaces of leaves, stems, flowers, and other above-ground parts of many plants. They contribute to important biological functions such as determent of herbivores, attraction of pollinators, and protection against abiotic stresses. Comparisons of glandular trichome-derived specialized metabolites from wild and cultivated tomato species have revealed that the ability to synthesize many of the defensive specialized metabolites has been lost during the process of domestication. Reintroduction of such traits into the cultivated tomato may prove to be an effective way of reducing crop loss and dependence on pesticides.

We investigated the different types of glandular trichomes present on the leaf surface of several different wild tomato species and on cultivated tomato by metabolite profiling and gene transcript profiling of the gland cells. Substantial differences within and between species and glandular trichome types were found for acyl-sugars, terpenoids, and flavonoids. Gene transcripts required for the synthesis of these classes of specialized metabolites were found in the gland cells of type 1, 4, and type 6 glandular trichomes.

In an in-depth study of one class of metabolites, we found that the wild tomato species, *S. habrochaites*, accumulates highly methylated derivatives of myricetin, a flavonol, in the glandular trichomes. Using collections of gland cells from the different glandular trichome types, we showed that secreting glandular trichomes (designated type 1 and 4) contained several-fold more of these compounds than storage glandular trichomes (type 6). We also identified transcripts of two genes expressed in the glandular trichomes, designated *ShMOMT1* (*Solanum habrochaites* myricetin *O*-methyltransferase) and *ShMOMT2*, and showed that they encode enzymes capable of methylating myricetin at the 3′ and 5′ and the 7 and 4′ positions, respectively. Both genes are preferentially expressed in secreting glandular trichome types 1 and 4, and to a lesser degree in storage trichome type 6, and ShMOMT1 and ShMOMT2 protein levels are correspondingly higher in type 1 and 4 glands compared with type 6 glands.

The large-scale comparative study of tomato glandular trichomes provides support for the hypothesis that gland cells are sites of synthesis and accumulation of defense-related specialized metabolites. By focusing on a select class of metabolites that accumulate in the glands of one wild tomato species we demonstrate the techniques and experiments that can be applied to investigating select metabolites and biosynthetic enzymes responsible for their synthesis in gland cells. The results of these investigations demonstrate that tomato glandular trichomes are a valuable biological system in which specialized metabolism can be investigated at all levels, in a single cell type.

Chapter 1

Introduction

Tomatoes are cultivated in nearly every part of the world and have become popular additions to most diets. They are annual plants that adapt well to most climates, and they can be cultivated successfully in greenhouses during less desirable seasons. This malleable character and ease of adapting has made the tomato a desirable vegetable crop and a favorite of backyard gardeners throughout North America and Europe. Its popularity varies from region to region; however, it is used in one form or another in nearly all major cultures. The fruit of garden varieties, especially heirloom varieties, can be found in a bewildering range of colors, shapes, sizes, and flavors. On the other hand, varieties found at grocery stores and those used in the production of sauces and pastes are often uniform in flavor; they differ only slightly in shape and are relatively high in solids content. The latter characteristic makes them more amenable to production technologies, but less palatable as a raw food. Today, large producers spend countless man-hours and resources trying to improve our domestic tomato using a combination of different breeding techniques and molecular technologies aimed at transferring beneficial characteristics from wild tomato relatives into the genetic background of our domestic tomato. These approaches have successfully introduced attributes that provide resistance to numerous pathogens, increase yield, and improve fruit taste, color and shape, to name a few.

The Food and Agriculture Organization of the United Nations (FAO) estimates from 2008 indicated that the 5 largest tomato producing countries contributed approximately 78 million tons of tomato (fresh and production grade) to the global market. China represented the largest producer with the United States, Turkey, India, and Egypt, following in that order. Combined, these five countries dedicated approximately 3 billion hectares to the cultivation of tomato. During this time, China’s tomato production

ranked 10th among all vegetable crops produced in that country and was valued at approximately $4,000 million. In the United States, production ranked 7th and was valued at approximately $8,720 million. A steady rise in production began in the mid-1990's when China began increasing its production to surpass that of the United States. Between 1995 and 2008 China increased tomato production 150% compared to a 16% increase in US production during this same time frame. Global consumption was also on the rise during this time, with estimates of consumption increasing annually at a rate of 3% between 1998 and 2008.

The growing popularity of the tomato within the past decade can be partly attributed to claims of various health benefits associated with its consumption. Especially prominent are studies evaluating the health benefits of lycopene, a powerful antioxidant and the source of the red color of the tomato, watermelon, pink grapefruit, and papaya, to name a few. It is estimated that tomatoes and tomato-based products make up 85% of the dietary intake of lycopene (Rao and Rao, 2007). The majority of studies assessing the physiological effects of lycopene have focused on its benefits to the heart and its effectiveness as an anticarcinogen (reviewed in (Palozza et al., 2010); (Borguini and Torres, 2009); (Singh and Goyal, 2008)). From a dietary perspective, tomatoes provide relatively high levels of vitamins and minerals, and are a good source of dietary fiber. They are rich in antioxidant compounds, in addition to lycopene, and are very low in sodium, saturated fat, and cholesterol. Health benefits associated with the consumption of tomatoes are more likely a complex synergism related to all of the naturally produced antioxidant compounds, vitamins, and sequestered minerals contained within the fruit. Determining the contributions of individual compounds, or even classes of compounds, to perceived health benefits is difficult to generalize among a population. Therefore, results of such studies should be considered in respect to their associative effects rather than their absolute context.

Domestic and wild tomato species belong to the Solanaceae family and are classified in the genus Solanum. The Solanaceae family includes several other important crop species such as potato, tobacco, chili pepper, and eggplant, as well as numerous toxic species. Members of this family provide a rich source of specialized chemicals that have been sought after by humans for use as spices, flavorings, medicines, and toxins. All

of our domestic tomato varieties are classified under one species, *Solanum lycopersicum*, and are further differentiated by designating the specific variety, such that *Solanum lycopersicum* var. *cerasiforme* correctly identifies a particular form of the domestic species. There are ten wild species of tomato endemic to western South America. These species are distributed in varied habitats along the coast and the Andean range from Chile north to Ecuador, including the Galapagos Islands (Spooner et al., 2005). Wild species have become a treasure trove of genetic material sought after for the improvement of our domestic crop species. The true number of wild species and their interrelationships has been a source of controversy until recent advances in molecular phylogeny provided detailed evidence delineating their relationships (Peralta and Spooner, 2001; Spooner et al., 2005).

The origins of today's domestic tomato, *Solanum lycopersicum*, can be most accurately traced back to Central America, in present day Mexico. It was here, in the early 16th century, that conquests of the New World first encountered domesticated varieties of tomato in cultivation throughout the area (Jenkins, 1948). Distribution of the tomato began soon after, with reports of its occurrence in Italy prior to 1544 and by 1554 its distribution had been documented throughout Europe to included France, Germany, and Greece (Matthiolus 1544, in Jenkins 1948). While this historical account of where the tomato was domesticated and its subsequent early distributions are fairly well established and accepted, the exact period of time and the location of its first uses and earliest forms of cultivation leading up to domestication in Central America are still regarded as a mystery today. Determining these early occurrences has been confounded by a lack of archeological, historical, and linguistic evidence to support its use or cultivation by civilizations living in areas where wild tomato species are found today. Studies on the origin and geography of cultivated plants by Vavilov (Vavilov, 1926; Vavilov, 1940) present a well-accepted view that the ancestral origin of a given cultivated plant can be traced back to the region where there is the highest diversity of that plant growing today. Following this point of view, it is well acknowledged that the center of origin of today's domestic tomato is most likely the diverse populations of wild species endemic to Peru. To date, there are 10 distinct wild tomato species growing in diverse habitats along the Western coast of South America in Chile, Peru, and Ecuador, including

the Galapagos Islands. In Peru alone 8 of the 10 wild species are growing in established populations compared to only 5 species in Ecuador, including 2 species endemic to the Galapagos Islands, and there are only 3 species found in Chile (C.M. Rick Tomato Genetic Resource Center, accessed online Feb. 2011).

The most recent ancestor of the domestic tomato was first discerned by Jenkins (1948) and represents the only wild variety of *S. lycopersicum* recognized today. This wild form, *Solanum lycopersicum* var. *cerasiforme*, has since been further supported as the progenitor of *S. lycopersicum* using a combination of genetic and historical data (Rick et al., 1979). *Cerasiforme* is a weedy, opportunistic plant found throughout Central and South America. It is most commonly found in present day Mexico City, growing unattended in a variety of diverse habitats created by the activities of people living and working in that area. This ability to grow well in disturbed soils and strong colonizing tendencies have obscured its true native range (Rick, 1978). An important characteristic supporting a direct link between the wild form, *cerasiforme*, and *S. lycopersicum* is the ability of the former to produce red-colored fruit. A significant characteristic separating wild species endemic to the western coast of South America from all forms of *S. lycopersicum* is the fact that these wild species produce mature green fruit. However, two exceptions to this can be found in the wild species *Solanum pimpinellifolium* and *Solanum cheesmanii*. The latter, being endemic and isolated to the Galapagos Islands, produces a mature fruit that is yellow to orange in color. Genetic evidence strongly supports its evolution under complete geographic isolation, effectively removing it from consideration as a direct ancestor of *S. lycopersicum* (Rick and Fobes, 1975). The other colored-fruit producing wild species, *S. pimpinellifolium*, is native to the western coast of South America and several lines of genetic evidence, although not conclusive, suggest that this wild species is the most likely progenitor of the *cerasiforme* variety of *S. lycopersicum*, and not the most recent ancestor (Rick et al., 1974; Rick and Fobes, 1975).

The process of domestication inevitably reduced the genetic diversity of *S. lycopersicum*. As cultivation of the wild form developed in Central America, people naturally selected plants with the most desirable traits (e.g. fruit color, taste, vigor) and took care to remove plants that did not conform to their needs. Selective pressure aimed at making the tomato more desirable as a food source and cash crop continued, albeit for

different traits and attributes, throughout the course of its distribution to Europe and eventually North America and Asia. Today we have a very homogenous tomato crop (fresh and production market) that grows to a uniform height and bears consistently red ripe fruit similar in size, shape, and number. We cater to these plants, ensuring that they receive the proper amount of water, that the soil is of the best quality, and we defend them against common pests and pathogens with an arsenal of chemicals. Our stewardship has created a new species of tomato, which fertilizes itself (self-compatible), making it completely independent of pollinating insects and relatively easy to cultivate worldwide in a variety of farming systems. While this is desirable and necessary for ensuring profitability in a modern marketplace, the tradeoff has been the loss of genetic elements essential for the production of flower scent, fruit scent, fruit taste, and defensive chemicals (Tadmor et al., 2005; Matsui et al., 2007; Mathieu et al., 2009). The logic follows that domestic tomatoes do not benefit from producing scent chemicals in their flowers because they lack the need to attract pollinators. They have no need to attract animals to eat their fruit for seed dispersal, so they gain nothing from producing taste or scent compounds in their fruit. Likewise, there is little benefit gained from producing an arsenal of chemicals in the leaves and stems to defend against herbivores when we apply the chemical defense for them. The selection for traits that improve production such as larger fruit, earlier fruit set, thicker stems, self-pollinating flowers, and fruit solids content inadvertently affect the plants' ability to allocate resources to producing specialized chemicals evolved to serve protective roles or to aid in fruit dispersal.

The amazing array of chemicals that plants produce for purposes of defense, scent, taste, and color have evolved as a result of their sessile existence, and are considered specialized metabolites because they are not necessarily essential for cellular metabolism. For this reason, the genetic elements required for their production, maintenance, and storage in the plant are often the first to be lost during the processes of domestication. As this reduction in genetic diversity occurs, the species becomes less able to adapt to changes in the environment and to new biological threats because there is less genetic background from which spontaneous mutations can arise to affect the necessary physiological changes. The traditional means of effectively enhancing the genetic background of a crop species is through breeding with a related species, for example a

wild tomato species that is resistant to a particular pathogen or produces a desirable taste-related chemical. The most notable example of this in the development of the tomato crop was the introduction of disease resistance beginning in the early 1940's. Prior to this time there was no knowledge of specific disease resistance in cultivated tomatoes (Rick 1986). These initial efforts aimed at improving the tomato crop have been regarded as the most extensive introduction of traits into the *S. lycopersicum* background and it appears to be responsible for propelling the rate of production to levels realized since (Rick 1986).

Today, breeding for improved nutrition and organoleptic (flavor and taste) qualities of the fruit has become a primary focus. The process of breeding introgression lines has proven a very effective means of identifying genetic elements linked to these qualities. This technique involves an initial cross between the cultivated tomato and a wild species, followed by multiple rounds of self- and back-crossing of the offspring in each generation to the *S. lycopersicum* parent (Eshed and Zamir, 1995). This process results in offspring that are genetically similar to the domesticated parent, but contain small, defined fragments of DNA from the wild species. These resulting introgression lines provide a source of germplasm from which traits, acquired from the wild species, can be identified and further bred without jeopardizing the desirable, performance traits of the cultivated tomato. This breeding technique has proven valuable for the introduction of genetic elements linked to the production of specialized metabolites important for enhanced nutrition and organoleptic qualities of the tomato fruit (Mathieu et al., 2009; (Schauer et al., 2006). Recent advancements in high-throughput analysis of plant-derived metabolites applied to characterization of introgression lines have provided a rich future for the improvement of our domestic tomato fruit (Levin et al., 2004; Giovannoni, 2006; Iijima and Aoki, 2009). The fact that such improvements can be accomplished within a traditional, non-GMO (Genetically Modified Organism), context is enormously valuable for the continued improvement of the crop, and will probably be championed as a significant contribution to future crop developments.

All of the ten wild species have been used in one way or another as sources of genetic material for introgression into the *S. lycopersicum* genetic background (summarized in Spooner et al., 2005). Traits ranging from drought and salt resistance to cold and frost tolerance have extended the range of cultivation and the growing season.

While other traits, ranging from insect and pathogen resistance to higher sugar content in the fruit, have improved performance and organoleptic qualities of the crop. Two wild species stand out for their contributions to the identification of genetic loci linked to improved organoleptic properties, fruit yield, and fruit production qualities. These wild species are *Solanum pennellii* and *Solanum habrochaites*. Introgression lines derived from *S. pennellii* provided the first hints of the value of introgressed germplasm for improving the genetic diversity of cultivated tomato (Rick, 1959). These introgression lines continue to be a significant source of new discoveries and advancements in our understanding of fruit organoleptic properties and insect resistance (McNally and Mutschler 1997; Bleeker et al., 2009; Mathieu et al., 2009(McNally and Mutschler, 1997; Bleeker et al., 2009). Introgressions of *S. habrochaites* have had similarly significant contributions in respect to identifying genetic loci associated with organoleptic properties and improved yield, and continue to provide a source of new discoveries related to the complexity of genetic loci associated with insect resistance (Bernacchi et al., 1998; Bernacchi et al., 1998; Frelichowski and Juvik, 2005; Momotaz et al., 2005; Hanson et al., 2007).

The contributions of these wild species to discoveries aimed at discerning the basis of insect resistance have been closely linked to the occurrence of epidermal structures called trichomes. These structures are regarded as a first line of defense against herbivores (Peiffer et al., 2009; Tooker et al., 2010) and early attempts at classifying wild tomato species were partly based on differences in morphologies and densities of trichomes (Luckwill 1943). These structures are present on the surface of nearly all above-ground parts of the plant and can be divided into two distinct classes, glandular and non-glandular. The non-glandular trichomes resemble linear hairs protruding from the epidermis. They lack apical gland/storage cells and do not appear to be involved in the synthesis or storage of specialized metabolites. The glandular trichomes have been traditionally divided into four types (1, 4, 6, and 7) and differ morphologically based on the length of the supporting stalk and the number of gland/storage cells making up the glandular tip. Glandular trichomes are especially important for conferring insect resistance because they preferentially synthesize and store many of the chemicals (i.e. specialized metabolites) directly linked to insect resistance (Ben-Israel et al., 2009; Kang

et al., 2010; Kang et al., 2010; Schilmiller et al., 2010). The glandular trichomes of *S. pennellii* and *S. habrochaites* accumulate a vast array of different acylsugars and terpenes, in addition to other specialized metabolites, in varying amounts distributed preferentially in the gland cells of the different types of glandular trichomes (McDowell et al., 2011). Specific examples of compounds from both classes of these specialized metabolites (acylsugars and terpenes) have been directly linked to the deterrence of several different insect pests (Guo et al., 1993; Juvik et al., 1994; Liedl et al., 1995). The densities of glandular trichomes have also been shown to correlate with levels of insect-deterring metabolites and with the degree of resistance conferred to the plant (Goffreda and Mutschler, 1989; Goffreda et al., 1989; Kennedy, 2003; Wosula et al., 2009). Introgression of genetic loci responsible for accumulations of acylsugars in glandular trichomes of *S. pennellii* and those of sesquiterpene acids in *S. habrochaites* have been an area of significant interest, as these classes of chemicals appear to provide a broad spectrum of insect resistance (Frelichowski and Juvik, 2001; Mutschler et al., 2001). However, identifying genetic loci linked to their production and accumulations in trichomes has been difficult because introgression lines exhibiting levels of metabolite accumulations comparable to the wild parent have not always been attainable (Frelichowski and Juvik, 2001; Frelichowski and Juvik, 2005; Bleeker et al., 2009; Schilmiller et al., 2010). The challenge of breeding all of the genetic complexity of these specialized metabolite pathways into a single introgression line is also compounded by the fact that the biosynthetic genes and regulatory genes appear to be widely distributed throughout the genomes of wild germplasm (Mutschler et al., 1996; Lawson et al., 1997). Additionally, since the major classes of specialized metabolites conferring insect resistance are nearly exclusively localized to glandular trichomes, the task of breeding these select metabolic pathways into the genetic background of *S. lycopersicum* depends equally on the ability to breed the necessary developmental genetics required for the production of specific types of glandular trichomes at similar densities. The cultivated tomato suffers from a lack of innate resistance to insect pests partly because it lacks the full complement and similar densities of glandular trichomes apparent in *S. pennellii* and *S. habrochaites* (McDowell et al., 2011). This presents a paramount challenge for

improving the insect resistance qualities of the cultivated tomato that has yet to be fully realized.

Our basic understanding of the functions of glandular trichomes in plant defense has been limited to associating specialized metabolites found in crude preparations of trichomes with deterrence of a particular insect pest and/or pathogen. This established that glandular trichomes store the specialized metabolites of interest, and demonstrated that different types (1, 4, and 6) appear to accumulate specific classes of metabolites more than others. However, fundamental questions concerning the capacities of different types of glandular trichomes to synthesize these specialized metabolites had not been clearly established. More recently, attempts aimed at localizing specific metabolites and their related biosynthetic enzymes to a certain type of glandular trichome have proven successful to varying degrees (Fridman et al., 2005; van Schie et al., 2007; Slocombe et al., 2008; Schilmiller et al., 2009; Schilmiller et al., 2010; Schilmiller et al., 2010). The results of these studies strongly suggest that the biosynthetic enzymes, their chemical products, and related precursor molecules are localized to specific types of glandular trichomes, mainly types 1 and 4, or type 6. These efforts have significantly advanced our understanding of the biochemical capacities of glandular trichomes and have provided strong evidence that the different types of glandular trichomes specialize in the synthesis of select classes of specialized metabolites. A caveat to all of these studies is the presence of contaminating tissues such as non-glandular trichomes, different types of glandular trichomes, leaf epidermal cells, and other types of trichome cells (e.g. cells that make up the linear stalk and those that surround the base of the stalk) in the collections of trichomes used for localizing metabolites, biosynthetic enzymes, and gene transcripts that were assigned to specific type(s) of glandular trichome. The techniques used in these studies rely on bulk shearing of trichomes off of the leaf or stem surface, in most cases this is followed by one or more successive filtering steps designed to aid in the enrichment of the sample for a particular type of glandular trichome (Gershenzon et al., 1987; Gang et al., 2001; Wang et al., 2001). These enrichment techniques cannot effectively exclude other tissues, or control for the rupture of, and subsequent inclusion of cell contents from leaf epidermal cells or from other glandular trichome types. While these contaminants may constitute only a small portion of the enriched preparation, and

probably did not affect the outcome of these particular studies, the degree and type of contamination is not measureable and not consistently controlled using these enrichment techniques. Considering the significance of the studies that link gene transcripts, biosynthetic enzymes, and special classes of metabolites to enriched collections of different types of glandular trichomes it became apparent that developing a collection technique that further minimized contamination from other cell types could contribute significantly to the growing interest in characterizing the biological functions and chemical contents of the different types of glandular trichomes.

Our solution to further eliminate contaminating cell types from collections of individual glandular trichome types was to 'pick' the apical gland cells off of the linear stalk of the trichome structure using a thin glass probe. The picking technique can be accomplished under magnification from a dissecting microscope and it does not require harvesting of leaf or stem material. The dissecting microscope can be placed on a moveable jack and the height adjusted to accommodate a wide range of leaf and stem material on the plant. Using this technique, gland cells can be collected *in situ* by simply bending plant parts under the microscope optics without breaking them from the plant.

The picking technique relies on the use of thin glass probes that are made by pulling capillary tubes (1.6-1.8 mm diameter) over a flame. This creates a very thin, hair-like, probe at one end. The probes are then flame-sealed at each end causing a small bubble to form at the tip of the probe. When collecting, gland cells adhere to the tip of the probe and are gently pulled off of the trichome stalk, leaving the stalk attached to the plant. This can be done many times over, resulting in the collection of 20 to 50 individual gland cells on the tip of the glass probe. Using this technique it is possible to collect gland cells from a single type of glandular trichome while eliminating contamination from other cell types.

We have applied this technique to characterizing metabolites and gene transcripts from gland cells of different glandular trichome types that were collected from the leaves of the cultivated tomato and several wild tomato species. The chapters that follow present two bodies of work that contributes to our understanding of the biological functions and chemical contents of the different types of glandular trichomes. These studies demonstrate the effectiveness of using the single-gland collection technique to localize

specific metabolites and related biosynthetic enzymes to different glandular trichome types.

The first describes a large-scale, comparative genomic and metabolomic analysis of glandular trichome types from a range of tomato species. This study provides quantitative differences in metabolite profiles of different types of glandular trichomes between and within species. It identifies gene transcripts required for the synthesis of major classes of specialized metabolites and those associated with photosynthesis and carbon fixation. Both of these findings lend additional support to the view that gland cells are sites of synthesis of specialized metabolites, as opposed to being only sites of accumulation. Finally, the lack of differences of metabolites and gene transcripts identified from type 1 and type 4 glandular trichomes reveal that they may be two morphotypes, type 4 being a shorter version of type 1, rather than distinct types of glandular trichomes.

The second body of work provides evidence for the synthesis and accumulations, in the gland cells, of several methylated forms of the flavonol, myricetin, and identifies two novel transcripts encoding enzymes required for their synthesis. The single-gland collection technique was applied to measuring levels of these specialized metabolites, expression levels of the gene transcripts, and for localizing the two enzymes in type 1/4 and type 6 gland cells. The results of these experiments demonstrate that different types of glandular trichomes serve distinct biological roles in the synthesis and storage of specialized metabolites and that these attributes are localized in the apical gland cells of the glandular trichome structure.

Together, these investigations provide a source of data and demonstrate techniques that can be used in future studies to characterize trichome-specific specialized metabolic pathways. Since the vast majority of specialized metabolites accumulating in glandular trichomes are of such low concentrations, it will be essential to synthesize specific metabolites *in vitro* for detailed characterizations of their biological functions. This approach may be valuable for the continued development of the cultivated tomato by defining the metabolites required for reintroducing broad-spectrum insect resistance associated with glandular trichomes.

Literature Cited

Ben-Israel I, Yu G, Austin MB, Bhuiyan N, Auldridge M, Nguyen T, Schauvinhold I, Noel JP, Pichersky E, Fridman E (2009) Multiple biochemical and morphological factors underlie the production of methylketones in tomato trichomes. Plant Physiology **151:** 1952-1964

Bernacchi D, Beck-Bunn T, Eshed Y, Inai S, Lopez J, Petiard V, Sayama H, Uhlig J, Zamir D, Tanksley S (1998) Advanced backcross QTL analysis of tomato. II. Evaluation of near-isogenic lines carrying single-donor introgressions for desirable wild QTL-alleles derived from Lycopersicon hirsutum and L-pimpinellifolium. Theoretical and Applied Genetics **97:** 170-180

Bernacchi D, Beck-Bunn T, Eshed Y, Lopez J, Petiard V, Uhlig J, Zamir D, Tanksley S (1998) Advanced backcross QTL analysis in tomato. I. Identification of QTLs for traits of agronomic importance from Lycopersicon hirsutum. Theoretical and Applied Genetics **97:** 381-397

Bleeker PM, Diergaarde PJ, Ament K, Guerra J, Weidner M, Schutz S, de Both MTJ, Haring MA, Schuurink RC (2009) The role of specific tomato volatiles in tomato-whitefly interaction. Plant Physiology **151:** 925-935

Borguini RG, Torres E (2009) Tomatoes and tomato products as dietary sources of antioxidants. Food Reviews International **25:** 313-325

C.M. Rick Tomato Genetics Resource Center (2011) Geographic data on wild species accessions, http://tgrc.ucdavis.edu/Data/Acc/dataframe.aspx?start=GIS_dataoption.aspx&navstart=nav.html

Eshed Y, Zamir D (1995) An introgression line population of Lycopersicon pennellii in the cultivated tomato enables the identification and fine mapping of yield-associated QTL. Genetics **141:** 1147-1162

Frelichowski JE, Jr., Juvik JA (2001) Introgression of the genes for sesquiterpene carboxylic acids into cultivated tomatoes for enhanced insect resistance. Hortscience **36:** 491-492

Frelichowski JE, Juvik JA (2001) Sesquiterpene carboxylic acids from a wild tomato species affect larval feeding behavior and survival of Helicoverpa zea and Spodoptera exigua (Lepidoptera : Noctuidae). Journal of Economic Entomology **94:** 1249-1259

Frelichowski JE, Juvik JA (2005) Inheritance of sesquiterpene carboxylic acid synthesis in crosses of Lycopersicon hirsutum with insect-susceptible tomatoes. Plant Breeding **124:** 277-281

Fridman E, Wang JH, Iijima Y, Froehlich JE, Gang DR, Ohlrogge J, Pichersky E (2005) Metabolic, genomic, and biochemical analyses of glandular trichomes from the wild tomato species Lycopersicon hirsutum identify a key enzyme in the biosynthesis of methylketones. Plant Cell **17:** 1252-1267

Gang DR, Wang JH, Dudareva N, Nam KH, Simon JE, Lewinsohn E, Pichersky E (2001) An investigation of the storage and biosynthesis of phenylpropenes in sweet basil. Plant Physiology **125:** 539-555

Gershenzon J, Duffy MA, Karp F, Croteau R (1987) Mechanized techniques for the selective extraction of enzymes from plant epidermal glands. Analytical Biochemistry **163:** 159-164

Giovannoni JJ (2006) Breeding new life into plant metabolism. Nature Biotechnology **24:** 418-419

Goffreda JC, Mutschler MA (1989) Inheritance of potato aphid resistance in hybrids between Lycopersicon esculentum and Lycopersicon pennellii. Theoretical and Applied Genetics **78:** 210-216

Goffreda JC, Mutschler MA, Ave DA, Tingey WM, Steffens JC (1989) Aphid deterrence by glucose esters in glandular trichome exudate of thewild tomato, Lycopersicon pennellii. Journal of Chemical Ecology **15:** 2135-2147

Guo ZH, Weston PA, Snyder JC (1993) Repellency to 2-spotted spider mite, Tetranychus urticae Koch, as related to leaf surface chemistry of Lycopersicon hirsutum accessions. Journal of Chemical Ecology **19:** 2965-2979

Hanson PM, Sitathani K, Sadashiva AT, Yang RY, Graham E, Ledesma D (2007) Performance of Solanum habrochaites LA1777 introgression line hybrids for marketable tomato fruit yield in Asia. Euphytica **158:** 167-178

Iijima Y, Aoki K (2009) Application of metabolomics to improve tomato fruit productivity and quality. Journal of the Japanese Society for Horticultural Science **78:** 14-22

Jenkins JA (1948) The origin of the cultivated tomato. Econ Bot **2:** 379-392

Juvik JA, Shapiro JA, Young TE, Mutschler MA (1994) Acylglucoses from wild tomatoes alter behavior and reduce growth and survival of Helicoverpa zea and Spodoptera exigua (Lepidoptera, Noctuidae). Journal of Economic Entomology **87:** 482-492

Kang JH, Liu GH, Shi F, Jones AD, Beaudry RM, Howe GA (2010) The tomato odorless-2 mutant is defective in trichome-based production of diverse specialized metabolites and broad-spectrum resistance to insect herbivores. Plant Physiology **154:** 262-272

Kang JH, Shi F, Jones AD, Marks MD, Howe GA (2010) Distortion of trichome morphology by the hairless mutation of tomato affects leaf surface chemistry. Journal of Experimental Botany **61:** 1053-1064

Kennedy GG (2003) Tomato, pests, parasitoids, and predators: Tritrophic interactions involving the genus Lycopersicon. Annual Review of Entomology **48:** 51-72

Lawson DM, Lunde CF, Mutschler MA (1997) Marker-assisted transfer of acylsugar-mediated pest resistance from the wild tomato, Lycopersicon pennellii, to the cultivated tomato, Lycopersicon esculentum. Molecular Breeding **3:** 307-317

Levin I, Lalazar A, Bar M, Schaffer AA (2004) Non GMO fruit factories strategies for modulating metabolic pathways in the tomato fruit. Industrial Crops and Products **20:** 29-36

Liedl BE, Lawson DM, White KK, Shapiro JA, Carson WG, Trumble JT, Mutschler MA (1995) Acylsugars of the wild tomato (Lycopersicon pennellii (Corr.) D'Arcy) alters settling and reduces oviposition of Bemisia argentifolii (silverleaf whitefly). Hortscience **30:** 827

Luckwill LC (1943) The Genus Lycopersicon: An Historical, Biological and Taxonomic Survey of the Wild and Cultivated Tomatoes. Aberdeen University Press, Aberdeen, UK

Mathieu S, Cin VD, Fei ZJ, Li H, Bliss P, Taylor MG, Klee HJ, Tieman DM (2009) Flavour compounds in tomato fruits: identification of loci and potential pathways affecting volatile composition. Journal of Experimental Botany **60:** 325-337

Matsui K, Ishii M, Sasaki M, Rabinowitch HD, Ben-Oliel G (2007) Identification of an allele attributable to formation of cucumber-like flavor in wild tomato species (Solanum pennellii) that was inactivated during domestication. Journal of Agricultural and Food Chemistry **55:** 4080-4086

McDowell ET, Kapteyn J, Schmidt A, Li C, Kang JH, Descour A, Shi F, Larson M, Schilmiller A, An L, Jones AD, Pichersky E, Soderlund CA, and Gang DR (2011) Comparative functional genomic analysis of Solanum glandular trichome types. Plant Physiolgy **155:** 524-539

McNally KL, Mutschler MA (1997) Use of introgression lines and zonal mapping to identify RAPD markers linked to QTL. Molecular Breeding **3:** 203-212

Momotaz A, Scott JW, Schuster DJ (2005) Searching for silverleaf whitefly and begomovirus resistance genes from Lycopersicon hirsutum accession LA1777. Proceedings of the 1st International Symposium on Tomato Diseases**:** 417-422

Mutschler MA, Doerge RW, Liu SC, Kuai JP, Liedl BE, Shapiro JA (1996) QTL analysis of pest resistance in the wild tomato Lycopersicon pennellii: QTLs controlling acylsugar level and composition. Theoretical and Applied Genetics **92:** 709-718

Mutschler MA, Wally AM, Rojas K, Cobb E (2001) Transferal of acylsugar-mediated multiple pest resistance to cultivated tomato. Hortscience **36:** 492

Palozza P, Parrone N, Simone RE, Catalano A (2010) Lycopene in atherosclerosis prevention: An integrated scheme of the potential mechanisms of action from cell culture studies. Archives of Biochemistry and Biophysics **504:** 26-33

Peiffer M, Tooker JF, Luthe DS, Felton GW (2009) Plants on early alert: glandular trichomes as sensors for insect herbivores. New Phytologist **184:** 644-656

Peralta IE, Spooner DM (2001) Granule-bound starch synthase (GBSSI) gene phylogeny of wild tomatoes (Solanum L. section Lycopersicon Mill. Wettst. subsection Lycopersicon). American Journal of Botany **88:** 1888-1902

Rao AV, Rao LG (2007) Carotenoids and human health. Pharmacological Research **55:** 207-216

Rick CM (1959) Non-random gene distribution among tomato chromosomes. Proceedings of the National Academy of Sciences of the United States of America **45:** 1515-1519

Rick CM (1978) Tomato. Scientific American **239:** 77-&

Rick CM (1979) Tomato. In N.W. Simmonds, ed, Crop Evolution. Longman, London.

Rick CM, Fobes JF (1975) Symposium on biochemical systematics, genetics and origin of cultivated plants. 10. Allozyme variation in cultivated tomato and closely related species. Bulletin of the Torrey Botanical Club **102:** 376-384

Rick CM (1986) Tomato. In J Smartt, N. W. Simmonds, eds, Evolution of Crop Plants, Ed 2 Longman Scientific & Technical, Essex, pp 452-457

Schauer N, Semel Y, Roessner U, Gur A, Balbo I, Carrari F, Pleban T, Perez-Melis A, Bruedigam C, Kopka J, Willmitzer L, Zamir D, Fernie AR (2006) Comprehensive metabolic profiling and phenotyping of interspecific introgression lines for tomato improvement. Nature Biotechnology **24:** 447-454

Schilmiller A, Shi F, Kim J, Charbonneau AL, Holmes D, Jones AD, Last RL (2010) Mass spectrometry screening reveals widespread diversity in trichome specialized metabolites of tomato chromosomal substitution lines. Plant Journal **62:** 391-403

Schilmiller AL, Miner DP, Larson M, McDowell E, Gang DR, Wilkerson C, Last RL (2010) Studies of a Biochemical Factory: Tomato Trichome Deep Expressed Sequence Tag Sequencing and Proteomics. Plant Physiology **153:** 1212-1223

Schilmiller AL, Schauvinhold I, Larson M, Xu R, Charbonneau AL, Schmidt A, Wilkerson C, Last RL, Pichersky E (2009) Monoterpenes in the glandular trichomes of tomato are synthesized from a neryl diphosphate precursor rather than geranyl diphosphate. Proceedings of the National Academy of Sciences of the United States of America **106:** 10865-10870

Singh P, Goyal GK (2008) Dietary lycopene: Its properties and anticarcinogenic effects. Comprehensive Reviews in Food Science and Food Safety **7:** 255-270

Slocombe SP, Schauvinhold I, McQuinn RP, Besser K, Welsby NA, Harper A, Aziz N, Li Y, Larson TR, Giovannoni J, Dixon RA, Broun P (2008) Transcriptomic

and reverse genetic analyses of branched-chain fatty acid and acyl sugar production in Solanum pennellii and Nicotiana benthamiana. Plant Physiology **148:** 1830-1846

Spooner DM, Peralta IE, Knapp S (2005) Comparison of AFLPs with other markers for phylogenetic inference in wild tomatoes Solanum L. section Lycopersicon (Mill.) Wettst. Taxon **54:** 43-61

Tadmor Y, King S, Levi A, Davis A, Meir A, Wasserman B, Hirschberg J, Lewinsohn E (2005) Comparative fruit colouration in watermelon and tomato. Food Research International **38:** 837-841

Tooker JF, Peiffer M, Luthe DS, Felton GW (2010) Trichomes as sensors: detecting activity on the leaf surface. Plant Signal Behav **5:** 73-75

van Schie CCN, Haring MA, Schuurink RC (2007) Tomato linalool synthase is induced in trichomes by jasmonic acid. Plant Molecular Biology **64:** 251-263

Vavilov N (1926) Studies on the origin of cultivated plants. Bull Appl Bot & Plant Breeding **16:** 139-248

Vavilov NI (1940) (The study of origin of cultivated plants since Darwin's time). Sovietskaya Nauka [Soviet Sci] **2:** 55-75

Wang EM, Wang R, DeParasis J, Loughrin JH, Gan SS, Wagner GJ (2001) Suppression of a P450 hydroxylase gene in plant trichome glands enhances natural-product-based aphid resistance. Nature Biotechnology **19:** 371-374

Wosula EN, Knapp M, Agong SG (2009) Resistance to Tetranychus evansi in Lycopersicon esculentum X L. hirsutum var. glabratum hybrids. Journal of Horticultural Science & Biotechnology **84:** 360-364

Chapter 2

Comparative Functional Genomic Analysis of *Solanum* Glandular Trichome Types

McDowell ET, Kapteyn J, Schmidt A, Li C, Kang JH, Descour A, Shi F, Larson M, Schilmiller A, An L, Jones AD, Pichersky E, Soderlund CA, and Gang DR (2011) Comparative functional genomic analysis of Solanum glandular trichome types. Plant Physiolgy **155:** 524-539

Abstract

Glandular trichomes play important roles in protecting plants from biotic attack by producing defensive compounds. We investigated the metabolic profiles and transcriptomes to characterize the differences between different glandular trichome types in several domesticated and wild *Solanum* species: *Solanum lycopersicum* (glandular trichome types 1, 6, and 7), *Solanum habrochaites* (types 1, 4, and 6), *Solanum pennellii* (types4 and 6), *Solanum arcanum* (type 6), and *Solanum pimpinellifolium* (type 6). Substantial chemical differences in and between *Solanum* species and glandular trichome types are likely determined by the regulation of metabolism at several levels. Comparison of *S. habrochaites* type 1 and 4 glandular trichomes revealed few differences in chemical content or transcript abundance, leading to the conclusion that these two glandular trichome types are the same and differ perhaps only in stalk length. The observation that all of the other species examined here contain either type 1or 4 trichomes (not both) supports the conclusion that these two trichome types are the same. Most differences in metabolites between type1 and 4 glands on the one hand and type 6 glands on the other hand are quantitative but not qualitative. Several glandular trichome types express genes associated with photosynthesis and carbon fixation, indicating that some carbon destined

for specialized metabolism is likely fixed within the trichome secretory cells. Finally, *Solanum* type 7 glandular trichomes do not appear to be involved in the biosynthesis and storage of specialized metabolites and thus likely serve another unknown function, perhaps as the site of the synthesis of protease inhibitors.

Introduction

Trichomes are epidermal structures widely conserved across the plant kingdom (Kim and Mahlberg, 1991; Wagner, 1991; Alonso et al., 1992; Yu et al., 1992; Kolb and Muller, 2003; Valkama et al., 2003; Giuliani and Bini, 2008). These structures perform important biological functions, such as discouraging herbivory, attracting pollinators, and maintaining a boundary layer (Nihoul, 1993; Van Dam and Hare, 1998; Kennedy, 2003; Moyano et al., 2003; Simmons and Gurr, 2005; Liu et al., 2006; Horgan et al., 2007; Gonzalez et al., 2008; Romero et al., 2008; Nonomura et al., 2009; Kang et al., 2010). Many of these functions are the result of the specialized nature of glandular trichomes (glands) as sites for the synthesis and storage of biologically active specialized metabolites (Alonso et al., 1992; Antonious, 2001; Iijima et al., 2004; Siebert, 2004; Deschamps et al., 2006; Nagel et al., 2008; Wang et al., 2008; Biswas et al., 2009; Sallaud et al., 2009). Comparisons between domesticated crop species and their wild progenitors have revealed that many of the more potent, glandular trichome-derived specialized metabolites have been lost during domestication (Rodriguez et al., 1993; Oghiakhe, 1997; Medeiros and Tingey, 2006; Zhang et al., 2008; Besser et al., 2009). The loss of these important compounds has led to an increased susceptibility of domesticated crops to pathogen and herbivore attack compared with their wild counterparts (Rodriguez et al., 1993; Puterka et al., 2003; Chao et al., 2006; Nonomura et al., 2009), and reintroduction of such compounds into crop species may prove to be an effective way to combat crop loss due to insects and disease.

The genus *Solanum* possesses two general categories of trichomes: nonglandular and glandular. The nonglandular trichomes are generally linear trichomes that lack secretory/storage cells at their tips (Schwab et al., 2000) and thus are not of interest for this investigation. The glandular trichomes of *Solanum*, on the other hand, first described by Luckwill (1943) and later reviewed extensively by Simmons and Gurr (2005), have been described as consisting of four distinct classes (types 1, 4, 6, and 7). The density of these glandular trichome types can vary according to species, cultivar, tissue, and environmental conditions (Luckwill, 1943; Wilkens et al., 1996; Economou et al., 2006; Maluf et al., 2007; Kang et al., 2010). The glandular trichome types differ according to

the size and length of the supporting stalk as well as the number of secretory cells making up the glandular tip. In addition, other differences, such as in chemical content, have been proposed between most of these four types of glandular trichomes. Indeed, type 6 glandular trichomes are known to be the major site of terpenoid production in cultivated tomato (*Solanum lycopersicum*; Schilmiller et al., 2009; Kang et al., 2010).

To determine the biological roles and chemical contents of individual glandular trichome types in various *Solanum* species, we have taken a comparative functional genomics approach with particular emphasis on analysis of the glandular trichome secretory cell transcriptome and metabolic profile. This analysis has allowed us to address several important questions. What are the roles of the different glandular trichome types? Do some plants make more than one type of glandular trichome? What specialized functions do different glandular trichome types possess? And where do specific specialized metabolic processes occur (e.g. terpenoid versus acyl sugar production)?

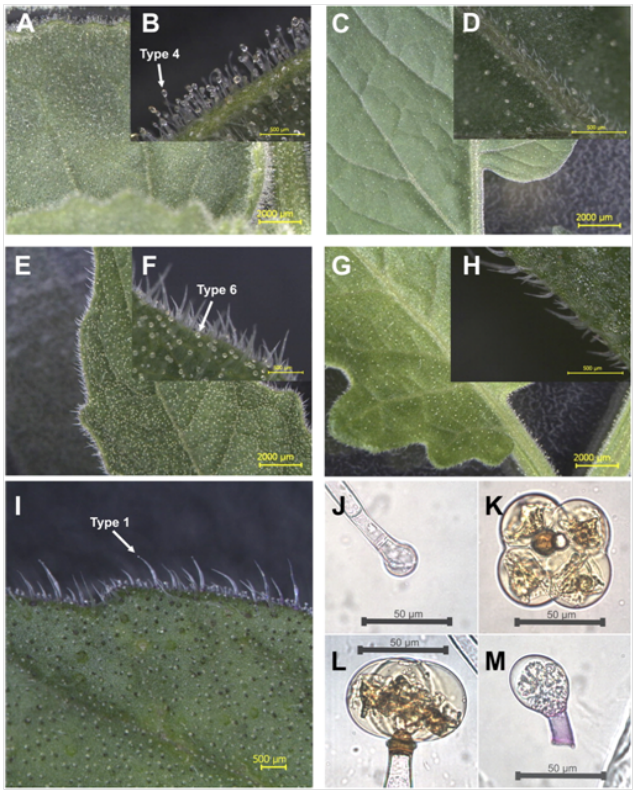

Figure 2.1. Glandular trichome density and distribution among four of five Solanum species used in this study. A, S. pennellii accession LA0716 leaf. B, A closer look at S. pennellii glandular trichomes. C, S. pimpinellifolium accession LA1589 leat. D, A closer look at S. pimpinellifolium glandular trichomes. E, S. habrochaites accession LA1777 leaf. F, A closer look at S. habrochaites glandular trichomes. G, S. arcanum accession LA1708 leaf. H, A closer look at S. arcanum glandular trichomes. I, S. lycopersicum accession LA3475 (M82) leaf. J to M, S. lycopersicum glandular trichomes. J, Type 1. K and L, Type 6. M, Type 7.

Isolation and Analysis of Different Trichome Types in Different *Solanum* Species

Accessions from five *Solanum* species were chosen for analysis: *Solanum habrochaites* (LA1777), *Solanum pimpinellifolium* (LA1589), *Solanum pennellii* (LA0716), *Solanum arcanum* (= *Solanum peruvianum*; LA1708), and *S. lycopersicum* (= *Lycopersicon esculentum*; M82). Within these species, several types of glandular trichomes are present and vary in abundance (Fig. 1; Table I). Of specific interest were secretory cells of type 1, 4, 6, and 7 glandular trichomes, which remain largely uncharacterized at the individual level across *Solanum* species. A recent report (Slocombe et al., 2008) describes the analysis of total trichome preparations from *S. pennellii*, which formed a reference point for our analysis, but did not analyze individual trichome type secretory cells.

Table 2.I. The accessions used in this study along with information on the glandular trichome density, metabolite profile, and EST approach.

A, Abundant; E, EST sequencing using the 454 pyrosequencing approach, more than 100,000 resulting ESTs; ES, EST sequencing using the Sanger approach, less than 1,000 resulting ESTs; M, metabolite profile was performed; S, sparse; ^{S}, sticky residue/profuse secretion

Species (Accession No.)	Glandular Trichome Type			
	Type 1	Type 4	Type 6	Type 7
S. lycopersicum (M82/LA3475), domesticated	A, M, ES	S, --, --	A, M, EP	S, --, ES
S. pimpinellifolium (LA1589), current	--, --, --	--, --, --	A, M, EP	--, --, --
S. Arcanum (LA1708), wild	A, --, --	--, --, --	A, M, --	--, --, --
S. habrochaites (LA1777), wild	S^{S}, M, ES	A^{S}, M, ES	A, M, EP	S, M, --
S. pennellii (LA0716), wild	S^{S}, --, --	A^{S}, M, ES	S, M, ES	S, --, --

The trichomes referred to as types 1 and 4 glandular trichomes, as shown in Figure 1, A, B, I, and J, appear to be physically similar to nonglandular hairy trichomes but terminate with globe- or oblong-shaped one- to two-cell storage/secretion units that may or may not be covered by a waxy cuticle. One hypothesis explaining the physical similarities between these two glandular trichome types is that type 1 and type 4 trichomes represent different stages of development (Kang et al., 2010). However, both are present on very young leaves as well as on fully mature leaves. Despite their apparent physical differences, both types accumulate small droplets on their tips that contain sticky acyl sugar compounds (Rodriguez et al., 1993; Alba et al., 2009; Nonomura et al., 2009). The accumulation of such compounds is pronounced in *S. pennellii* and *S. habrochaites*, which have abundant type 4 trichomes (Weston et al., 1989; Snyder et al., 1998), resulting in a sticky residue when leaves of these species are handled. The opposite is true for *S. arcanum* and *S. lycopersicum*, which possess type 1 trichomes but lack the profuse secreting nature of *S. habrochaites* and *S. pennellii* type 1 or 4 trichomes.

The other dominant glandular trichome in *Solanum* species is the type 6 gland, shown in Figure 1, F, K, and L. Composed of four disc cells at the end of a two-celled stalk, these glands are found on all species used in this study but are present in low abundance on *S. pennellii* leaves and stems. Unlike the secreting type 1 and 4 glands of *S. habrochaites* and *S. pennellii*, type 6 glands appear to be specialized to produce metabolites and then store them under a waxy cuticle, as has been described for other "peltate" glandular trichomes found in mint (*Mentha* x *piperita*), basil (*Ocimum basilicum*), and other species (Croteau, 1991; Turner et al., 2000; Gang et al., 2001; Deschamps et al., 2006; Gunnewich et al., 2007). In *Solanum* type 6 glands, the area under the cuticle is filled completely and ready to release its contents given either the correct environmental conditions or physical contact (Lin et al., 1987; Maluf et al., 2007; Ben-Israel et al., 2009).

The final glandular trichome type of interest is the type 7 glandular trichome depicted in Figure 1M. Of all glandular trichomes analyzed, this gland is both of low abundance (Simmons et al., 2003) and the least characterized, due not only to its scarcity but also to its general physical properties. Located in close proximity to the epidermis, this glandular trichome consists of a small multicellular glandular head situated on a

short, single-celled stalk, making it very difficult to isolate. Like the type 6 gland, type 7 glandular trichomes also possess a waxy cuticle that has been observed in our studies to be removable with harsh abrasive treatment. The exact content of the mixture under the waxy cuticle of type 7 glands remains unclear and is discussed below.

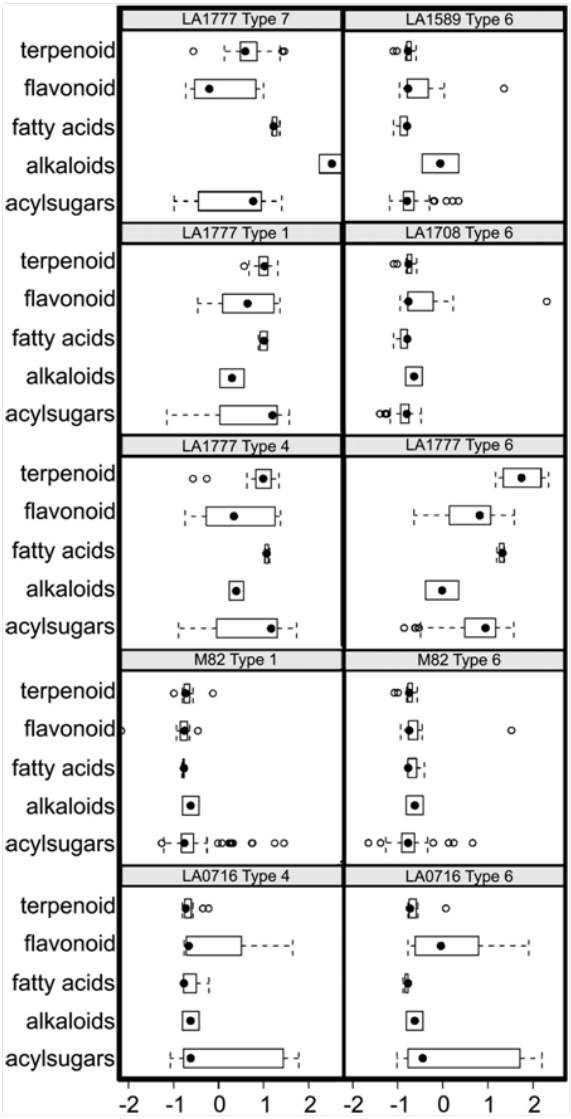

Figure 2.2. Summary of major identifiable metabolites by species and trichome types. Each panel represents one species/trichome type. In each panel, the *x* axis is the normalized log2 (peak area), the *y* axis represents the five compound classes, and the panel title (at the top of each panel) lists the corresponding species/trichome type. Black circles indicate metabolite class medians, while the dotted lines indicate the limits of the 90th percentile and lower 10th percentile. White circles or semicircles indicate individual data points outside the range of 10th to 90th percentiles. For the purposes of this study, peak areas for each of the identified trichome metabolites were averaged within each species/trichome type. Using these averages, a log2 transformation was performed to decrease the effect of extreme values. Following log2 transformation, the resulting values were normalized across all 10 species/trichome types.

To collect enough glandular secretory cells for metabolomic and transcriptomic analyses, a variety of methods were employed. To collect the type 1 and 4 glands from the various *Solanum* species, microscissors were used to clip the glandular heads off of the stalks. This leads to very pure fractions of just the glandular head cells. Two alternative approaches were used to isolate the type 6 gland heads. The first approach involved directly "picking" type 6 glandular trichome heads using stretched glass pipettes (Schilmiller et al., 2009; Kang et al., 2010), while the second approach utilized glass beads in buffer to abrasively remove trichomes from the leaf surface (Gang et al., 2001; Fridman et al., 2005). Fractions enriched in type 7 glandular trichome secretory cells were obtained using the bead-beater procedure. Methods employing liquid N2 or dry ice (Yerger et al., 1992) did not work well for our purposes, as these preclude the ability to separate different types of trichomes from each other and lead to trichome fractions that consist mostly of the non-glandular stalks. The methods used in this investigation allowed us to obtain very pure preparations consisting almost exclusively of the secretory cells of interest. Secretory cells collected for transcriptome profiling were flash frozen in liquid nitrogen, whereas cells destined for metabolite profiling were immediately suspended in ice-cold solvent before being further processed (see "Materials and Methods").

Gross Comparisons of Trichome Metabolite Profiles in *Solanum* Species

Metabolite profiles obtained for the 10 species/type entries marked as abundant or sparse in Table I were produced using a liquid chromatography (LC)-time of flight-mass spectrometry (MS)-based method and revealed that the majority (79%) of the detected compounds were unknowns (Supplemental Table S1). However, 119 known compounds were detected and their relative quantities determined between gland types and between species. It was impossible to determine absolute levels for these compounds in our samples because of differences in ionization efficiencies and potential ion suppression due to variable matrix effects. Moreover, potential intrametabolite contamination from the type 1/4 trichome exudates for the type 6 trichome samples may exist, especially for the type 6 samples from *S. habrochaites* and *S. pennellii*. Thus, it was also not possible to determine accurate differences in abundance for compound/compound comparisons.

Nevertheless, trends in compound class abundance between trichome types and between species, based on relative quantification values, were determined. The box plot in Figure 2 shows the distribution of normalized peak areas for aggregate metabolite classes for known compounds detected in the various *Solanum* species and trichome types, providing a general concept of the prevalence of various compound classes in different glandular trichome extracts. The results presented in this figure must be evaluated with caution, however, in light of the issues of non-uniform ionization efficiencies and potential ion suppression and matrix effects mentioned above. Nevertheless, these results suggest interesting trends regarding metabolite production in these trichomes, where metabolite modules appear to be present and imply mechanisms involved in controlling the production of specific compounds and groups of compounds (Fig. 3; Supplemental Figs. S1 and S2; Supplemental Table S2; Xie et al., 2009).

The normalized data used to produce Figure 3 revealed that the known metabolites observed in *Solanum* trichomes are differentially distributed between trichome types and species and that this variation is generally more evident between species than within. For example, *S. habrochaites* glands contain the most diverse set of known fatty acids, sesterterpenes, and acyl sucroses of all species and glandular trichome types (Supplemental Table S2; Supplemental Fig. S2, clusters 2A–2Y). Likewise, *S. pennellii* glands were dominated by acyl glucoses (Supplemental Fig. S2, clusters 1A–1H) compared with other species and gland types. It is also clear from Figure 2 that cultivated tomato (M82) lacks the chemical diversity of many of the wild species and is more similar to *S. arcanum* and *S. pimpinellifolium* than to *S. pennellii* and *S. habrochaites*, a conclusion further supported by the data shown in Figures 2 to 4 and Supplemental Figures S2 and S3. Figure 4, displaying results from additional multivariate statistical analyses (principal component analysis [PCA] and partial least squares-discriminant analysis [PLS-DA]) of the metabolite data set with individual samples from all species viewed separately instead of by analyzing means of replicates, clearly shows that *S. lycopersicum*, *S. arcanum*, and *S. pimpinellifolium* are closely related metabolically, regardless of trichome type. The similar metabolite profiles and morphologies of *S. lycopersicum*, *S. arcanum*, and *S. pimpinellifolium* is consistent with the close phylogenetic relationship among these species (Peralta and Spooner, 2001).

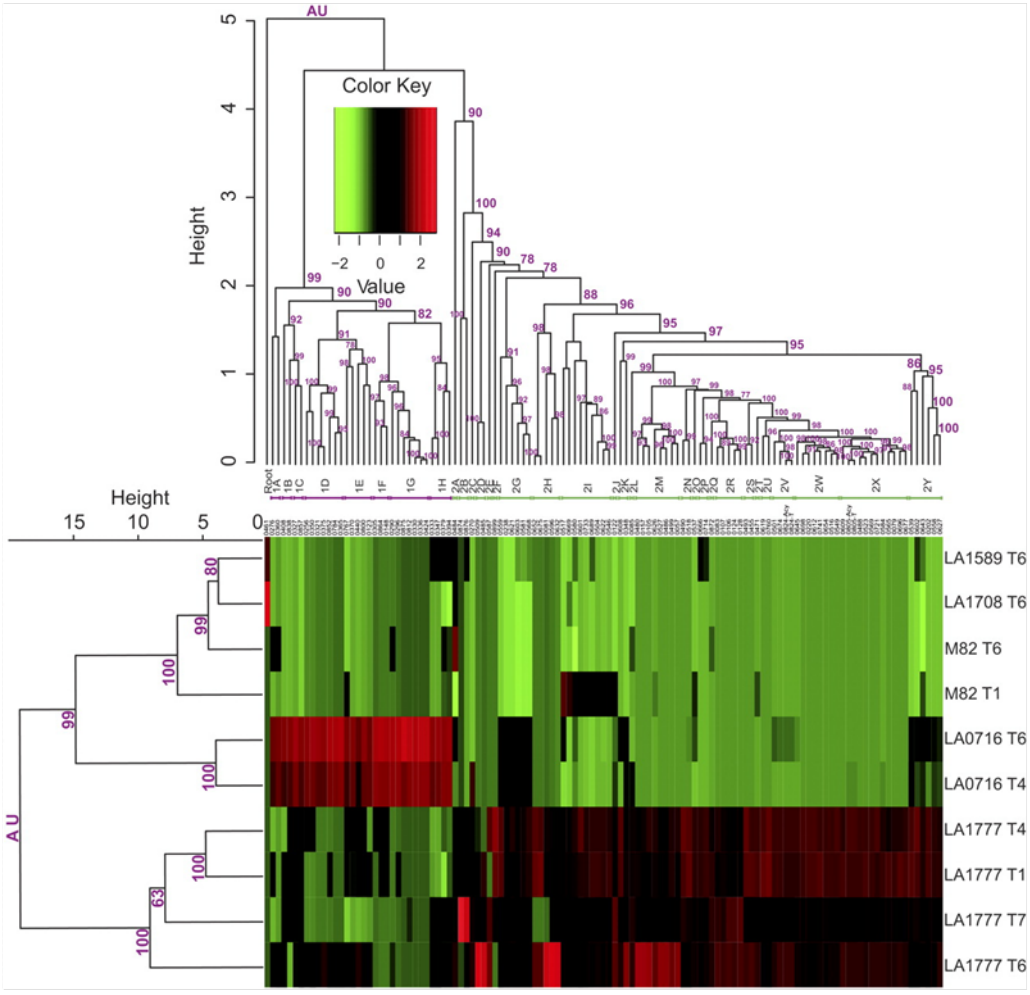

Figure 2.3. Two-way cluster analysis of normalized LC-MS metabolite peak areas from *Solanum* glandular trichomes. In the heat-map plot, each column represents a feature, and the dendrogram of cluster tree for features is displayed at the top; each row represents a species/trichome type, and the dendrogram of cluster tree for types is displayed on the left margin. Dendrograms and bootstrap values (magenta numbers) are calculated using the R package pvclust (Shimodaira, 2002, 2004). Four-digit numbers along the top edge of the heat map indicate unique metabolite identifiers listed in Supplemental Figure S1. Two-digit alpha-numeric identifiers (1A–1H, 2A–2Y) immediately below the top dendrogram indicate metabolite clusters also listed in Supplemental Figures S1 and S2. Accession numbers represent the *Solanum* species examined: LA1589, *S. pimpinellifolium*; LA1777, *S. habrochaites*; LA0716, *S. pennellii*; LA1708, *S. arcanum*; M82, *S. lycopersicum*.

These profiles are also illustrative of *S. lycopersicum*'s limited ability to produce and/or store the metabolites measured in our analysis within its glandular trichomes, although it does produce significant levels of a handful of monoterpenoids and sesquiterpenoids (Kang et al., 2010). This reduced chemical diversity relative to wild species may help to explain observations that the resistance of domesticated tomato cultivars to certain

arthropod herbivores is less than that of many wild tomato species (Kumar et al., 1995; Pico et al., 1998; Martins Santana et al., 2001).

What was quite surprising was that greater differences were observed in overall metabolite profiles for the same glandular trichome type across species than were observed for comparisons of different gland types within the same species. For example, PLS-DA (Fig. 4C) and PCA (Fig. 4, C–F) analyses of metabolite data obtained for *S. habrochaites* (accession LA1777), the only accession that had readily isolatable glandular trichomes for all types (1, 4, 6, and 7), demonstrated that glandular trichome types 1 and 4 were indistinguishable from each other. Hierarchical cluster analysis (Supplemental Fig. S3A) also failed to separate type 1 and 4 trichomes based on overall or aggregate metabolite profiles, regardless of the method used for data normalization. The normalization used for the data presented above was log2-transformed data. Other normalization methods, such as autoscaling, pareto scaling, or range scaling, gave even poorer resolving power, where type 6 trichomes were also not readily differentiated from the type 1 or 4 trichomes. Interestingly, glandular trichomes from stems could be differentiated from glandular trichomes isolated from leaf surfaces (Fig. 4, D and F), depending on which principal components were considered, suggesting that significantly different metabolite profiles may exist for stems versus leaves. Such results only present an aggregate picture of a greater metabolomic content, however, and do not allow for closer inspection of how specific compounds that might be involved in specific plant defenses may be produced or regulated.

When specific classes of compounds were compared, instead of gross aggregate profiles, a few notable differences were observed among the different trichome types within species. For example, *S. lycopersicum* type 1 and 6 glandular trichomes exhibited markedly dissimilar profiles for certain subsets of metabolites. Whereas the levels of acyl glucoses in both types of *S. lycopersicum* glands were very low (although they were more abundant in the type 6 glands than in type 1), type 1 extracts from the same species were dominated by acyl sucroses (Supplemental Fig. S2, clusters 1A, 1E, 1G, 1H, 2I, 2O, 2T, and 2Y), but such compounds did not appear to be present in type 6 glands from this particular species. In addition, *S. habrochaites* type 1 and 4 trichomes had approximately

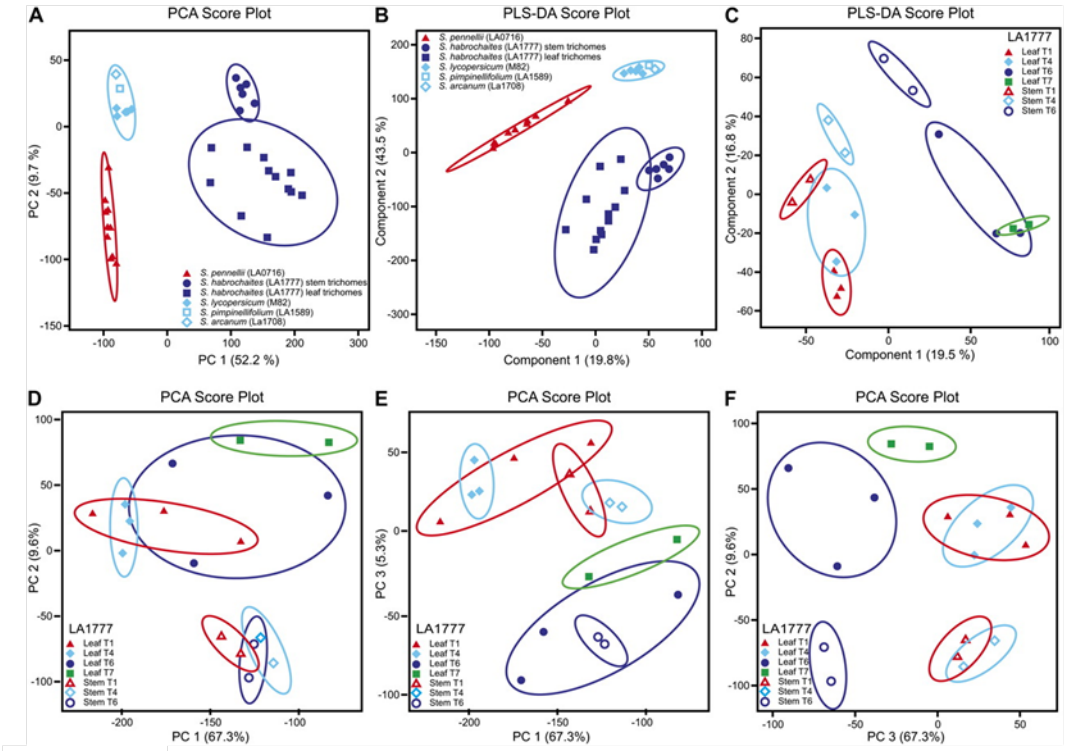

Figure 2.4. PCA and PLS-DA of metabolite profiling data for comparison of trichome types of all species evaluated in this investigation (A and B) and of all trichome types from S. habrochaites (LA1777; C–F).

5-fold higher levels of methylated myricetin (a flavonoid) than did type 6 (A. Schmidt and E. Pichersky, unpublished data).

We observed great variability in relative amounts of acyl sugars between different preparations of the same gland type, especially for *S. pennellii* type 6 and 4 gland preparations. And, despite the possibility of variable matrix effects, the differences between preparations of a single gland type were very large compared with the likely variation resulting from matrix effects. Therefore, we are not convinced that further chemical analyses (even if acyl sugar standards were available) would enhance our understanding of the differences between gland chemistries.

Trichome Transcriptomes in *Solanum* Species

The transcriptomes of the secretory cells of various glandular trichome types from the different species were analyzed using a transcriptome sequencing approach, with six and eight libraries sequenced using Sanger and 454 approaches, respectively (Table I),

resulting in 1.4 x 10^6 ESTs. The ESTs for the five species were separately assembled with PAVE (Soderlund et al., 2009) and annotated with UniProt (UniProt Consortium, 2010) and Rstat (Stekel et al., 2000). The ESTs from all trichome/species libraries were also assembled together, resulting in 32,261 contigs and 49,958 singletons. Annotation of these trichome/species contigs and singletons resulted in 80% of sequences being assigned a UniProt identifier, of which 33,092 had UniProt identifiers from plants as a top match. The resulting transcriptomic data can be viewed and analyzed at http://www.agcol.arizona.edu/pave/*Solanum*/. This approach contrasts to what has been reported before for *S. pennellii*, where total trichomes, including stalks, were aggregately (trichome types were not distinguishable) analyzed for gene expression level by hybridization to the *S. lycopersicum* TOM2 microarray, an array containing sequences from a different *Solanum* species than what was used in the hybridization analysis (Slocombe et al., 2008). Such cross-species microarray experiments, while capable of differentiating rough relative expression levels between tissues within the same species for many (but not all) genes in the target species, are not capable of providing absolute expression levels or of being useful when comparing expression for any particular gene between species (Chain et al., 2008; Gilad et al., 2009). Thus, it is unfortunately practically impossible to draw comparisons between our approach and what has been previously published with regard to observed levels of expression for any particular gene, as our approach was fundamentally different from what has been described before.

Comparison of Type 6 Glandular Trichomes between *Solanum* Species

Analysis of metabolites from type 6 glandular trichomes across all five species resulted in the same trends discussed in the gross comparisons of metabolites across all species and glandular trichome types. Compared with the other species, *S. habrochaites* and *S. pennellii* type 6 glands have more in common with one another than they do with *S. lycopersicum*, *S. arcanum*, and *S. pimpinellifolium* (Figs. 2 and 3). Moreover, the *S. habrochaites* type 6 extracts also contain the most diverse sets of metabolites (which are specific to *S. habrochaites* type 6) compared with other species (Supplemental Fig. S2), being dominated by acyl sucroses, terpenoids, and fatty acids (Supplemental Fig. S2). *S. pennellii* type 6 glands possess the second most diverse complement of specialized

metabolites specific to one species, containing the most diverse set of acyl glucoses in our comparisons (Supplemental Fig. S2). In contrast, type 6 gland extracts from *S. lycopersicum*, *S. pimpinellifolium*, and *S. arcanum* are very similar to each other (Supplemental Fig. S2), and both the diversity and quantity of metabolites in these three species are extremely limited. The unique type 6 glandular trichome metabolite profiles may play important roles in conferring to wild *Solanum* species resistance to disease and insect herbivory (Kumar et al., 1995; Pico et al., 1998; Martins Santana et al., 2001).

Gross analysis of *Solanum* type 6 transcriptomes revealed that transcripts for enzymes and proteins associated with photosynthesis light reactions, photosynthetic carbon fixation, glycolysis/gluconeogenesis, starch and Suc metabolism, and the citrate cycle were prevalent, in addition to many other downstream primary metabolic processes (Supplemental Table S3; Supplemental Figs. S4–S7; a reference iPath map can be accessed at http://pathways.embl.de/default_map.html for comparison), suggesting that *Solanum* type 6 glandular trichomes may be able to produce specialized compounds de novo, perhaps without the requirement for transport and uptake of source carbon from stalk cells. This contrasts somewhat with the report that in *S. pennellii* total trichomes, the expression level for photosynthesis-related genes was greatly reduced (Slocombe et al., 2008), based on hybridization to a nonspecies microarray platform (the TOM2 Affy array is based on a limited set of genes from a specific *S. lycopersicum* cultivar and not on *S. pennellii*). However, the trichome stalk cells provided the vast majority of the cell mass and presumably RNAs in that study (see Fig. 2, G and H, in Slocombe et al., 2008). In our study, we analyzed only the secretory cells for the majority of the trichome types analyzed, or only small portions of the stalks were included when microscissors were used to clip off the trichome heads at their connection to the stalk. This may have led to our ability to detect significant levels of expression of some photosynthesis-related genes, whereas the other report did not observe this.

Developing oil seed embryos from some species do not necessarily rely solely on imported Suc and the oxidative pentose phosphate pathway but rather also utilize an endogenous photosynthetic apparatus to provide both carbon skeletons and reducing power for oil (triglyceride) synthesis (Goffman et al., 2004; Alonso et al., 2007; Junker et al., 2007; Allen et al., 2009). Similarly, Wang et al. (2009) recently claimed that

photosynthesis genes are expressed at very high levels in the glandular trichomes of *Artemisia annua*, with chlorophyll *a/b*-binding protein and ribulose bisphosphate carboxylase small subunit being among the top 10 most highly expressed transcripts in the trichomes of that species, and that in situ carbon fixation may be involved in the production of artemisinin in these trichome secretory cells. However, close inspection of figure 5 (isolation of glandular trichomes) from that report reveals significant contamination by green mesophyll cells in the final glandular trichome preparation used for 454 transcriptome analysis. The glandular trichomes shown in that figure appear to be colorless. Thus, it is not clear whether or not de novo carbon fixation in the secretory cells is indeed involved in the production of artemisinin, and the transcript levels observed may be due to expression not only in the trichome but also in underlying mesophyll cells that contaminated the trichome preparations. Indeed, species such as *Glycine max, Mentha* species, and basil possess glandular trichomes with plastids that lack developed thylakoid membrane systems and any apparent ability to perform photosynthesis (Franceschi and Giaquinta, 1983; Croteau, 1991; Gershenzon et al., 1992; McCaskill et al., 1992; McCaskill and Croteau, 1995; Lange et al., 2000; Turner et al., 2000; Gang et al., 2001; Turner and Croteau, 2004; Rios-Estepa et al., 2008; Xie et al., 2008). In these species, nonphotosynthetic plastids appear to be heavily involved in specialized metabolite synthesis. The glandular trichomes of *A. annua* appear to be of this type.

In contrast, work on tobacco (*Nicotiana tabacum*) glandular trichomes clearly suggested that some glandular trichomes in the *Solanaceae* have the ability to fix carbon and synthesize metabolites from sugar produced directly in the trichomes, although carbon imported into the trichome may also be involved (Keene and Wagner, 1985; Kandra and Wagner, 1988; Nielsen et al., 1991). The type 6 trichomes from *S. lycopersicum, S. arcanum, S. pimpinellifolium*, and *S. habrochaites* used for 454 sequencing in this analysis were isolated using the glass-bead-shaking method. However, the type 1/4 trichomes from all species and type 6 trichomes from *S. pennellii* used for both metabolite analysis and sequencing in this project were hand picked (Supplemental Fig. S20), leading to analysis of only the secretory cells and perhaps part of a stalk cell for those collected by the microscissors technique but no possible contamination by

underlying mesophyll or other cell types. It must be noted that such photosynthesis-related genes were not among the most highly expressed in our analysis, as can be seen in Supplemental Tables S14 to S19, where many of them are listed. Therefore, the identification of transcripts for photosynthesis genes in the trichomes suggests the possibility that the secretory cells of *Solanum* species may possess the ability to have at least a rudimentary capacity for photosynthesis that may contribute to secreted metabolite synthesis. Thus, the role of imported versus de novo-synthesized sugars in glandular trichome secretory cell metabolism remains an area of intense interest.

Also observed in type 6 glands from all species, with the exception of *S. pennellii*, were transcripts representing the phenylpropanoid and flavonoid pathways. The lack of representation of the phenylpropanoid and flavonoid pathways in the transcriptome of *S. pennellii* type 6 glandular trichomes was likely the result of inadequate sampling of the transcriptome during sequencing (Supplemental Tables S4 and S5), as these trichomes were difficult to obtain due to the high densities of type 1/4 glands that obscured access, with the resulting production of only a small 454 library.

In further efforts to make quantitative comparisons between type 6 *Solanum* trichomes from these species, we utilized the methodology of Stekel et al. (2000) to identify differentially significantly expressed ESTs (Supplemental Tables S6 and S7) using summaries of three different annotations that were assigned as described in "Materials and Methods": UniProt identification (UPID), Enzyme Commission (EC), and Gene Ontology. Supplemental Tables S6 and S7 provide interspecies and intraspecies comparisons for UniProt and EC, showing the normalized counts for up-regulated genes for each of the two species compared. The elements of the metabolic network present in *Solanum* type 6 trichome secretory cells are listed in Supplemental Table S3 and are pictorially reconstructed using the iPATH software (Letunic et al., 2008; Supplemental Figs. S4–S8). To ensure legitimate comparisons between library data sets, we took a conservative approach and only used library comparisons that were of similar size, collection method, sequencing technologies, and within the same sequence assembly (Supplemental Tables S4–S7). Thus, the type 6 gland comparisons that are listed in Supplemental Tables S6 and S7 excluded the *S. arcanum* and *S. pennellii* type 6 data sets. The three type 6 transcript comparisons that were performed reflect the metabolite

profiles observed in the gross metabolite comparisons described above; this is shown in Supplemental Tables S8 to S15, which list overrepresented and underrepresented biological processes by Gene Ontology terms in each of the species. Interestingly, terpenoid-rich *S. habrochaites* appears to preferentially (compared with either *S. pimpinellifolium* or *S. lycopersicum*; Supplemental Table S14) express enzymes important for regulating flux into the terpenoid/isoprenoid pathway: 1-deoxy-D-xylulose 5-phosphate synthase 2 (annotated as Q68IP4_SOLHA), 4-hydroxy-3-methylbut-2-enyl diphosphate reductase (annotated as Q2XTB5_SOLTU, LYTB-like protein), and Z,Z-farnesyl pyrophosphate synthase (annotated as B8XA40_SOLHA). Also, *S. habrochaites* type 6 trichomes exhibit enriched expression of contig EC annotations implicated in processes associated with acyl sugar biosynthesis, including an acyl desaturase (EC 1.14.19.2) and an isopropylmalate synthase (EC 2.3.3.13; Supplemental Table S15; Slocombe et al., 2008). In contrast, it was not clear from this analysis why *S. habrochaites* type 6 glands contain limited quantities of Glc-derived acyl sugars compared with acyl sucroses, as ESTs for enzymes such as Suc synthase or gluconeogenesis pathway members were found in relatively equal abundance across species (Supplemental Tables S14 and S15). The mechanism responsible for regulating the production of these compounds remains unidentified, but based on our experiments, it is not likely to involve direct control by modulation of transcript levels.

In addition to the observations described above (i.e. that the specialized metabolites stored within the type 6 glandular trichome can be derived from imported, leaf-produced Suc or from carbon fixed within the trichome itself), the data also suggest that transcripts for general metabolic pathways that were detected were expressed at similar levels across species (Supplemental Tables S14 and S15). Additionally, it was evident that differences in type 6 gland biochemistry are likely due to differential up-regulation of select segments or branches of a pathway, not the whole pathway, as is suggested by Supplemental Figures S9 to S14. The differential regulation of select enzymes within type 6 glands is consistent with the biochemistries outlined in Figure 3, Supplemental Table S2, and Supplemental Figure S4, specifically with *S. habrochaites* compared with either *S. lycopersicum* or *S. pimpinellifolium*. It also appears that some differences in metabolite profiles between the species are most likely regulated at both

the transcriptional and genomic levels. Unique EC annotations for the "same" enzyme between different species suggested that not only differences in expression levels for gene family members but also alterations in sequence leading to potentially differential activity may produce altered pathway functions.

A final determination was that type 6 glands also express genes not directly contributing to specialized metabolism. *S. lycopersicum* is the best example, and genes encoding enzymes and other proteins such as lipoxygenase, pathogenesis-related protein isoform b1, Arg decarboxylase, superoxide dismutase, various heat shock-related proteins, and of course polyubiquitin were apparently expressed at high levels (Supplemental Tables S14 and S15). It is likely that these proteins are important in preserving the viability of these cells, which are exposed to varied environmental conditions due to their location at the end of a long trichome stalk. Moreover, it is also notable that despite the presence of transcripts for transcription factor genes, none of these appear to be preferentially expressed between species, at least not in a manner that was detectable using our sampling technique, which we acknowledge can only provide an approximation of expression levels. The lack of preferentially expressed transcription factors between species is likely an indicator that those transcription factors detected had biological roles more in line with the development or maintenance of cell fate functions than with the regulation of specialized metabolism. More detailed measurements of expression and function for individual members of such protein classes is definitely warranted.

Comparison of Type 1 and 4 Trichomes

Comparisons across all species for the physically similar type 1 and type 4 trichomes revealed that there are substantial differences between species for these glandular trichome types. Again the *S. pennellii* and *S. habrochaites* type 1/4 glands contained the most diverse sets of acyl sugars, phenylpropanoids, terpenoids, and alkaloids compared with other species (Fig. 2; Supplemental Fig. S2). For instance, *S. pennellii* type 4 glands, despite the presence of a few acyl sucroses (Supplemental Fig. S2, cluster 2G), contain mostly acyl glucoses. Also, *S. habrochaites* type 1/4 trichomes contain largely acyl sucroses rather than acyl glucoses (Supplemental Fig. S2). As with

the other trichome and species comparisons listed above, cultivated tomato type 1 glands are deficient in most of the specialized metabolites detected in this study.

Another trend evident in the type 1/4 comparison was the striking similarity between *S. habrochaites* type 1 and 4 trichomes at both the chemical and transcript levels (Figs. 3 and 4; Supplemental Fig. S2). While there were a few select compounds that exhibited differences in this comparison, such as a triacyl glucose with 20 acyl carbons, and two terpenoid metabolites tentatively assigned as glycosides of sesterterpene malonate esters, being more concentrated in type 1 than in type 4 (Supplemental Fig. S2, clusters 1A, 1B, and 2B), these differences were specific to only a few compounds and did not represent the overall metabolite profiles that were measured. As type 1 glandular trichomes are typically taller than type 4 trichomes, the relative differences in their metabolite contents may simply be a product of variation in cell size or trichome development.

Analysis of transcript levels (Supplemental Tables S6 and S7) demonstrated that the acyl sugar, phenylpropanoid, flavonoid, terpenoid, and specific alkaloid pathways are expressed in *S. habrochaites* type 1/4 glands, as are enzymes from core metabolism, as was observed for type 6 glands. Together, these data suggest that, like type 6 glands, *S. habrochaites* type 1/4 glands are most likely capable of both fixing carbon and metabolizing imported sugars. Not surprisingly, enzymes involved in the production of keto acids, fatty acids, lipids, and their subsequent derivatization are represented as well. Type 1/4 glands possess characteristic cuticle-enclosed heads that act as the site of the biosynthesis and storage of specialized metabolites, although these trichomes also apparently secrete the majority of the acyl sugars that are exuded from glands and coat the surface of *Solanum* leaves. The mechanism whereby these compounds are secreted from the gland cells has not yet been identified.

Comparison of transcript levels for annotated genes, whether from the EC or UPID standpoint, identified no significant differences between *S. habrochaites* type 1 and 4 glandular trichomes. Thus, the distinction of a trichome type as being either type 1 or 4 may be artificial. For this reason, comparisons to *S. lycopersicum* type 1 and *S. pennellii* type 4 were performed with a combined library referred as *S. habrochaites* type 1/4. Only one protein, a nonspecific lipid transfer protein, was preferentially expressed (in *S.*

lycopersicum type 1 glands) in these comparisons. Not only was this the only gene with preferential expression in all of the *Solanum* type 1/4 comparisons, but it was also one of the most prevalent transcripts in all species sampled. It is no surprise that this particular protein is highly expressed, as it has been previously shown to be induced by both biotic and abiotic stress (Torres-Schumann et al., 1992; Ooi et al., 2008). Clearly, trichomes are exposed to "the weather" more than most cell types. In addition, the lack of differences in EST counts for UPID and EC annotations (Supplemental Figs. S15–S18) may be due to limited sampling of cells that were difficult to obtain. We expected to observe at least a few differences between species, considering the differences in metabolite content and quantities as shown in Figures 2 and 3 and Supplemental Table S2. An alternative explanation may be that regulation of compound production in this glandular trichome type may occur at levels not evaluated in this study, such as by protein turnover, biochemical control, substrate availability, or altered enzyme activity due to posttranslational modifications.

Comparison of *Solanum* Type 6 and Type 1/4 Trichomes

To test for processes specific to either type 6 or type 1/4 glandular trichomes, we made three intraspecies comparisons (*S. lycopersicum* type 6 versus type 1, *S. habrochaites* type 6 versus type 1/4, and *S. pennellii* type 6 versus type 4; Supplemental Tables S18–S20) using the method of Stekel et al. (2000). Comparisons of type 6 and type 1/4 transcriptomes identified a limited number of significant differences between the trichome types in each of the three species. The *S. pennellii* comparison between the Sanger type 6 and 4 libraries identified only one gene (A1XEL0_TOBAC) annotated as a cytochrome P450 of unknown function that was preferentially expressed in the type 6 gland (Supplemental Table S20). However, for the *S. lycopersicum* and *S. habrochaites* comparisons, which use two libraries of dissimilar size and sequencing methodologies, these comparisons must be more carefully considered. The results of the *S. lycopersicum* and *S. habrochaites* comparisons nevertheless demonstrate that a small number of known, annotated genes are preferentially expressed in either trichome type. Genes associated (Table II; Supplemental Tables S18 and S19) with the type 6 gland include several involved in terpenoid biosynthesis and stress response (B8XA40_SOLHA, Z,Z-

farnesyl pyrophosphate synthase; Q9FQ28_SOLLC, sesquiterpene synthase 2; B8XA41_SOLHA, bergamotene/santalene synthase; EC 2.4.1.115, anthocyanidin 3-O-glucosyltransferase; EC 1.10.3.1, catechol oxidase; and EC 1.13.11.12, Q96573_SOLLC, lipoxygenase [Stekel et al., 2000]). We have used the observation that transcripts of the *S. lycopersicum* homologs of B8XA40, B8XA41, and Q9FQ28 are abundant in type 6 glands of *S. lycopersicum*, but not in other *S. lycopersicum* glands, as the starting point to identify the enzymes responsible for the synthesis of monoterpenes in the type 6 glands, but not in other glands, of this species (Schilmiller et al., 2009). In that work, we used biochemical assays and genetic analysis of near-isogenic lines to show that the B8XA40 homolog in *S. lycopersicum* encodes neryl diphosphate synthase. Neryl diphosphate is used as the substrate by the Q9FQ28 homolog, a terpene synthase, to synthesize β-phellandrene and other monoterpenes.

On the other hand, both *S. habrochaites* and *S. lycopersicum* type 1/4 trichomes preferentially express a nonspecific lipid-transfer protein (NLTP1_SOLLC) when compared with type 6 glands; this gene may play an important role in the secretion of acyl sugars (Slocombe et al., 2008). Together, all three *Solanum* type 1/4 versus type 6 gland comparisons indicate that there appears to be no quantitative disparity in the expression of genes involved with specialized metabolite pathways, such as acyl sugar or terpenoid biosynthesis (Table II). In addition, the preferential expression of a nonspecific lipid-transfer protein in type 1/4 trichomes in two of the three species is not surprising given the secretory activity of this trichome type, as evidenced by acyl sugar exudate accumulation on the leaves of these species, and may implicate this gene in the secretory activity of these cells.

It is important to note that some of the individual type 1 and 4 gland EST databases are limited in size, so that the prevalence of some transcripts that are not highly represented could not be reliably compared with that in other types of glands. For example, we recently showed by quantitative PCR that a rare transcript found in the *S. habrochaites* type 4 trichome EST database is nevertheless present in type 1 and 4 trichomes at about a 10-fold higher level than in type 6 trichomes. Biochemical assays showed that the transcript encodes an enzyme that methylates myricetin, thus explaining the above-noted observation that type 1 and 4 glands of *S. habrochaites* contain several

fold higher levels of methylated myricetin than do type 6 glands (A. Schmidt and E. Pichersky, unpublished data).

Characterization of *Solanum* Type 7 Trichomes

The type 7 glandular trichome is a short, multicelled trichome (Fig. 1M) that has been largely uncharacterized. We were able to collect type 7 trichomes from *S. habrochaites* for metabolite and transcriptome profile analysis. However, this gland type was either absent or too difficult to obtain from the other species to be included in our analysis. Surprisingly, type 7 glands from *S. habrochaites* were found to possess considerably higher concentrations of most metabolite classes than many of the other trichome types from the other species (Figs. 2 and 3). However, most of the compounds observed were also present at similar levels in other trichome types from *S. habrochaites*, suggesting contamination by the exudates produced by type 1/4 glands. The exceptions were the alkaloids tomatine and dehydrotomatine (Supplemental Fig. S2, cluster 2B), which were present in *S. habrochaites* type 7 glands but essentially absent from all other glandular trichome types.

Further investigations into the biological roles of this particular glandular trichome type led us to sequence 1,980 ESTs using the Sanger method and analyze chemical extracts from individually isolated *S. lycopersicum* type 7 glands. This analysis revealed that this gland type contains few if any transcripts with gene ontologies associated with specialized metabolism (Supplemental Fig. S19; Supplemental Tables S21–S24). In contrast, Cys protease inhibitors were strongly up-regulated in this trichome type, suggesting a role separate from the other glandular trichome types in plant defense.

Table 2.II. Selected pathways and known enzyme expression in different trichome types across *Solanum* species
Per 10K, Parts per 10,000.

UniProt Identifier/Pathway	Description	*S. habrochaites* Type 6 (per 10K)	*S. habrochaites* Type 1 (per 10K)	*S. habrochaites* Type 4 (per 10K)	*S. habrochaites* Type 1/4 (per 10K)	*S. lycopersicum* Type 6 (per 10K)	*S. lycopersicum* Type 1 (per 10K)	*S. lycopersicum* Type 7 (per 10K)	*S. pennellii* Type 4 (per 10K)	*S. pimpinellifolium* Type 6 (per 10K)
Terpenoid biosynthetic pathway										
A9ZN10_HEVBR	2-*C*-Methyl-D-erythritol 4-phosphate cytidylyltransferase	0	0	0	0	4	0	0	0	0
Q9XH50_SOLLC	1-D-Deoxyxylulose 5-phosphate synthase	0	0	0	0	1	0	0	0	2
Q2XTB5_SOLTU	LYTB-like protein-like	1,269	1	1	2	226	0	0	0	509
Q1A746_SOLLC	Geranyl pyrophosphate synthase	1	0	0	0	1	0	0	0	3
B8XA40_SOLHA	*Z,Z*-Farnesyl pyrophosphate synthase (*S. habrochaites*)/neryl diphosphate synthase (*S. lycopersicum*)	7,116	0	3	3	1,202	0	0	0	170
B8XA41_SOLHA	Santalene and bergamotene synthase (*S. habrochaites*)/β-phelandrene synthase (*S.*	1,879	0	2	2	669	0	0	0	624

(Table continues on following page.)

Table 2.II. (Continued from previous page.)

UniProt Identifier/Pathway	Description	*S. habrochaites* Type 6 (per 10K)	*S. habrochaites* Type 1 (per 10K)	*S. habrochaites* Type 4 (per 10K)	*S. habrochaites* Type 1/4 (per 10K)	*S. lycopersicum* Type 6 (per 10K)	*S. lycopersicum* Type 1 (per 10K)	*S. lycopersicum* Type 7 (per 10K)	*S. pennellii* Type 4 (per 10K)	*S. pimpinellifolium* Type 6 (per 10K)
	lycopersicum)									
Q9ZS34_TOBAC	Geranylgeranyl reductase	42	0	0	0	94	2	1	0	78
O64961_SOLLC	Epidermal germacrene C synthase (sesquiterpene synthase 1)	39	0	0	0	1	0	0	0	423
O64962_SOLLC	Germacrene C synthase	0	0	0	0	445	0	0	0	5
Q4A570_SOLLC	Putative squalene epoxidase	2	0	0	0	7	0	0	0	1
Q68IP4_SOLHA	Putative squalene epoxidase	880	0	0	0	300	2	0	0	340
Q9FQ28_SOLLC	Sesquiterpene synthase 2 (fragment)	14	0	0	0	1,938	3	1	0	1
Acyl sugar biosynthetic pathway										
Q0VH87_GOSHI	3-Ketoacyl-CoA reductase 2	0	0	0	0	3	1	0	0	2
A9XU45_GOSHI	3-Ketoacyl-CoA synthase 3	11	0	0	0	11	0	0	0	47
KCS19_ARATH	3-Ketoacyl-CoA synthase 19	7	0	0	0	9	0	0	0	6
ILV5_ARATH	Ketol acid reductoisomerase, chloroplastic	0	0	0	0	14	0	0	0	0

(Table continues on following page.)

Table 2.II. (Continued from previous page.)

UniProt Identifier/Pathway	Description	*S. habrochaites* Type 6 (per 10K)	*S. habrochaites* Type 1 (per 10K)	*S. habrochaites* Type 4 (per 10K)	*S. habrochaites* Type 1/4 (per 10K)	*S. lycopersicum* Type 6 (per 10K)	*S. lycopersicum* Type 1 (per 10K)	*S. lycopersicum* Type 7 (per 10K)	*S. pennellii* Type 4 (per 10K)	*S. pimpinellifolium* Type 6 (per 10K)
Q52QX_MANES	Aldo/keto reductase	4	0	1	1	0	0	0	0	1
B5LAT2_CAPAN	Putative acetolactate synthase	6	0	0	0	3	1	0	1	1
Q9SMC2_NICPL	Acetolactate synthase small subunit	0	0	0	0	2	0	0	0	1
B5LAV3_CAPAN	Putative isopropylmalate synthase	0	0	0	0	4	0	0	0	1
LEU1B_SOLPN	2-Isopropylmalate synthase B	1	0	0	0	1	0	0	0	6
Q9FEN7_SOLTU	Dihydrolipoyl dehydrogenase	9	0	1	1	2	0	0	0	1
IVD1_SOLTU	Isovaleryl-CoA dehydrogenase 1, mitochondrial	29	0	0	0	52	0	1	0	36

Conclusion

The type 6 and type 1/4 trichomes from the *Solanum* species analyzed in this study contain somewhat overlapping and modular sets of specialized metabolites, particularly acyl sugars, when compared within species. Despite this overlap, there are quantitative differences in metabolite profiles between *Solanum* species. These differences mirror previously determined *Solanum* phylogenies (Peralta and Spooner, 2001; Medeiros and Tingey, 2006). Glandular trichomes of *S. habrochaites* contain the most diverse sets of acyl sugars, fatty acids, alkaloids, and terpenoids compared with all other species, with sesterterpenes and acyl sucroses as the dominant forms of their respective metabolite classes (terpenoids and acyl sugars). The species with the second most diverse array of specialized metabolites is *S. pennellii*, dominated by the acyl glucose class of compounds. The remaining two wild species, *S. arcanum* and *S. pimpinellifolium*, have metabolite profiles that are very similar to *S. lycopersicum* and possess only modest differences when compared with their domesticated counterpart. Also, the transcriptomes of each of the trichome types generally mirror their respective biochemistries. Analysis of the glandular trichome EST collections reveals that all of the type 1/4 and 6 glands appear to contain most of the genes necessary for specialized metabolite biosynthesis, such as for the acyl sugar, terpenoid, or flavonoid pathways. More quantitative transcript comparisons (Supplemental Tables S14–S20) between species and gland types indicate that distinct chemical profiles may be due to differential regulation of specific genes or gene pathway segments on a transcriptional level or by other processes that are not directly connected to transcription, such as posttranslational modification of proteins, protein turnover, or biochemical control and cross-talk between pathways, among other possibilities.

Notable differences between different glandular trichome types were observed within species. For example, *S. lycopersicum* type 1 glandular trichomes are dominated by acyl glucoses (although even these compounds were present at relatively low levels in this trichome type from this species), while type 6 glands from this species are dominated by acyl sucroses. Complementary analysis of type 6 gland transcripts across species mirrored some of the traits observed in the different species' metabolite profiles.

Unfortunately, the comparison of metabolite levels with transcript levels was unable to identify specific genes whose expression levels could explain the differences in acyl sucrose and acyl glucose content for *S. habrochaites* or *S. pennellii* type 6 trichomes. Thus, unlike terpenoid biosynthesis in *S. habrochaites*, control of acyl sugar metabolism is likely exerted at a level not observable by the transcriptome analysis used in this study, a fact observed in the type 1/4-type 6 transcript comparisons of *S. lycopersicum* and *S. habrochaites*. However, this conclusion may be limited due to the small sampling size of the type 1/4 EST collections.

Many of the genes involved in photosynthesis and carbon fixation are expressed at significant (although not particularly high) levels in the *Solanum* trichome types investigated, in contrast to what has been observed in some other species (Turner et al., 2000; Gang et al., 2001; Deschamps et al., 2006; Gunnewich et al., 2007; Marks et al., 2009). Therefore, it is likely that at least some of the carbon required for the synthesis of the specialized metabolites found in *Solanum* glandular trichomes may be fixed within the trichome secretory cells. The relationship between de novo carbon fixation and import of Suc as the source for carbon skeletons, however, remains to be determined.

The least characterized of all glandular trichome types, the type 7 glandular trichome, appears to have a more limited metabolite profile than the other types. Because of the method required to collect type 7 glands, we cannot be sure that the type 7 transcriptome and metabolic profile sampled are completely exclusive to the type 7 gland. Nevertheless, it is clear that specialized metabolite production is limited in this glandular trichome type compared with the other types.

Finally, the distinction between type 1 and type 4 glandular trichomes, at least in *S. habrochaites*, may represent an artificial classification system, due to the lack of wholesale differences between the metabolic profile or the transcriptome of either cell type. Therefore, it may be more reasonable to consider type 4 glandular trichomes as simply a morphotype of a larger type 1 class.

Materials and Methods

Plants and Growth Conditions

All *Solanum* germplasm used in this study was obtained from the C.M. Rick Tomato Genetics Resource Center. Seeds were treated with 10% sodium tripolyphosphate for 20 min and rinsed in 10% bleach for 1 min. After rinsing thoroughly with sterile water, seeds were spread out on moist 3M Whatman filter paper in a sealed container. After 4 to 5 d, the seeds were transferred to peat pellets. The plants were grown in a growth room under a 16-h-light (27°C)/8-h-dark (18°C) cycle with the light intensity at approximately 200 µE m–2 s–1. Plants in peat pellets were watered daily with Peter's Professional general purpose 20:20:20 diluted to give 100 µL L–1 nitrogen. After 3 to 4 weeks, depending on the species, seedlings were transferred to 4-inch square pots and grown in the same growth room until analysis.

Production of 454 Libraries

Production of 454 libraries was exclusive to the type 6 trichome for all species except *Solanum pennellii*. For *Solanum lycopersicum*, *Solanum arcanum*, *Solanum pimpinellifolium*, and *Solanum habrochaites*, 15 to 20 g of young leaves approximately 1 cm wide was collected and covered for 15 min with 200 mL of ice-cold wash buffer (50 mM Tris-HCl, pH 7.5, 200 mM sorbitol, 20 mM Suc, 10 mM KCl, 5 mM MgCl2, 0.5 mM K2HPO4, 5 mM succinic acid, 1 mM EGTA, diethyl pyrocarbonate-treated water, 1 mM aurintricarboxylic acid, and 14 mM β-mercaptoethanol). Fifty milliliters of 0.5-mm glass beads (Biospec Products) was added to the beaker and then sealed shut using Parafilm. Once sealed, the beaker containing the glass beads and leaves was shaken by hand 300 times followed by 60 s on ice, repeated two more times. After shaking was complete, the leaf slurry was poured through a series of plastic funnels, each with an attached nylon mesh cloth with different pore sizes. The flow-through was collected in an ice-cold 1-L beaker at each step. The order of these meshes was as follows: 350 µm/105 µm/73 µm/54 µm/40 µm; with the type 6 trichomes collected on the final 40-µm mesh. The type 6 trichome fraction was immediately transferred to RNAlater and stored at –80°C until processed using the Qiagen RNEasy kit. cDNA was synthesized according to

the protocol described by Kapteyn et al. (2010) and sequenced by 454 sequencing (GS FLX) at the Michigan State University Research Technology Support Facility.

Production of Sanger Libraries

In order to produce the remaining glandular trichome EST libraries from *S. lycopersicum*, *S. pennellii*, and *S. habrochaites*, a protocol utilizing stretched glass pipettes (Supplemental Fig. S20) or microscissors (for accessions where the glands would not stick to the glass pipettes) was used to collect samples consisting of 4,000 each of type 1 (*S. lycopersicum*, *S. habrochaites*), type 4 (*S. pennellii*, *S. habrochaites*), and type 6 (*S. pennellii*) trichomes. These were transferred immediately into RNAlater and stored at –80°C until processed using the Qiagen RNEasy kit. Again, the resulting cDNA synthesis was performed using the protocol described by Kapteyn et al. (2010) and then subcloned into the plasmid pCR2.1.

S. lycopersicum type 7 trichome fractions used for EST analysis were produced in a manner similar to those of the *Solanum* type 6 fractions described above; however, an additional set of filters were added to further remove as many type 6, type 1, and hairy trichomes as possible from the initial type 6 flow-through. Additional steps include further filtration through a 73-µm and a 33-µm mesh. The final, enriched type 7 fraction was collected on the 33-µm mesh and used to produce cDNA as described (Kapteyn et al., 2010).

LC-MS Analysis of Trichome Extracts

S. habrochaites type 7 trichomes were collected in the manner described above, transferred to a microfuge tube, spun down (3,000g, 30 s), and resuspended in extraction solvent after the wash buffer was removed. For the remaining trichome types, picked trichome fractions of approximately 1,500 glandular trichome secretory cell clusters (heads) were immediately transferred to 50 µL/50 glands ice-cold extraction solvent, 2-propanol:CH3CN:water (3:3:2, v/v/v). The gland/solvent mixture was then sonicated for 5 min followed by vortexing for 30 s and centrifugation at 5,000g for 10 min. The supernatant was then transferred to a glass autosampler vial equipped with a 100-µL glass insert. LC-MS analysis of isolated gland metabolites was performed using a model LCT

Premier (Waters) mass spectrometer coupled to an LC-20AD pump and SIL-5000 autosampler (Shimadzu). All analyses utilized electrospray ionization in negative ion mode and employed a custom-packed Supelco Discovery Bio C18 column (1 x 150 mm, 3-µm particles). Mobile phase gradients were based on solvent A (0.15% aqueous formic acid) and solvent B (methanol), with a total flow rate of 0.05 mL min–1. The gradient consisted of initial condition 95% A, a linear gradient to 50% A at 5 min, a linear gradient to 5% A at 33 min, and then to 0% A at 35 min. The mobile phase was held constant until 38 min, when the composition returned to the original composition. Spectra were acquired using two quasisimultaneous conditions: high energy (aperture 1, 80 V) and low energy (aperture 1, 10 V) in the instrument source. Mass spectra were acquired at 1 Hz. Peak integration and alignment were performed using MarkerLynx software (Waters), and an array of peak areas was exported as a text file. Following acquisition of mass spectra, replicate peak areas for each metabolite were averaged within each species/trichome. Due to the calculated data being distributed dramatically over a wide range (0–800,000+), a log2 transformation was performed in order to compensate for the huge variation in the data. As log2(0) has no mathematical definition, log2(0+1) was used for transforming zero values. Transformed values were then normalized across 10 species/trichomes using the following equation: for values

Once normalized, cluster analysis was performed on the known compound data that contains 119 annotated metabolites, as shown in Supplemental Table S2. To produce the box plot in Figure 2, these values were aggregated according to metabolite class, and the class medians, averages, and both upper and lower quartiles were calculated. The uncertainty in hierarchical cluster analysis was assessed using the bootstrap resampling method, which was implemented by the R package pvclust (Shimodaira, 2002, 2004). The P values listed are the approximately unbiased P values, which are computed by multiscale bootstrap resampling and are a better approximation to unbiased P value than those computed by normal bootstrap resampling using a P value cutoff chosen as 95%. PCA and PLS-DA were performed using MetaboAnalyst (http://www.metaboanalyst.ca).

Analysis and Comparisons of EST Libraries

ESTs were assembled and annotated using the PAVE system (Soderlund et al., 2009; http://www.agcol.arizona.edu/pave/*Solanum*/). Annotation of the assembled contigs was primarily accomplished via the use of BLAST comparisons with first the UniProt (UniProt Consortium 2010 [www.uniprot.org]) database, followed by the lesser annotated GenBank (http://www.ncbi.nlm.nih.gov/GenBank/). The resulting annotation of the trichome contigs using either the UniProt or GenBank database permitted associated BLAST hits to be used as a basis for cross-species comparison of trichome transcriptomes on the basis of either EC numbers or UniProt identifiers. In addition, the Rstat values for each of the EC and UniProt identifiers were calculated as well as the minimum Rstat values necessary for the determination of a greater than 99% believability between libraries with a comparison (Stekel et al., 2000). Cross-species comparisons were specifically performed via PAVE annotation software and custom scripts, and only between EST collections of similar size and sequencing methodology. The results of these comparisons are summarized in Supplemental Tables S5 to S7, and the results of the assemblies and comparisons can be viewed at www.agcol.arizona.edu/pave/*Solanum*. EC annotation of the contents of all available *Solanum* trichome metabolic pathways were pictorially reconstructed using the iPATH software (Letunic et al., 2008), which can be accessed at http://pathways.embl.de.

Supplemental data from this article can be accessed online at http://www.plantphysiol.org/cgi/content/full/pp.110.167114/DC1

Sequence data from this article can be found in the GenBank EST and Sequence Read Archives under accession numbers GT157943 to GT161597, GT162273 to GT165033, GT166527 to GT168680, GT168709 to GT183821, SRR015435, SRR015436, and SRR027939 to SRR027943.

Literature Cited

Alba JM, Montserrat M and Fernández-Muñoz R (2009) Resistance to the two-spotted spider mite (Tetranychus urticae) by acylsucroses of wild tomato (Solanum pimpinellifolium) trichomes studied in a recombinant inbred line population. Exp Appl Acarol **47:** 35–47

Allen DK, Ohlrogge JB and Shachar-Hill Y (2009) The role of light in soybean seed filling metabolism. Plant J **58:** 220–234

Alonso AP, Goffman FD, Ohlrogge JB and Shachar-Hill Y (2007) Carbon conversion efficiency and central metabolic fluxes in developing sunflower (Helianthus annuus L.) embryos. Plant J **52:** 296–308

Alonso WR, Rajaonarivony JIM, Gershenzon J and Croteau R (1992) Purification of 4S-limonene synthase, a monoterpene cyclase from the glandular trichomes of peppermint (Mentha x piperita) and spearmint (Mentha spicata). J Biol Chem **267:** 7582–7587

Antonious GF (2001) Production and quantification of methyl ketones in wild tomato accessions. J Environ Sci Health B **36:** 835–848

Ben-Israel I, Yu G, Austin MB, Bhuiyan N, Auldridge M, Nguyen T, Schauvinhold I, Noel JP, Pichersky E and Fridman E (2009) Multiple biochemical and morphological factors underlie the production of methylketones in tomato trichomes. Plant Physiol **151:** 1952–1964

Besser K, Harper A, Welsby N, Schauvinhold I, Slocombe S, Li Y, Dixon RA and Broun P (2009) Divergent regulation of terpenoid metabolism in the trichomes of wild and cultivated tomato species. Plant Physiol **149:** 499–514

Biswas KK, Foster AJ, Aung T and Mahmoud SS (2009) Essential oil production: relationship with abundance of glandular trichomes in aerial surface of plants. Acta Physiol Plant **31:** 13–19

Chain F, Ilieva D and Evans B (2008) Single-species microarrays and comparative transcriptomics. PLoS ONE **3:** e3279

Chao WS, Serpe MD, Anderson JV, Gesch RW and Horvath DP (2006) Sugars, hormones, and environment affect the dormancy status in underground adventitious buds of leafy spurge (Euphorbia esula). Weed Sci **54:** 59–68

Croteau R (1991) Metabolism of monoterpenes in mint (Mentha) species. Planta Med (Suppl) **57:** S10–S14

Deschamps C, Gang D, Dudareva N and Simon JE (2006) Developmental regulation of phenylpropanoid biosynthesis in leaves and glandular trichomes of basil (Ocimum basilicum L.). Int J Plant Sci **167:** 447–454

Economou LP, Lykouressis DP and Barbetaki AE (2006) Time allocation of activities of two heteropteran predators on the leaves of three tomato cultivars with variable glandular trichome density. Environ Entomol **35:** 387–393

Franceschi VR and Giaquinta RT (1983) Glandular trichomes of soybean leaves: cytological differentiation from initiation through senescence. Bot Gaz **144:** 175–184

Fridman E, Wang JH, Iijima Y, Froehlich JE, Gang DR, Ohlrogge J and Pichersky E (2005) Metabolic, genomic, and biochemical analyses of glandular trichomes from the wild tomato species Lycopersicon hirsutum identify a key enzyme in the biosynthesis of methylketones. Plant Cell **17:** 1252–1267

Gang DR, Wang JH, Dudareva N, Nam KH, Simon JE, Lewinsohn E and Pichersky E (2001) An investigation of the storage and biosynthesis of phenylpropenes in sweet basil. Plant Physiol **125:** 539–555

Gershenzon J, McCaskill D, Rajaonarivony JIM, Mihaliak C, Karp F and Croteau R (1992) Isolation of secretory cells from plant glandular trichomes and their use in biosynthetic studies of monoterpenes and other gland products. Anal Biochem **200:** 130–138

Gilad Y, Pritchard JK and Thornton K (2009) Characterizing natural variation using next-generation sequencing technologies. Trends Genet **25:** 463–471

Giuliani C and Bini LM (2008) Insight into the structure and chemistry of glandular trichomes of Labiatae, with emphasis on subfamily Lamioideae. Plant Syst Evol **276:** 199–208

Goffman FD, Ruckle M, Ohlrogge J and Shachar-Hill Y (2004) Carbon dioxide concentrations are very high in developing oilseeds. Plant Physiol Biochem 42: 703–708

Gonzalez WL, Negritto MA, Suarez LH and Gianoli E (2008) Induction of glandular and non-glandular trichomes by damage in leaves of Madia sativa under contrasting water regimes. Acta Oecologica **33:** 128–132

Gunnewich N, Page JE, Kollner TG, Degenhardt J and Kutchan TM (2007) Functional expression and characterization of trichome-specific (–)-limonene synthase and (+)-alpha-pinene synthase from Cannabis sativa. Natural Product Communications **2:** 223–232

Horgan FG, Quiring DT, Lagnaoui A and Pelletier Y (2007) Variable responses of tuber moth to the leaf trichomes of wild potatoes. Entomol Exp Appl **125:** 1–12

Iijima Y, Gang DR, Fridman E, Lewinsohn E and Pichersky E (2004) Characterization of geraniol synthase from the peltate glands of sweet basil. Plant Physiol **134:** 370–379

Junker BH, Lonien J, Heady LE, Rogers A and Schwender J (2007) Parallel determination of enzyme activities and in vivo fluxes in Brassica napus embryos grown on organic or inorganic nitrogen source. Phytochemistry **68**: 2232–2242

Kandra L and Wagner GJ (1988) Studies of the site and mode of biosynthesis of tobacco trichome exudate components. Arch Biochem Biophys **265:** 425–432

Kang JH, Shi F, Jones AD, Marks MD and Howe GA (2010) Distortion of trichome morphology by the hairless mutation of tomato affects leaf surface chemistry. J Exp Bot **61:** 1053–1064

Kapteyn J, He R, McDowell ET and Gang DR (2010) Incorporation of non-natural nucleotides into template-switching oligonucleotides reduces background and improves cDNA synthesis from very small RNA samples. BMC Genomics **11:** 413

Keene CK and Wagner GJ (1985) Direct demonstration of duvatrienediol biosynthesis in glandular heads of tobacco trichomes. Plant Physiol **79:** 1026–1032

Kennedy GG (2003) Tomato, pests, parasitoids, and predators: tritrophic interactions involving the genus Lycopersicon. Annu Rev Entomol **48:** 51–72

Kim ES and Mahlberg PG (1991) Secretory cavity development in glandular trichomes of Cannabis sativa L. (Cannabaceae). Am J Bot **78:** 220–229

Kolb D and Muller M (2003) Different trichome types on the leaves of Styrian oil pumpkin. Phyton Ann Rei Bot **43:** 365–379

Kumar NKK, Ullman DE and Cho JJ (1995) Frankliniella occidentalis (Thysanoptera, Thripidae) landing and resistance to tomato spotted wilt tospovirus among Lycopersicon accessions with additional comments on Thrips tabaci (Thysanoptera, Thripidae) and Trialeurodes vaporariorum (Homoptera, Aleyrodidae). Environ Entomol **24:** 513–520

Lange BM, Wildung MR, Stauber EJ, Sanchez C, Pouchnik D and Croteau R (2000) Probing essential oil biosynthesis and secretion by functional evaluation of expressed sequence tags from mint glandular trichomes. Proc Natl Acad Sci USA **97:** 2934–2939

Letunic I, Yamada T, Kanehisa M and Bork P (2008) iPath: interactive exploration of biochemical pathways and networks. Trends Biochem Sci **33:** 101–103

Lin SYH, Trumble JT and Kumamoto J (1987) Activity of volatile compounds in glandular trichomes of Lycopersicon species against 2 insect herbivores. J Chem Ecol **13:** 837–850

Liu J, Xia KF, Zhu JC, Deng YG, Huang XL, Hu BL, Xu XP and Xu ZF (2006) The nightshade proteinase inhibitor IIb gene is constitutively expressed in glandular trichomes. Plant Cell Physiol **47:** 1274–1284

Luckwill LC (1943) The Genus Lycopersicon: An Historical, Biological and Taxonomic Survey of the Wild and Cultivated Tomatoes. Aberdeen University Press, Aberdeen, UK

Maluf WR, Inoue IF, Ferreira R, Gomes LAA, de Castro EM and Cardoso MDG (2007) Higher glandular trichome density in tomato leaflets and repellence to spider mites. Pesquisa Agropecu Bras **42:** 1227–1235

Marks MD, Tian L, Wenger JP, Omburo SN, Soto-Fuentes W, He J, Gang DR, Weiblen GD and Dixon RA (2009) Identification of candidate genes affecting Delta9-tetrahydrocannabinol biosynthesis in Cannabis sativa. J Exp Bot **60:** 3715–3726

Martins Santana F, Ribeiro SD, Moita AW, Moreira DJ and Giordano LD (2001) Sources of resistance in Lycopersicon spp. to a bipartite whitefly-transmitted geminivirus from Brazil. Euphytica **122:** 45–51

McCaskill D and Croteau R (1995) Monoterpene and sesquiterpene biosynthesis in glandular trichomes of peppermint (Mentha x piperita) rely exclusively in plastid-derived isopentenyl diphosphate. Planta **197:** 49–56

McCaskill D, Gershenszon J and Croteau R (1992) Morphology and monoterpene biosynthetic capabilities of secretory cell clusters isolated from glandular trichomes of peppermint (Mentha x piperita). Planta **187:** 445–454

Medeiros AH and Tingey WM (2006) Glandular trichomes of Solanum berthaultii and its hybrids with Solanum tuberosum affect nymphal emergence, development, and survival of Empoasca fabae (Homoptera: Cicadellidae). J Econ Entomol **99:** 1483–1489

Moyano F, Cocucci A and Sersic A (2003) Accessory pollen adhesive from glandular trichomes on the anthers of Leonurus sibiricus L. (Lamiaceae). Plant Biol **5:** 411–418

Nagel J, Culley LK, Lu YP, Liu EW, Matthews PD, Stevens JF and Page JE (2008) EST analysis of hop glandular trichomes identifies an O-methyltransferase that catalyzes the biosynthesis of xanthohumol. Plant Cell **20:** 186–200

Nielsen MT, Akers CP, Jarlfors UE, Wagner GJ and Berger S (1991) Comparative ultrastructural features of secreting and nonsecreting glandular trichomes of 2 genotypes of Nicotiana tabacum L. Bot Gaz **152:** 13–22

Nihoul P (1993) Do light-intensity, temperature and photoperiod affect the entrapment of mites on glandular hairs of cultivated tomatoes. Exp Appl Acarol **17:** 709–718

Nonomura T, Xu L, Wada M, Kawamura S, Miyajima T, Nishitomi A, Kakutani K, Takikawa Y, Matsuda Y and Toyoda H (2009) Trichome exudates of Lycopersicon pennellii form a chemical barrier to suppress leaf-surface germination of Oidium neolycopersici conidia. Plant Sci **176:** 31–37

Oghiakhe S (1997) Trichomes and resistance to major insect pests in cowpea, Vigna unguiculata (L.) Walp.: a review. Discov Innov **9:** 173–178

Ooi LSM, Tian L, Su MX, Ho WS, Sun SSM, Chung HY, Wong HNC and Ooi VEC (2008) Isolation, characterization, molecular cloning and modeling of a new lipid transfer protein with antiviral and antiproliferative activities from Narcissus tazetta. Peptides **29:** 2101–2109

Peralta IE and Spooner DM (2001) Granule-bound starch synthase (GBSSI) gene phylogeny of wild tomatoes (Solanum L. section Lycopersicon [Mill.] Wettst. subsection Lycopersicon). Am J Bot **88:** 1888–1902

Pico B, Diez M and Nuez F (1998) Evaluation of whitefly-mediated inoculation techniques to screen Lycopersicon esculentum and wild relatives for resistance to Tomato yellow leaf curl virus. Euphytica **101:** 259–271

Puterka GJ, Farone W, Palmer T and Barrington A (2003) Structure-function relationships affecting the insecticidal and miticidal activity of sugar esters. J Econ Entomol **96:** 636–644

Rios-Estepa R, Turner GW, Lee JM, Croteau RB and Lange BM (2008) A systems biology approach identifies the biochemical mechanisms regulating monoterpenoid essential oil composition in peppermint. Proc Natl Acad Sci USA **105:** 2818–2823

Rodriguez AE, Tingey WM and Mutschler MA (1993) Acylsugars of Lycopersicon pennellii deter settling and feeding of the green peach aphid (Homoptera, Aphididae). J Econ Entomol **86:** 34–39

Romero GQ, Souza JC and Vasconcellos-Neto J (2008) Anti-herbivore protection by mutualistic spiders and the role of plant glandular trichomes. Ecology **89:** 3105–3115

Sallaud C, Rontein D, Onillon S, Jabès F, Duffé P, Giacalone C, Thoraval S, Escoffier C, Herbette G, Leonhardt N, (2009) A novel pathway for sesquiterpene biosynthesis from Z,Z-farnesyl pyrophosphate in the wild tomato Solanum habrochaites. Plant Cell **21:** 301–317

Schilmiller AL, Schauvinhold I, Larson M, Xu R, Charbonneau AL, Schmidt A, Wilkerson C, Last RL and Pichersky E (2009) Monoterpenes in the glandular trichomes of tomato are synthesized from a neryl diphosphate precursor rather than geranyl diphosphate. Proc Natl Acad Sci USA **106:** 10865–10870

Schwab B, Folkers U, Ilgenfritz H and Hulskamp M (2000) Trichome morphogenesis in Arabidopsis. Philos Trans R Soc Lond B Biol Sci **355:** 879–883

Shimodaira H (2002) An approximately unbiased test of phylogenetic tree selection. Syst Biol **51:** 492–508

Shimodaira H (2004) Approximately unbiased tests of regions using multistep-multiscale bootstrap resampling. Ann Stat **32:** 2616–2641

Siebert DJ (2004) Localization of salvinorin A and related compounds in glandular trichomes of the psychoactive sage, Salvia divinorum. Ann Bot (Lond) **93:** 763–771

Simmons AT and Gurr GM (2005) Trichomes of Lycopersicon species and their hybrids: effects on pests and natural enemies. Agric For Entomol **7:** 265–276

Simmons AT, Gurr GM, McGrath D, Nicol HI and Martin PM (2003) Trichomes of Lycopersicon spp. and their effect on Myzus persicae (Sulzer) (Hemiptera: Aphididae). Aust J Entomol **42:** 373–378

Slocombe SP, Schauvinhold I, McQuinn RP, Besser K, Welsby NA, Harper A, Aziz N, Li Y, Larson TR, Giovannoni J, et al (2008) Transcriptomic and reverse genetic analyses of branched-chain fatty acid and acyl sugar production in Solanum pennellii and Nicotiana benthamiana. Plant Physiol **148:** 1830–1846

Snyder JC, Simmons AM and Thacker RR (1998) Attractancy and ovipositional response of adult Bemisia argentifolii (Homoptera: Aleyrodidae) to type IV trichome density on leaves of Lycopersicon hirsutum grown in three day-length regimes. J Entomol Sci **33:** 270–281

Soderlund CA, Johnson E, Bomhoff M and Descour A (2009) PAVE: program for assembling and viewing ESTs. BMC Genomics **10:** 400

Stekel DJ, Git Y and Falciani F (2000) The comparison of gene expression from multiple cDNA libraries. Genome Res **10:** 2055–2061

Torres-Schumann S, Godoy JA and Pintor-Toro JA (1992) A probable lipid transfer protein gene is induced by NaCl in stems of tomato plants. Plant Mol Biol **18:** 749–757

Turner GW and Croteau R (2004) Organization of monoterpene biosynthesis in Mentha: immunocytochemical localizations of geranyl diphosphate synthase,

limonene-6-hydroxylase, isopiperitenol dehydrogenase, and pulegone reductase. Plant Physiol **136:** 4215–4227

Turner GW, Gershenzon J and Croteau RB (2000) Development of peltate glandular trichomes of peppermint. Plant Physiol **124:** 665–680

UniProt Consortium (2010) The Universal Protein Resource (UniProt) in 2010. Nucleic Acids Res **38:** D142–D148

Valkama E, Salminen JP, Koricheva J and Pihlaja K (2003) Comparative analysis of leaf trichome structure and composition of epicuticular flavonoids in Finnish birch species. Ann Bot (Lond) **91:** 643–655

Van Dam NM and Hare JD (1998) Biological activity of Datura wrightii glandular trichome exudate against Manduca sexta larvae. J Chem Ecol **24:** 1529–1549

Wagner GJ (1991) Secreting glandular trichomes: more than just hairs. Plant Physiol **96:** 675–679

Wang GD, Tian L, Aziz N, Broun P, Dai XB, He J, King A, Zhao PX and Dixon RA (2008) Terpene biosynthesis in glandular trichomes of hop. Plant Physiol **148:** 1254–1266

Wang W, Wang YJ, Zhang Q, Qi Y and Guo DJ (2009) Global characterization of Artemisia annua glandular trichome transcriptome using 454 pyrosequencing. BMC Genomics **10:** 465

Weston PA, Johnson DA, Burton HT and Snyder JC (1989) Trichome secretion composition, trichome densities, and spider-mite resistance of 10 accessions of Lycopersicon hirsutum. J Am Soc Hortic Sci **114:** 492–498

Wilkens RT, Shea GO, Halbreich S and Stamp NE (1996) Resource availability and the trichome defenses of tomato plants. Oecologia **106:** 181–191

Xie Z, Kapteyn J and Gang DR (2008) A systems biology investigation of the MEP/terpenoid and shikimate/phenylpropanoid pathways points to multiple levels of metabolic control in sweet basil glandular trichomes. Plant J **54:** 349–361

Xie Z, Ma XQ and Gang DR (2009) Modules of co-regulated metabolites in turmeric (Curcuma longa) rhizome suggest the existence of biosynthetic modules in plant specialized metabolism. J Exp Bot **60:** 87–97

Yerger EH, Grazzini RA, Hesk D, Cox-Foster DL, Craig R and Mumma RO (1992) A rapid method for isolating glandular trichomes. Plant Physiol **99:** 1–7

Yu HF, Kowalski SP and Steffens JC (1992) Comparison of polyphenol oxidase expression in glandular trichomes of Solanum and Lycopersicon species. Plant Physiol **100:** 1885–1890

Zhang XM, Thacker RR and Snyder JC (2008) Occurrence of 2,3-dihydrofarnesoic acid, a spidermite repellent, in trichome secretions of Lycopersicon esculentum x L. hirsutum hybrids. Euphytica **162:** 1–9

Chapter 3

Polymethylated Myricetin in Trichomes of the Wild Tomato Species *Solanum habrochaites* and Characterization of Trichome-specific 3′/5′ and 7/4′ Myricetin *O*-methyltransferases

Schmidt A, Li C, Shi F, Jones AD, Pichersky E (2011) Polymethylated myricetin in the trichomes of the wild tomato species *Solanum habrochaites* and characterization of trichome-specific 3′/5′ - and 7/4′ -myricetin *O*-methyltransferases. Plant Physiology **155:** 1999-2009

Abstract

Flavonoids are a class of metabolites found in many plant species. They have been reported to serve several physiological roles such as in defense against herbivores and pathogens, and in protection against harmful UV radiation. They also serve as precursors of pigment compounds found in flowers, leaves, and seeds. Highly methylated derivatives of myricetin, a flavonoid, have been previously reported from a variety of plants, but an *O*-methyltransferase responsible for their synthesis have not yet been identified. Here we show that secreting glandular trichomes (designated type 1 and 4) and storage glandular trichomes (type 6) on the leaf surface of wild tomato (*Solanum habrochaites* acc. LA1777) plants contain 3,7,3′-trimethyl myricetin, 3,7,3′,5′-tetramethyl myricetin, and 3,7,3′,4′,5′-pentamethyl myricetin, with gland types 1 and 4 containing several fold more of these compounds than type 6 glands and with the tetramethylated compound predominating in all three gland types. We have also identified transcripts of two genes expressed in the glandular trichomes, designated *ShMOMT1* and *ShMOMT2*, and showed that they encode enzymes capable of methylating myricetin at the 3′ and 5′ and the 7 and 4′ positions, respectively. Both genes are preferentially expressed in

secreting glandular trichome types 1 and 4, and to a lesser degree in storage trichome type 6, and ShMOMT1 and ShMOMT2 protein levels are correspondingly higher in type 1 and 4 glands compared with type 6 glands.

Introduction

Flavonoids constitute a large and structurally diverse family of metabolites synthesized in plants. The core structure of flavonoids is either a 2-phenylchromen-4-one (flavonoids), 3-phenylchromen-4-one (isoflavonoids), or 4-phenylcoumarin (neoflavonoids). The great structural diversity of flavonoids stems from the possible substitution on up to 10 carbons of the core structure. Some common functional group substitutions include hydroxylation, methylation, sulfonation, methylation, and (iso)prenylation (Ibrahim and Anzellotti, 2003). In addition to these core substitutions, hydroxyl functional groups can be further modified by the addition of a wide range of different sugar moieties, which can be further modified themselves. Current estimates of the number of structurally distinct, plant-derived, flavonoids probably exceed 9,000 (Williams and Grayer, 2004). This rich structural diversity extends well into the functional diversity of flavonoids. They play crucial roles in plants in pathogen and herbivore defense, protection from harmful UV radiation, pigmentation of flowers, fruits and seeds. They also act as plant-microbe signaling molecules, inhibitors in biochemical pathways, and developmental regulators (reviewed in Buer et al., 2010; Taylor and Grotewold, 2005; Treutter, 2005).

The flavonoid pathway in flowering plants can be traced back to the first plants to colonize land. The most primitive form of the pathway probably terminated at the production of flavonols (Rausher, 2008). Dihydroflavonols, the reduced forms of flavonols, represent an important step in the evolution of the structural and functional diversity of flavonoids seen in extant flowering plants. All anthocyanins, flavonols, and derivatives of these come from one of the three dihydroflavonols - dihydrokaempferol, dihydroquercetin, and dihydromyricetin - the latter being the most highly substituted, with hydroxyl groups on the 3, 5, 7, 3′, 4′ and 5′ carbons. The enzyme flavonol synthase (FLS) converts the dihydroflavonoids to their corresponding flavonols; kaempferol, quercetin, and myricetin, by oxidation of the C2-C3 bond of the C ring **(Figure 1)**.

In plants that synthesize methylated and glycosylated derivatives of myricetin, levels of unmodified myricetin are generally very low or not detectable (Stevens et al., 1995 and 1996; Kumar et al., 2009; Michodjehoun-Mestres et al., 2009; Riihinen et al., 2008; Reynertson et al., 2008). Methylation has been reported at 5 of the 6 available

hydroxyl groups: C3 (C ring), C7 (A ring), and C-3′, -4′, and -5′ of the B ring, but not on the C5 (A Ring), from a variety of different families of flowering plants (Stevens et al., 1995; Kumari et al., 1984; Jung et al., 2003; Jay et al., 1980). Glycosylation of myricetin occurs consistently at C3 of the C ring, and appears to be reversible *in vitro* (Modolo et. al., 2009; Singh et al., 2009; Kumari et al., 1984; Gerats et al., 1983). Glycosylation renders the flavonoids more water-soluble and facilitates transport into the vacuole, where they are often stored (reviewed in Vogt and Jones, 2000). Myricetin, myricetin methyl ethers, and 3-*O*-glycosylated myricetin derivatives have been reported in leaf tissues (Braca et al., 2001; Oliveira et al., 2007; Lee et al., 2006; Motta et al., 2005), fruits (Riihinen et. al., 2008; Gorbatsova et al., 2007; Lako et al., 2007; Le et al., 2007), flowers (Kumar et. al., 2008; Wu et al., 2008; Liu et al., 2008; Tabart et al., 2006), stems and bark (Min et al., 2003), and in roots (Ojong et al., 2008).

In plants that synthesize highly methylated flavonols, the process occurs in a stepwise manner with *O*-methylation at position 3 being the first step in the process (Huang et al., 2004; Ibrahim et al., 1987; Thresh and Ibrahim, 1985; Macheix and Ibrahim, 1984). In *Chrysosplenium americanum*, methylation of quercetin (Q) proceeds from 3-methylquercetin (3-MeQ) to 3,7-MeQ to 3,7,4′-MeQ. Several species of the genus *Aeonium* accumulate highly methylated quercetin and myricetin. In these species the methylation pattern appears to follow the same stepwise addition of methyl groups beginning with position 3. The myricetin methyl ethers that accumulate in the leaves include 3,7,3′-trimethylmyricetin, 3,7,3′,4′-tetramethylmyricetin, and 3,7,3′,4′,5′-pentamethylmyricetin (Stevens et al., 1995). To date an enzyme responsible for the synthesis of polymethylated myricetin in these species has not been identified. An

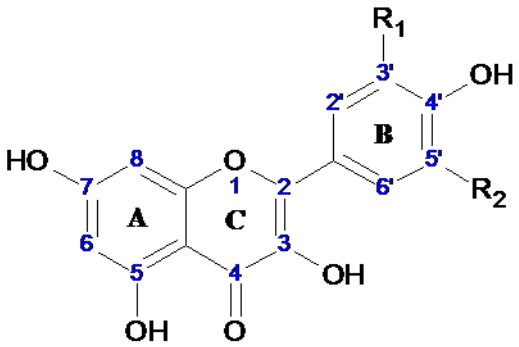

Kaempferol (R1 = R2 = H)
Quercetin (R1 = OH, R2 = H)
Myricetin (R1 = R2 = OH)

Figure 3.1. Generic flavonol structure showing the lettering system for the three rings and the numbering system for the carbons. Addition of hydroxyl groups at the 3′ position or 3′ and 5′ positions designate quercetin and myricetin, respectively.

enzyme isolated from *Catharanthus roseus* was shown to methylate free myricetin *in vitro*, and this reaction was hypothesized to occur *in vivo* prior to the further modifications of myricetin into the anthocyanins observed in the plant, but analysis of the kinetic parameters of the enzyme was not reported (Cacace et al. 2003).

Glandular trichomes are specialized storage and secreting organs that develop on the surface of areal parts of a wide variety of different plant species (Wagner, 1991; Schilmiller et al., 2008). They synthesize, store, and secrete specialized metabolites important to plant defense, and serve as the major source of essential oils (Ambrsio et al., 2008; Iijima et al., 2004; Croteau et al., 2005). They are a valuable resource for elucidating specialized biochemical pathways because they are biochemically highly active in select pathways, metabolite accumulation is species-specific, and their metabolites and gene transcripts can be easily extracted and analyzed (Schilmiller et al., 2008 and 2010). In the *Solanum* genus, glandular trichomes can be divided into two main groups, secreting glands and storage glands (Luckwill, 1943; Schilmiller et al., 2010). The secreting glands (of which there are two types, 1 and 4, with type 4 being shorter) are supported atop a relatively long multicellular stalk that varies in length, and the gland itself appears to be unicellular. Droplets rich in specialized metabolites are often observed on the surface of these glands or on the stalk near the gland. The storage glands, defined as type 6 glands, are multicellular and sit atop a relatively short multicellular stalk. The storage glands consist of four cells arranged such that each makes up one quarter of the round structure.

Here we report the identification of polymethylated myricetin from isolated types 1, 4 and 6 glandular trichomes from the wild tomato *Solanum habrochaites*. We also report the identification and the biochemical characterization of two myricetin *O*-methyltransferases encoded by transcripts found in the *Solanum habrochaites* glandular trichomes, and show that one of them, ShMOMT1, is likely responsible for *O*-methylation of the 3′ and 5′ hydroxyl groups and the second, ShMOMT2, is likely responsible for *O*-methylation of the 7 and 4′ hydroxyl groups.

Glandular trichomes of *Solanum habrochaites* (accession LA1777) contain methylated, non-glycosylated, myricetin

In an initial screen for flavonoids present in leaves of *Solanum habrochaites* (accession LA1777), whole leaves were ground and extracted with MTBE, and the extract analyzed by LC/MS. This analysis revealed that the leaves contain several glycosylated flavonoids, mostly kaempferol diglucoside but also rutin and quercerin diglucoside **(Figure 2)**. In addition, several non-glycosylated flavonoids were detected, including 3,7,3′- trimethyl myricetin (3,7,3′-MeM), 3,7,3′,5′- tetramethyl myricetin (3,7,3′,5′-MeM), 3,7,3′,4′,5′- pentamethyl myricetin (3,7,3′,4′,5′-MeM), and 3- methyl quercetin (3-MeQ) **(Figure 2)**. When the trichomes were physically removed before the leaves were extracted, the levels of kampferol diglucoside, rutin, quercetin diglucoside, and 3-MeQ detected remained similar, but no 3,7,3′-MeM, 3,7,3′,5′-MeM, and

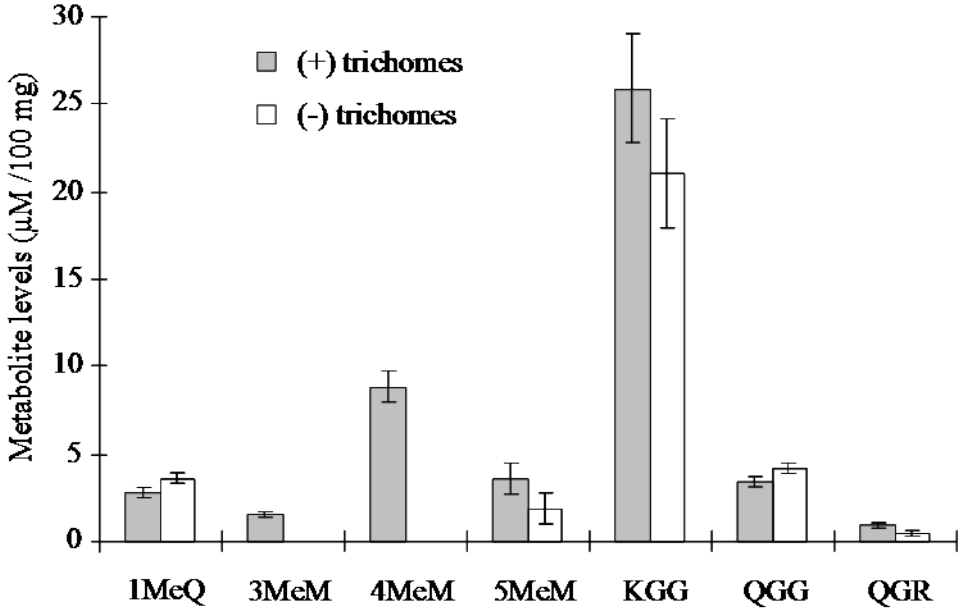

Figure 3.2. Levels of flavonoid compounds extracted from *S. habrochaites* leaf with trichomes and with trichomes removed. Flavonoid compounds detected were: 3-methyl quercetin (1MeQ), 3,7,3′-trimethyl myricetin (3MeM), 3,7,3′,5′-tetramethyl myricetin (4MeM), 3,7,3′,4′,5′-pentamethyl myricetin (5MeM), kaempferol diglucoside (KGG), quercetin diglucoside (QGG), and rutin (QGR). Results are averages of 3 biological replicates +/- SE.

approximately half the levels of 3,7,3′,4′,5′-MeM, were detected, suggesting that these compounds were completely or mostly located in the trichomes **(Figure 2)**.

To examine the relative distribution of the non-glycosylated myricetins in specific types of trichomes, secreting glands and storage glands were collected individually from leaves of *Solanum habrochaites* for metabolic profiling **(Figure 3 and Supplemental Figure 1)**. Secreting glands (types 1 and 4) contained higher levels per gland of all three methylated myricetins compared to storage glands (type 6). Levels of myricetin tetramethyl ether (3,7,3′,5′-MeM) were greatest in both secreting and storage gland types compared to the myricetin trimethyl ether (3,7,3′-MeM) and myricetin pentamethyl ether (3,7,3′,4′,5′-MeM). However, the levels of all myricetin methyl ethers were 5 to 6 fold greater in secreting type 1 and 4 glands compared to the corresponding levels in storage glands. Also, in secreting glands the levels of myricetin pentamethyl ether were slightly higher than levels of myricetin trimethyl ether, whereas in storage glands levels of the tri- and penta-methylated myricetins were not significantly different.

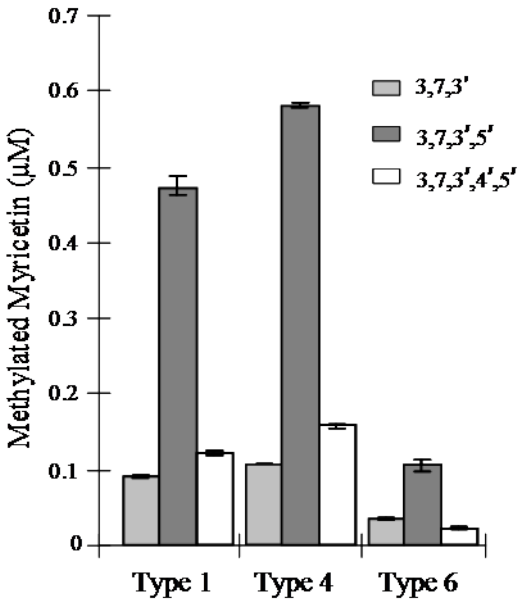

Figure 3.3. Levels of *O*-methylated myricetin compounds measured in extracts from 50 glandular trichomes from *S. habrochaites* leaf. *O*-Methylated myricetin compounds detected were: (3,7,3')-trimethyl myricetin; (3,7,3',5')- tetramethyl myricetin; (3,7,3',4',5')- pentamethyl myricetin. Results are averages of 3 biological replicates +/- SE.

Characterization of substrate specificity of ShMOMT1 and ShMOMT2

We have recently constructed EST libraries from the secreting and storage glands (types 1, 4, and type 6, respectively) of *Solanum habrochaites* leaves (http://www.trichome.msu.edu/; McDowell et al., 2011). A bioinformatics search of these

libraries using BLAST sequence comparisons with known *O*-methyltransferase (OMT) sequences identified three OMT sequences in *S. habrochaites* trichomes. All three cDNAs were expressed in *E. coli* and the crude extracts were tested for OMT activity with a battery of substrates **(Table I)** and [methyl-^{14}C]-S-adenosyl-L-methionine ([^{14}C]-SAM) as the methyl donor. One cDNA encoded a protein with similarity to plant *N*-methyltransferases and had no methylating activity with myricetin, quercetin, kaempferol, or any other flavonol tested in this investigation (see **Table I** for list of tested compounds). Consequently, it was not investigated further. A second cDNA encoded a protein, subsequently named ShMOMT1, with methylating activity toward myricetin and quercetin but not kaempferol, suggesting that this protein has 3′/5′ *O*-methyltransferase activity. A third cDNA encoded a protein, subsequently named ShMOMT2, with methylating activity against all these three flavonols.

ShMOMT1 and ShMOMT2 were further tested with a range of substrates related to myricetin that could be obtained in sufficient concentrations for these assays. ShMOMT1 catalyzed the transfer of a methyl group to the 3′ hydroxyl of myricetin as indicated by co-migration with an authentic standard of 3′-methylmyricetin in radioactive thin-layer chromatography (RTLC) **(Supplemental Figure 2)** and by LC/MS **(Supplemental Figure 3)** (the 3′ and 5′ hydroxyl positions in this compound are equivalent, and by convention the product is designated as 3′-methyl myricetin, or laricitin) and the equivalent position of several other related compounds, including quercetin, 3-methyl quercetin, and 7-methyl quercetin (i.e. rhamnetin) **(Table I)**. When the 3′ hydroxyl of the substrate was already methylated, as in laricitin, ShMOMT1 transferred a methyl group to the 5′ hydroxyl, as determined by co-migration with an authentic standard of 3′,5′-methylmyricetin in RTLC and by LC/MS **(Table I and Supplemental Figures 2 and 3)**. When both 3′ and 5′ hydroxyls were already methylated, for example in the substrate 3′,5′-dimethyl myricetin (i.e. syringetin), ShMOMT1 could not transfer a methyl group to any other hydroxyl **(Table I)**.

ShMOMT2 transferred a methyl group to the 4′ hydroxyl of kaempferol, but to the 7 position of quercetin and myricetin **(Table I)**. When the hydroxyl at the 7 position was already methylated, it transferred a methyl to the 4′ hydroxyl (e.g. with substrate 7-methyl quercetin), and when the 4′ hydroxyl was already methylated, ShMOMT2

Table 3.I. **Relative activity of ShMOMT1 and ShMOMT2 with flavonol and *O*-methyl flavonol substrates[1].**

Substrate	Relative Activity[2](%)	ShMOMT1 Product	Relative Activity[2](%)	ShMOMT2 Product
Flavonols				
Kaempferol[3]	≤1	--	117	4′-methyl kaempferol
Quercetin[4]	51	3′-methyl quercetin	119	7-methyl quercetin
Myricetin[5]	100	3′-methyl myricetin	100	7-methyl myricetin[11]
O-methyl flavonols				
4′-methyl kaempferol[6]	≤ 1	—	105	7,4′-dimethyl kaempferol
3,7,4′-trimethyl kaempferol	≤ 1	—	3	--
3′-methyl quercetin[7]	≤ 1	—	23	3′,4′-dimethyl quercetin
3-methyl quercetin	61	3,3′-dimethyl quercetin	19	3,7-dimethyl quercetin
7-methyl quercetin[8]	70	7,3′-dimethyl quercetin	120	7,4′-dimethyl quercetin
3,7,3′,4′-tetramethyl quercetin	≤ 1	—	3	--
3′-methyl myricetin[9]	64	3′,5′-dimethyl myricetin	5	3′,4′-dimethyl myricetin
3′,5′-dimethyl myricetin[10]	≤ 1	—	11	7,3′,5′-trimethyl myricetin
3′,4′,5′ trimethyl myricetin	≤ 1	—	36	7,3′,4′,5′-tetramethyl myricetin

[1] Additional substrates tested include; caffeic acid, eugenol, isoeugenol, chavicol, orcinol, and several different flavones, isoflavones, and anthocyanidins. Substrate concentration was 200 μM, and incubation time was 30 min.
[2] 100% relative activity represents total methylating activity; ShMOMT1 3.4 nmol min^{-1} mg^{-1}, ShMOMT2 0.02 nmol min^{-1} mg^{-1}, of the recombinant proteins assayed with myricetin as substrate.
[3-5] Structures in figure 1.
[6] Kaempferide
[7] Isorhamnetin
[8] Rhamnetin
[9] Laricitrin
[10] Syringetin
[11] After overnight incubation (>10 h), the main product is 7, 4′-dimethylmyricetin.

transferred the methyl group to the hydroxyl at the 7 position (e.g. with the substrate 3′,4′,5′-trimethyl myrecitin). It did not transfer a methyl group to any hydroxyl other than at the 7 or 4′ position **(Table I)**. Radioactive thin-layer chromatography of the reaction with myricetin revealed a single product that migrated between myricetin and 3′-methyl myricetin **(Supplemental Figure 2)**. This product was identified by LC/MS as 7-methyl myricetin. When myricetin was incubated with ShMOMT2 overnight, the product obtained was 7, 4′- methyl myricetin **(Supplemental Figure 4)**.

The structural relatedness of ShMOMT1 and ShMOMT2 to other OMTs

The protein encoded by the *ShMOMT1* cDNA is 362 amino acids long, with a calculated molecular mass of 40.7 kD, and it contains all of the recognized plant OMT domains known or hypothesized to be involved in binding to SAM and metal cofactors (Ibrahim, 1997) (analysis not shown). ShMOMT1 is most similar (40-49% identity) to a number of mostly 3′ and 3′/5′ *O*-methyltransferases **(Figure 4)**, consistent with its regiospecificity for the 3′ and 5′ positions.

The protein encoded by the *ShMOMT2* cDNA is 355 amino acids long, with a calculated molecular mass of 39.4 kD, and it also contains all of the recognized plant OMT domains known or hypothesized to be involved in binding to SAM and metal cofactors (analysis not shown). ShMOMT2 is most similar (29-47% identity) to several *O*-methyltransferases identified (with one exception) as specific for the 7 and/or 4′ position **(Figure 4)**, consistent with its regiospecificity for these positions. ShMOMT2 is only 27% identical to ShMOMT1.

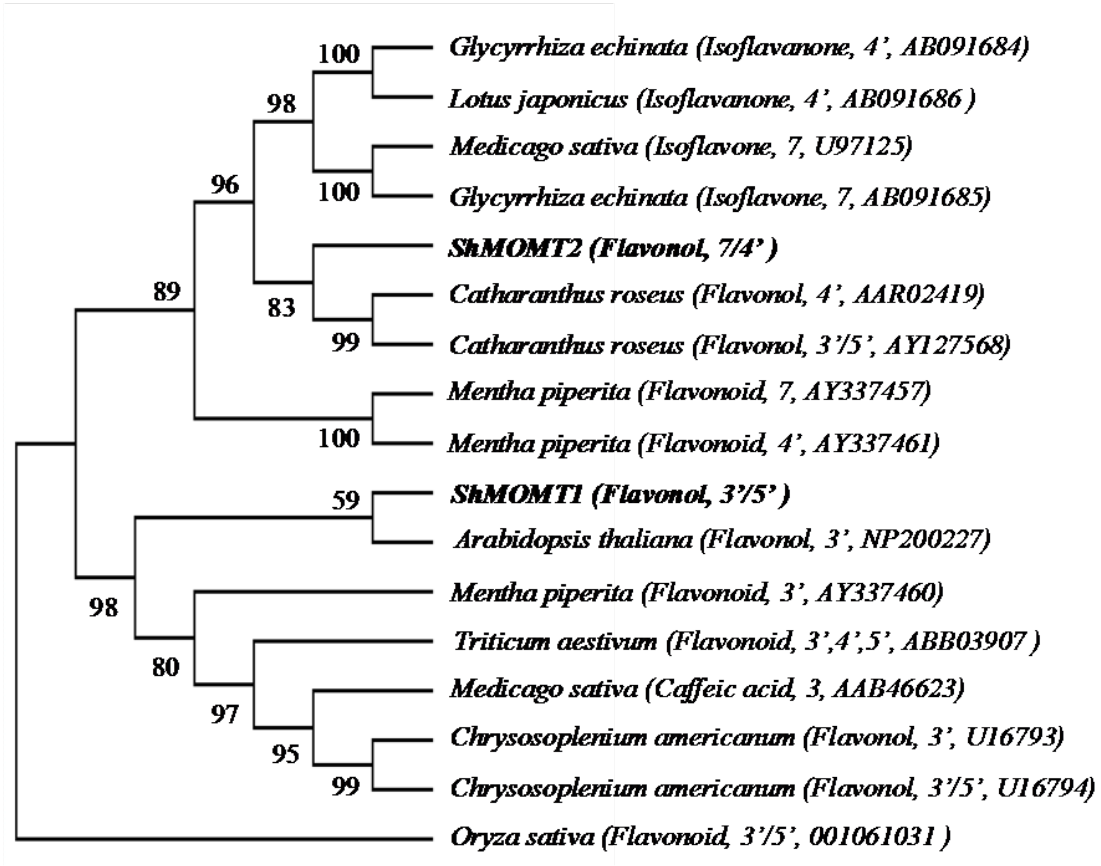

Figure 3.4. Analysis of the level of relatedness of the *ShMOMT1*-encoded protein and *ShMOMT2*-encoded protein to other plant *O*-methyltransferases. For each protein, descriptions in parentheses indicate the chemical class of the preferred substrate, the position(s) that are *O*-methylated by the enzyme, and the accession number of the sequence. The evolutionary history was inferred using the Neighbor-Joining method (Saitou and Nei, 1987). The percentage of replicate trees in which the associated taxa clustered together in the bootstrap test (1000 replicates) are shown next to the branches (Felsenstein, 1985). The evolutionary distances were computed using the Poisson correction method and are in the units of the number of amino acid substitutions per site (Zuckerkandl and Pauling, 1965). Phylogenetic analyses were conducted in MEGA4 (Tamura et al., 2007).

Distribution of ShMOMT1 and ShMOMT2 transcripts and protein in trichome glands

We used quantitative RT-PCR (qRT-PCR) and Western blot analyses to localize *ShMOMT1* and *ShMOMT2* transcript, and ShMOMT1 and ShMOMT2 proteins, respectively, in the different types of trichome glands. Extracts of collections of individual types of glands were compared to whole leaf extracts in both types of experiments. *ShMOMT1* transcript levels were 3.5 to 12.5 fold higher in secreting glands from types 4 and 1 trichomes, respectively, compared to storage glands of type 6 trichomes **(Figure 5)**. *ShMOMT2* transcript levels were 2 to 4 fold higher in secreting glands from types 4 and 1 trichomes, respectively, compared to storage glands of type 6 trichomes **(Figure 5)**. Comparison of transcript levels from leaf tissue with trichomes vs. leaf tissue from which the trichomes had been mechanically removed indicated that transcripts of both *ShMOMT1* and *ShMOMT2* are present exclusively in trichomes **(Figure 5)**. Protein blot analysis indicated that levels of ShMOMT1 protein were 7 to 8.6 fold higher in secreting glands compared to storage glands, and 1.9 to 2.4 fold higher compared to whole leaf extracts **(Figure 6)**. Levels of ShMOMT2 protein were 5 to 6.6 fold higher in secreting glands compared to storage glands, while ShMOMT2 was not detectable in whole leaf extracts **(Figure 6)**.

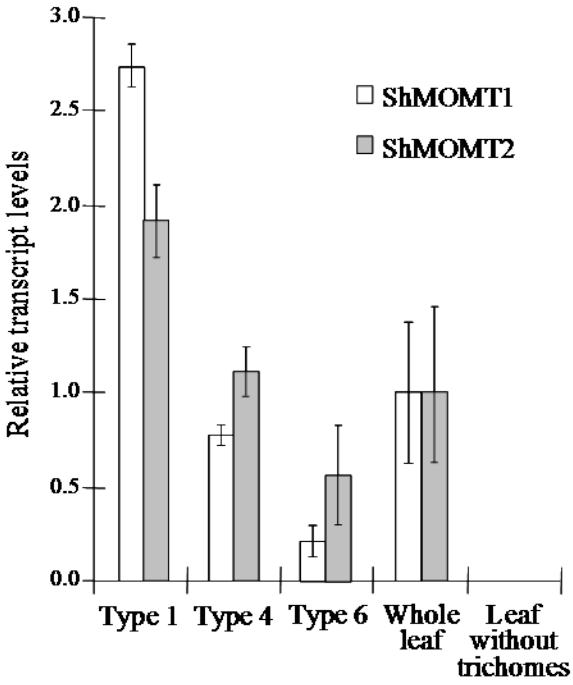

Figure 3.5. Relative levels of ShMOMT1 and ShMOMT2 transcript measured in trichomes, leaves, and leaves with trichomes removed by qRT-PCR. Results are averages of 3 biological replicates +/- SE.

Characterization of the kinetic parameters of ShMOMT1 and ShMOMT2

ShMOMT1 and *ShMOMT2* were expressed in *E. coli* BL21 (DE3) cells and the recombinant proteins were purified to near homogeneity by two successive anion exchange chromatography steps **(Figure 7)**. The purified ShMOMT1 protein catalyzed the formation of laricitrin (3′-methyl myricetin) from myricetin with an apparent K_m value of 0.46 µM and an apparent K_{cat} value of 1.59 s^{-1}. An apparent K_m value of 0.21 µM was measured for ShMOMT1 with laricitrin (giving the product syringetin, 3′,5′-dimethyl myricetin) as the substrate, with an apparent K_{cat} value of 0.45 s^{-1}. The apparent K_m value for SAM, with myricetin as co-substrate, was 16.64 µM with an apparent K_{cat} value of 0.47 s^{-1} **(Table II and Supplemental Figure 5)**.

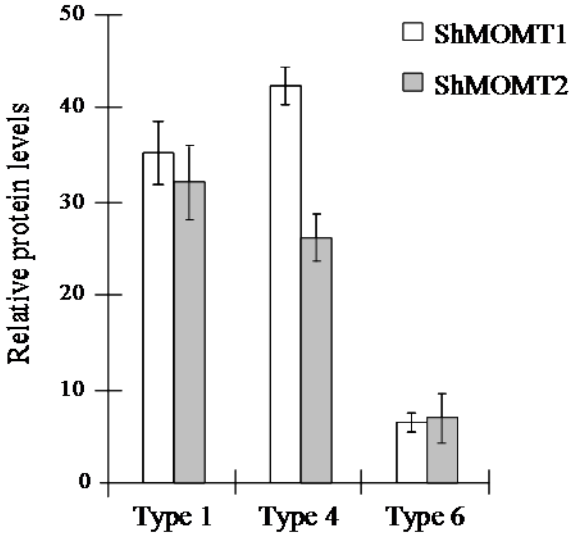

Figure 3.6. Relative levels of ShMOMT1 and ShMOMT2 protein measured in trichomes. Levels were determined by quantitative Western blot analysis with anti-ShMOMT1 or anti-ShMOMT2 and anti-α-tubulin. Results are averages of 3 biological replicates +/- SE.

Table 3.II. Kinetic parameters of ShMOMT1 with myricetin, laricitrin, and [^{14}C]-SAM as substrates. K_m and K_{cat} ± S.E. Values are averages of three assays.

Substrates	K_m (µM)	K_{cat} (s^{-1})	K_{cat}/K_m ($\mu M^{-1} s^{-1}$)
Myricetin[1]	0.46 ± 0.05	1.59 ± 0.15	3.46 ± 0.38
Laricitrin[2]	0.21 ± 0.04	0.45 ± 0.01	2.14 ± 0.27
SAM[3]	16.64 ± 2.10	0.47 ± 0.06	0.03 ± 4.0 x10^{-3}

[1]Structure in figure 1.
[2]3′- methyl myricetin.
[3]Adenosyl-L-methionine, S-[methyl-^{14}C]-

Purified ShMOMT2 catalyzed methylation of the 7 hydroxyl group of myricetin, the 7 hydroxyl group of kaempferide (4′-methyl kaempferol), and the 4′ hydroxyl group of rhamnetin (7-methyl quercetin). An apparent K_m of 1.68 µM was determined for myricetin with an apparent K_{cat} value of $7.4x10^{-3}$ s^{-1}. An apparent K_m of 2.27 µM was determined for kaempferide with an apparent K_{cat} value of $5.76x10^{-3}$ s^{-1}. And, an apparent K_m of 2.30 µM was determined for rhamnetin with an apparent K_{cat} value of $6.40x10^{-3}$ s^{-1}. The apparent K_m value for SAM with kaempferide as co-substrate was

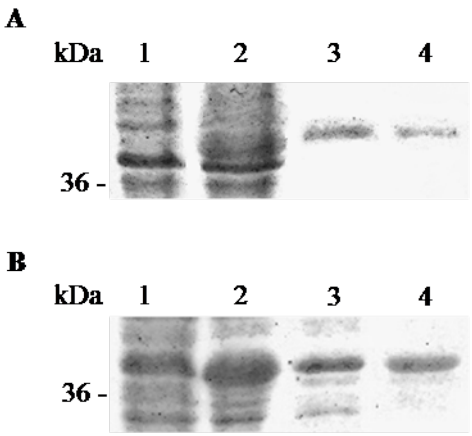

Figure 3.7. Purification of *E. coli*-produced ShMOMT1 (panel A) and ShMOMT2 (panel B). Lanes: 1, non-induced crude extract *E. coli* cells carrying the ShMOMT1 or ShMOMT2 expression vector but not induced with IPTG; 2, induced crude extract; 3, The fractions eluting from DE53 column (Panel A, 2 µg; Panel B, 10 µg) with the highest MOMT activity; 4, The fractions eluting from the HiTrapQ column (Panel A, 0.25 µg; Panel B, 5 µg) with the highest MOMT activity. SDS-PAGE visualized with Coomaise Brilliant Blue.

Table 3.III. Kinetic parameters of ShMOMT2 with myricetin, kaempferide, rhamnetin, and [^{14}C]-SAM as substrates. K_m and K_{cat} ± S.E. Values are averages of three assays.

Substrates	K_m (µM)	K_{cat} (s^{-1})	K_{cat}/K_m (μM^{-1} s^{-1})
Myricetin[1]	1.68 ± 0.23	$7.40x10^{3}$ ± $9.03x10^{4}$	$4.41x10^{3}$ ± $5.74x10^{4}$
4'-methylkaempferol[2]	2.27 ± 0.37	$5.76x10^{3}$ ± $8.89x10^{4}$	$2.53x10^{3}$ ± $3.27x10^{4}$
7-methylquercetin[3]	2.30 ± 0.20	$6.40x10^{3}$ ± $5.22x10^{4}$	$2.78x10^{3}$ ± $3.06x10^{4}$
SAM[4]	18.71 ± 2.51	$1.64x10^{2}$ ± $2.33x10^{3}$	$8.75x10^{4}$ ± $1.73x10^{4}$

[1]Structure in figure 1.
[2]Kaempferide
[3]Rhamnetin
[4]Adenosyl-L-methionine, S-[methyl-^{14}C]-

18.71 µM with an apparent K_{cat} value of $1.64x10^{-2}$ s^{-1} **(Table III and Supplemental Figure 6)**.

Characterization of optimal conditions for catalysis revealed that both ShMOMT1 and ShMOMT2 do not require the addition of Mg^{2+} or Mn^{2+} for activity. At levels below 2.5 mM, Mg^{2+} had little negative effect on activity (≤10%); however, concentrations above 2.5 mM had increasing inhibitory effects on activity with myricetin. Similarly, addition of Mn^{2+} to enzyme assays, using myricetin as substrate, had little negative effect (≤10%) on activity until levels exceeded 2.5 mM. ShMOMT1 activity with myricetin was observed in the pH range of 6.0-8.5 with optimal activity observed at pH 7.5. And, ShMOMT2 activity with myricetin was observed in the pH range of 6.0-9.0 with optimal activity observed at pH 8.0.

Discussion

Solanum habrochaites glandular trichomes contain methylated, non-glycosylated myricetin

Our metabolic profiling of trichome glands from *Solanum habrochaites* leaf identified three forms of *O*-methylated myricetin species: 3,7,3′-MeM, 3,7,3′,5′-MeM, and 3,7,3′,4′,5′-MeM. These three compounds have previously been shown to accumulate in tissues of several other plants (Stevens et al., 1995; Dachriyanus et al., 2003; Ariyanathan et al., 2010), but they have not yet been reported to be present in trichomes. By isolating individual types of glands, we were able to show that these compounds are found in three types of glandular trichomes – 1, 4, and 6 **(Figure 3)**, although they are most abundant in the secreting glands (types 1 and 4).

All of the myricetin methyl ethers that we detected in the glands of glandular trichomes were methylated at the 3 position (in the C ring). This position is often glycosylated, and the glycosylated form is then transported to the vacuole (Vogt and Jones, 2000). We did not find any glycosylated myricetin in the trichomes nor myricetin species that are not modified at the 3 position, suggesting that the 3-OMT responsible for this methylation reaction is quite efficient. However, our attempts to detect OMT activity in crude extracts of glands or whole leaves capable of adding a methyl group to the 3-hydroxyl position of myricetin was unsuccessful, nor could we identify a cDNA encoding such an enzyme in our EST databases. To our knowledge, no 3-OMTs capable of methylating myricetin or any other flavonols have been identified from any plant, although a cellular activity capable of methylating quercetin at the 3 position has been reported (De Luca and Ibrahim, 1985; Huang et al., 2004).

Our analyses of *S. habrochaites* leaves with trichomes and leaves with trichomes removed revealed that 3,7,3′-trimethyl myricetin and 3,7,3′,5′-tetramethyl myricetin were found in trichome gland cells only, and 3,7,3′,4′,5′-pentamethyl myricetin was found in both trichomes and the rest of the leaf organ **(Figure 2)**. All other flavonol compounds were apparently confined mostly to non-trichome leaf cells since their levels did not decrease significantly when trichomes were removed **(Figure 2**). The presence of 3,7,3′,4′,5′-pentamethyl myricetin, whose 3,7,3′,5′-tetramethyl myricetin precursor is

found only in the trichomes, outside the trichomes is most likely due to secretion, since our analysis indicates that *ShMOMT1* and *ShMOMT2* are not expressed in non-trichome leaf cells **(Figure 5)**.

ShMOMT1 is a 3′/5′ myricetin methyltransferase and ShMOMT2 is a 7 and 4′ myricetin methyltransferase

The characterization of the enzymatic properties of ShMOMT1 *in vitro* showed that it has high affinity for both myricetin and 3′-methyl myricetin, and its products are 3′-methyl myricetin (laricitrin) and 3′,5′-dimethyl myricetin (syringetin) **(Supplemental Figure 3)**. In previous studies, OMTs have been identified that can methylate myricetin at these positions, but in all such cases myricetin was not the best substrate for the enzyme and the tissue source of the enzyme did not actually contain methylated myricetin but only related compounds, such as quercetin, kaempferol, tricin, tricetin and luteolin (Muzac et al., 2000; Lee et al., 2008; Zhou et al., 2006). The catalytic efficiency of ShMOMT1 with both myricetin and laricitrin are significantly higher than for such 3′,5′-OMTs **(Table IV)**, and these enzymes had higher affinity to the substrates whose methylation led to the compounds actually observed in the plant.

Table 3.IV. **Kinetic parameters of ShMOMT1 with myricetin as a substrate compared with other 3′,5′-*O*-methyltransferase enzymes that exhibit activity with myricetin.**

Enzyme	K_m (μM)	K_{cat} (s^{-1})	K_{cat}/K_m ($\mu M^{-1} s^{-1}$)
ShMOMT1	0.46	1.59	3.46
AtOMT1[1]	3.38	0.01	3×10^{-3}
TaOMT2[2]	6.59	8.78	1.33
ROMT-17[3]	44	0.04	9×10^{-4}
ROMT-15[3]	80	0.22	2.74×10^{-3}

[1]Muzac et al., (2000).
[2]Zhou et al., (2006).
[3]Lee et al., (2008).

ShMOMT2 is most similar to some enzymes characterized as 4′ methyltransferases and some characterized as 7 methyltransferases, with one exception **(Figure 4)**. This exception is *Catharanthus roseus* flavonol 3′/5′ *O*-methyltransferase (Cacace et. al., 2003), which is very similar to *Cantharanthus roseus* flavonol 4′ *O*-methyltransferase (Schröder et. al., 2004) **(Figure 4)**, and may represent a recent case of gene duplication and divergence. When ShMOMT2 was incubated with kaempferol, a substrate missing both a 3′ and a 5′-hydroxyl, it added a methyl group to the 4′-hydroxyl **(Table I)**. However, with either quercetin or myricetin, ShMOMT2 initially added a methyl group to the 7-hydroxyl, suggesting that 3′ and/or 5′-hydroxyls might inhibit its activity with the 4′-hydroxyl. This is consistent with the observation that 3,7,3′-trimethyl myricetin is found in the glands, but no 3,3′,4′-trimethyl myricetin is observed **(Figure 3)**. Thus, it appears that after the 3-hydroxyl is methylated, the next hydroxyls to be methylated are at the 7 and 3′ position, although which of these two is methylated first cannot yet be resolved. This is also consistent with what has been shown in *Chrysosplenium americanum*, where methylation of quercetin proceeds first to 3-methylquercetin, then to 3,7-dimethyl quercetin (De Luca and Ibrahim, 1985). It can be deduced that the next hydroxyl to be methylated is at the 5′ position, since we see

accumulation of 3,7,3′,5′-tetra methyl myricetin but no 3,7,3′,4′-tetra methyl myricetin, and also because it appears that ShMOMT1 is not active with a substrate that has a methyl group at both the 3′,4′ positions **(Table I)**. ShMOMT2 clearly is capable of methylating the 4′-hydroxyl after it methylated the 7-hydroxyl (tested with 7-methyl quercetin for lack of 7-methyl myricetin, see **Table I**, and also by incubating myricetin with ShMOMT2 for an extended period (>10 h), after which the major product is 7,4′-myricetin **(Supplemental Figure 4)**). However, it seems to be less efficient at methylating the 4′ hydroxyl once the 3′ and/or the 5′ hydroxyls have been methylated **(Table I)**, consistent with the lower levels of 3,7,3′,4′,5′-pentamethyl myricetin observed in the trichomes.

A caveat for the kinetic analysis of ShMOMT1 and ShMOMT2 presented here is that, for lack of availability, we were not able to test them with 3-methylmyricetin or other combinations of polymethylated myricetin with one methyl group at the 3-position (for example, 3,7- dimethylmyricetin). However, we did obtain and test both enzymes with 3-methyl quercetin. The results with ShMOMT1 indicated that it had higher activity with the 3-methyl quercetin than with quercetin, although ShMOMT2 had lower activity **(Table I)**. It has been shown for many OMTs that they are regiospecific but not substrate-specific, meaning that their specificity is determined by the part of the molecule which is modified by their catalytic activity (Vogt, 2004). However, we note that the turnover rate of ShMOMT2 with the *in vitro* substrates tested were substantially lower than the turnover rates observed for ShMOMT1 **(Tables II, III)**. This might indicate that ShMOMT2 activity could possibly be rate limiting in the synthesis of polymethylated myricetins in the trichomes. Alternatively, this enzyme may be more sensitive to the lack of correct functional groups in the *in vitro* tested substrates. It is also possible that it may have additional, non-myricetin related substrates in the cell with which it is more efficient.

ShMOMT1 and ShMOMT2 are expressed in three different glandular trichomes

Our data indicate that *ShMOMT1* and *ShMOMT2* transcripts and proteins are found in all three types of glandular trichomes in *S. habrochaites* that are metabolically active. The levels of the transcripts and proteins in these gland types – 1, 4, and 6 –

correlate well with the amount of methylated myricetin found in them, with type 6 glands containing an order of magnitude less of each compared with type 1 and 4 glands, with the exception that type 4 glands have somewhat reduced amounts of both transcripts compared to type 1 glands. However, the level of *ShMOMT1* and *ShMOMT2* transcripts in type 4 glands are still 4-fold and 2-fold higher, respectively, than that found in type 6 glands. In addition to localizing ShMOMT1 and ShMOMT2 in glandular trichomes, we have detected transcripts of putative genes involved in flavonoid and flavonol biosynthesis in our EST databases created from isolated trichome glands (types 1, 4, and 6) **(Supplemental Table I)**. Transcripts of both flavonol 3′ hydroxylase and flavonol 3′,5′ hydroxylase, required for the synthesis of myricetin, were detected in these databases, with highest representation in type 1 glands.

Possible roles of methylated myricetins in tomato glandular trichomes

Flavonoids in general have been hypothesized to as act as UV protectants, chemical defense compounds, and in plant-insect, plant-microbe, plant-pathogen, and plant-plant interactions (reviewed by Treutter, 2005). While evidence for some of these roles (*e.g.*, in plant-microbe interactions) is strong, other roles are still tentative (Treutter, 2005). Furthermore, since flavonoids often occur as a mixture, assigning roles to specific compounds is difficult. Currently, no physiological function has been postulated specifically for laricitrin and syringetin in plants, nor for the more highly methylated myricetins found in the tomato trichomes. Laricitrin and syringetin, but not the more highly methylated myricetin ethers, are found in red grape and are probably responsible, along with several other flavonols and methylated derivatives, for the antioxidant potency of red grapes and wine (Mattivi et al., 2006). However, there is no evidence to support specific roles for these compounds in grape. Myricetin has also been linked to radical scavenging activity, xanthine oxidase inhibitory activity, and antioxidant activity in extracts of Ginkgo leaves and *Bridelia ferruginea* stem bark (Kobus et al., 2009; Cimanga et al., 2001), but in both investigations the tested mixture contained several other flavonols and methylated derivatives.

Thus, we can only hypothesize that in tomato trichomes the methylated myricetins contribute to some of the general roles postulated for flavonoids. Their synthesis and

accumulation in glandular trichomes along with their relatively lipophilic nature suggest that they are likely targeted to the cuticular space surrounding the secretory cells. In this location they are well placed to serve roles in chemical defense against herbivores, as UV protectants, or as radical scavengers to aid in preventing peroxidation of lipids.

Methods

Plant Material and Growth Conditions

Solanum habrochaites (accession LA1777) seeds were obtained from the C.M. Rick Tomato Genetics Resource Center (TGRC, University of California at Davis). The seeds were germinated on sterile filter paper in germination boxes and kept for approximately 5-7 days before transfer of seedlings to soil. Plants were grown in a mixture of regular soil:fine sand (3:1, v/v) in a growth chamber under a 14-h light/ 10-h dark photoperiod. Temperature was maintained at 22°C throughout the light period and 18°C during the dark period.

Gland cells were collected from glandular trichomes by hand with micropipettes under a dissecting microscope (Leica MZ6). Micropipettes were hand pulled and shaped from either 9" disposable pasteur pipettes or 1.8 mm X 100 mm capillary tubes. The micropipettes were approximately 6 cm in length and shaped to taper from one end, approximately 1.5-2.0 mm, down to approximately 0.25 mm diameter at the opposite end. Both ends of the pipette were flame sealed to prevent capillary action. Gland cells were picked from the top of glandular trichome structures using the thin tip of the micropipette. The cells adhered to the tip until being put into an appropriate buffer for downstream analyses. Trichomes were removed from leaf material using the same type of micropipettes, except, they were lightly scraped across the leaf surface in order to remove the bulk of trichomes without disturbing the leaf surface.

Chemicals

All chemicals were from Sigma-Aldrich (St. Louis, MO, USA) unless otherwise noted. Flavonols and methyl flavonols were purchased from Extrasynthese (B.P. 62 - 69730 Genay France) with the exception of the flavonol kaempferol which was purchased from Indofine Chemical Company, Inc. (12-1 Ilene Court, Belle Mead, NJ 08502). Deuterium labeled *S*-adenosyl-*L*- methionine was purchased from C/D/N isotopes (Quebec, Canada). And, methanol, 88% formic acid, and acetonitrile were purchased from VWR Scientific (West Chester, PA).

Metabolic profiling of leaf and trichome gland cells and metabolite identification

Approximately 50 mg fresh weight of leaf material were extracted in 100 µL of ice-cold acetonitrile:isopropanol:water (3:3:2 v/v/v) at room temperature overnight. Samples were evaporated to near dryness and resuspended in 50% methanol (v/v) for LC/MS analysis. For leaf material with trichomes removed, a glass probe (described previously) was used to gently scrape trichomes from the surface of the leaf prior to extraction with the 3:3:2 solvent mixture.

A total of 50 gland cells from each type of glandular trichome (types 1, 4, and 6) were collected with micropipettes and extracted in 50 µL of ice-cold acetonitrile:isopropanol:water (3:3:2 v/v/v). Samples were stored overnight at -20°C, evaporated to near dryness and resuspended in 50% methanol (v/v) for LC/MS analysis.

Samples were analyzed on a QTRAP™ 3200 mass spectrometer from Applied Biosystems/MDS Sciex (Concord, Ontario, Canada) coupled to a Shimadzu UFLC LC-20AD system and SIL-HTc autosampler. Separation was achieved with a Thermo Beta-basic C18 column (150 mm × 1.0 mm, 5 µm) at 30 C. The mobile phases were, (A) 0.5% formic acid, (B) 0.5% formic acid in 60% methanol+ 40% acetonitrile. A 15 min reverse phase gradient at a flow rate of 0.100 mL/min was used for separation. The linear gradient elution program was as follows: 10% B for 0.3 min, 40% B and linear increase to 100% from 0.31 to 8.5 min, followed by an isocratic hold at 100% B for 2.5 min. At 11 min. B was returned to 10% and the column was equilibrated for 4 min before the next injection.

The mass spectrometer was operated in the positive ion mode with a TurboIonSpray source. Enhanced product ion (MS/MS) scanning was accomplished with dynamic fill time and was used for ion detection at 40 V collision energy (CE). The other ionization parameters were as follows; curtain gas (CUR) 10, ion source gas 1 (GS1) 12, ion source gas 2 (GS2) 30, source temperature (TEM) 400°C, entrance potential (EP) 10 V, CAD high; IS voltage 5500 V. The mass spectrometer and the HPLC system were controlled by Analyst 1.4.2 software from Applied Biosystems/MDS Sciex.

All flavonol glycosides observed in leaf dip extracts were glycosylated in the 3-position judged by the high abundance of radical anion aglycone fragment ions in negative ion MS/MS spectra (Cuyckens and Claeys, 2005). Authentic standards of most

aglyconic polymethylated myricetin metabolites were not available from commercial sources. Owing to the substantial number of methylated isomers, their low levels in plant tissues, and their co-elution with other metabolites, comparisons to ultraviolet spectra of standards were not feasible, nor were sufficient amounts of purified metabolites available for detailed NMR structure determination. In view of these limitations, position of methyl groups in methylated myricetins were assigned based on co-elution of plant metabolites with authentic standards when available produced semi-synthetically from standards of myricetin or methylated myricetins when possible, predictions of relative LC retention times based on the ease of formation of intramolecular hydrogen bonds in some isomers, and on MS/MS product ion spectra that showed positional isomer-selective differences in fragmentation behavior. In the latter case, ion structure assignments were aided through enzymatic synthesis of individual *O*-d_3-methylated myricetin derivatives from d_3-*S*-adenosylmethionine. Product ion MS/MS spectra of $[M+H]^+$ ions derived from methylated myricetins yielded evidence for position-selective fragmentation chemistry. Abundances of fragments arising from loss of a methyl radical (-15 Da) relative to $[M+H]^+$ ions varied among methylated myricetins, and relative yields of these fragments decreased based on methyl position as $3 > 4' > 3' = 5' >> 7$. Assignments of myricetins methylated on the A-ring (either the 5- or 7-positions) were facilitated by observations of characteristic fragment ion masses observed in the MS/MS product ion spectra. In the absence of methylation in these positions, the fragment ion derived from the A-ring group (designated as $1,3A^+$) appears at m/z 153, but when either of the 5- or 7-positions are methylated, this fragment mass shifts upward in mass by 14 Da to appear at m/z 167. We considered methylation at the 5-position unlikely because this is a rare metabolite, and none of the metabolites gave MS/MS fragments suggestive of two methyl groups on the A-ring. One additional feature, the loss of 16 Da from the $[M+H]^+$ precursor, was shown using deuterium labeling to specifically occur when at least two methyl ether groups were present on the B-ring (3', 4', or 5' positions). The combinations of these features in the MS/MS spectra allow us to use a process of elimination to generate unambiguous evidence for the assignments of methyl group positions in methylated myricetin metabolites.

RNA isolation

Total RNA was extracted from 100 mg fresh weight of young leaf material or young leaf material from which trichomes had been removed. Tri Reagent (Molecular Research Center, Inc.) was used in accordance with the manufacturer's instructions to extract total RNA from leaf and from leaf with trichomes removed. First-strand cDNA was synthesized with SuperScript II reverse transcriptase (Invitrogen) using an anchored poly-T primer supplied by the manufacturer.

Quantitative RT-PCR

Total RNA from young leaf material and young leaf material with trichome removed were extracted as described above then treated with DNase using the DNA-free kit (Ambion). Superscript II Reverse Transcriptase (Invitrogen) and an anchored poly-T primer were used for first-strand cDNA synthesis. A negative control sample was run in parallel without reverse transcriptase added to the reaction mixture. All samples were normalized to the amplification of a *Solanum lycopersicum* actin gene (accession: BT013707). Quantitative expression analysis was performed using the StepOnePlus Real-Time PCR System (Applied Biosystems). The Fast Sybr Green Master Mix (Applied Biosystems) reagent was used according to the manufacturers' instructions in preparation of the qPCR reactions. The cycling conditions were: 40X 15 sec/95°C, 30 sec/60°C, 30 sec/72°C. Cycling was followed by a melting stage that ramped up from 55 to 95°C with an increasing gradient of 0.5°C, and a 10-s pause at each temperature. The entire experiment was performed in triplicate starting with total RNA isolation from gland cells, leaves, or leaves with trichomes removed. The threshold cycle (Ct) values from each experiment were averaged and the relative expression level of ShMOMT1 in each tissue was calculated using the comparative Ct method (Schmittgen and Livak, 2008). The results were expressed relative to expression levels of ShMOMT1 or ShMOMT2 in leaf material with trichomes.

Isolation, Expression, and purification of recombinant ShMOMT1 and ShMOMT2

The full-length ShMOMT1 and ShMOMT2 ORF's were cloned from cDNA made from *S. habrochaites* leaf RNA. Tri Reagent (Molecular Research center, Inc.) was

used to extract total RNA from approximately 100 mg of material and SuperScript II Reverse Transcriptase (Invitrogen) was used to synthesize first-strand cDNA. ShMOMT1 sequence was amplified using KOD Hot Start DNA polymerase (Novagen) from first-strand cDNA and ligated into the pGEM-T Easy vector (Promega), grown in *Escherichia coli* Top 10 cells, and full-length cDNAs were verified by DNA sequencing. The full-length ORF was amplified from the pGEM-T Easy vector using KOD Hot Start DNA Polymerase (Novagen), gel-purified using MinElute (Qiagen), and inserted into the pEXP5-CT/TOPO expression vector (invitrogen) with the native stop codon intact. The correct pEXP5-CT/TOPO construct was verified by DNA sequencing, isolated using QIAprep Spin Miniprep kit (Qiagen) and transformed into *E.coli* BL21(DE3)pLysS cells (Invitrogen). A colony carrying the correct construct was isolated and grown in LB medium containing 100 μg/mL ampicillin and 50 μg/mL chloramphenicol at 37°C to an OD_{600} of 0.5-0.8. Cultures were induced with 1 mM isopropylthio-β-galactoside and grown at 18°C for an additional 4 hours.

Induced cultures were pelleted by centrifugation, resuspended in 1/10 volume lysis buffer (50 mM Tris, 10 mM NaCl, 1 mM EDTA, 10% glycerol, 14 mM β-mercaptoethanol, pH 8.0), and lysed at 4°C by sonication. The cell lysate was cleared by centrifugation, and the supernatant was partially purified with DE53 anion exchanger (Whatman International, Ltd.). ShMOMT1 and ShMOMT2 were each purified by anion-exchange chromatography on an HiTrap Q HP column (GE Healthcare). A linear gradient of (10 - 1000 mM) NaCl in lysis buffer was used for the initial purification on the DE53 anion exchanger, and a linear gradient of (250 - 500 mM) NaCl in lysis buffer was used for the second round of purification on the HiTrap Q HP anion exchanger. ShMOMT1 eluted in the 400 - 500 mM and ShMOMT2 eluted in the 300-400 mM fractions from the DE53 anion exchanger and in the 350 - 400 mM and the 300 - 350 mM fractions from the HiTrap Q HP anion exchanger, respectively. The active fractions were identified by radiochemical enzyme assays as described above, using myricetin as substrate. SDS-PAGE was used to visualize the degree of homogeneity of the active fractions.

Enzyme assays and Product Identification

Radiochemical enzyme assays consisted of 50 mM Tris-HCl (pH 7.5, ShMOMT1 or pH 8.0, ShMOMT2), 5 µg of recombinant ShMOMT1 or ShMOMT2, 250 µM of substrate dissolved in 1:1 mixture DMSO:dd$H_2$0, and 200 µM SAM (Perkin Elmer Instruments), in a final volume of 50 µL. Assays were incubated at room temperature for 30 minutes and stopped by the addition of 2 N HCl. Reaction products were extracted with 200 µL of ethyl acetate and counted in a scintillation counter (model LS6500, Beckman Coulter, Fullerton, CA). Kinetic analyses were carried out within the linear range of reaction velocity by adjusting the concentration of recombinant protein in the assay. Raw data (counts per minute [cpm]) were converted to picokatals as previously described in D' Auria et al. (2002).

To produce ample product for LC/MS analyses, enzyme assays were performed using nonradiolabeled SAM and 10 fold reaction volumes. A Continuous Extraction Assay Method (CEAM) was designed to optimize product accumulation in these assays. Reactions were performed in 1.5 mL glass vials (Supelco Analytical, 27080-U) in a final volume of 500 µL (aq). A layer of 100% ethyl acetate (500 µL) was carefully applied over the aqueous assay volume to serve as a non-polar extraction phase. The reactions were set up on ice and mixed briefly before addition of the ethyl acetate layer. Reactions were sealed with a screw-top septum, and incubated overnight at room temperature. The ethyl acetate was removed, evaporated, and the residue resuspended in 50 µL, ethanol:ddH_2O (1:1).

Metabolite identities were determined using TLC following the method of Owens and McIntosh (2009) with the following modifications, Polygram Sil G/UV_{254} plastic sheets (Macherey-Nagel Inc.) and running buffer of toluene:ethylformate:formic acid (5:4:1, v/v/v), and by LC-MS using three different criteria: accurate mass, measured with time-of-flight mass spectrometry; retention time comparison with authentic standards; and comparison of mass spectra fragmentation patterns (see section Metabolic profiling of leaf and trichome gland cells and chemical identification above, and **Supplemental Figures 1, 3,** and **4**).

Protein Blot Analysis

Total protein was extracted from collections of 500 gland cells from each of the different types of glandular trichomes (type 1, 4, and 6) in 50 µL of SDS-PAGE sample buffer (100 mM Tris, 2% SDS, 5% ß-mercaptoethanol, 15% glycerol, 0.1% bromophenol blue). Total protein extraction from leaves followed the protocol given in Dudareva et al. 1996. Polyclonal antibodies to ShMOMT1 or ShMOMT2 were generated at Cocalico Biologicals (Reamstown, PA) in rabbit from recombinant ShMOMT1 or ShMOMT2 protein **(Supplemental Figure 7)**. Anti-α-tubulin was from Sigma-Aldrich and served as an internal control to standardize samples from gland cells and leaves. All antibodies (anti-ShMOMT1, anti-ShMOMT2, and anti- α-tubulin) were used at a 1:3,000 dilution and incubated with gel blots for 1 h. All other conditions of the protein gel blots were performed as described previously (Dudareva et al., 1996)

Sequence data from this article can be found in the GenBank archives under accession numbers JF499656 and JF499656 for ShMOMT1 and ShMOMT2, respectively.

Supplemental Data

Supplemental Figures

S3.1

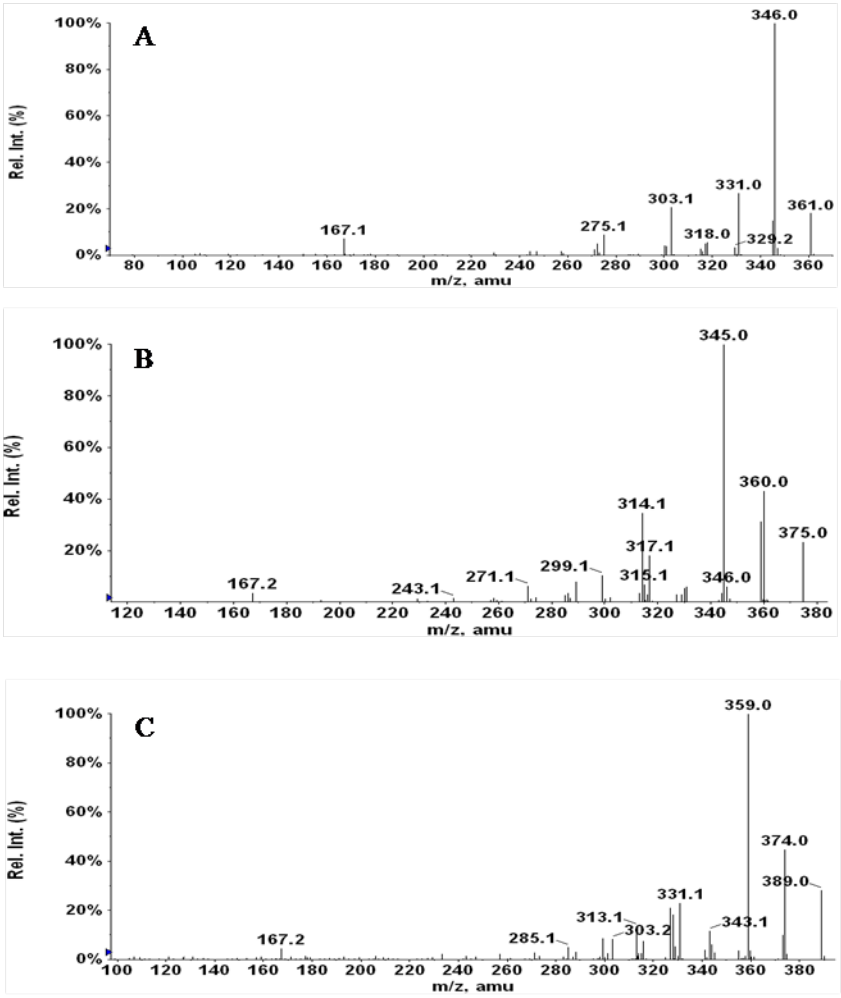

Supplemental Figure S3.1. Mass fragmentation patterns of methyl myricetin compounds detected in trichome glands of *S. habrochaites*. A, 3,7,3′-trimethyl myricetin (RT =9.68); B, 3,7,3′,5′-tetramethyl myricetin (RT =10.48); C, 3,7,3′,4′,5′-pentamethyl myricetin (RT =11.18).

S3.2

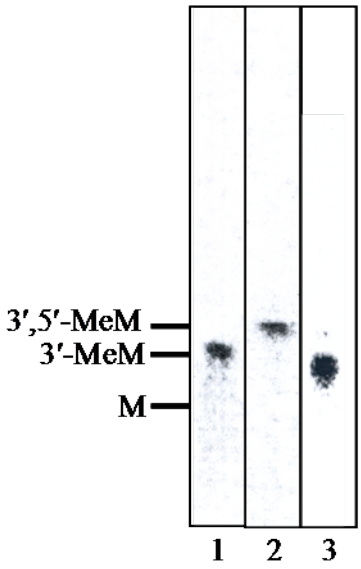

Supplemental Figure S3.2. Radioactive thin-layer chromatography showing products extracted from enzyme assays of ShMOMT1 (lanes 1, 2) and ShMOMT2 (lane 3). Authentic standards; myricetin (M, R_f 0.23), 3′-methylmyricetin (3′-MeM, R_f 0.33), 3′,5′-methylmyricetin (3′,5′-MeM, R_f 0.39). Products; lane 1, 3′-methylmyricetin (R_f 0.34), lane 2, 3′,5′-methylmyricetin (R_f 0.39), lane 3, 7-methylmyricetin (R_f 0.28).

S3.3

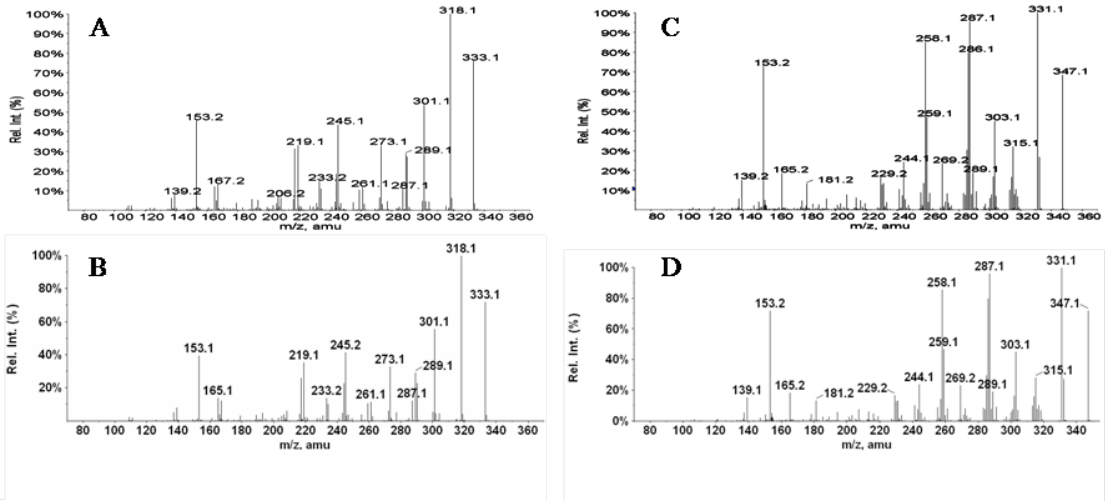

Supplemental Figure S3.3. Mass fragmentation patterns of authentic standards and products extracted from enzyme assays of ShMOMT1. A, 3′-methyl myricetin authentic standard (RT =8.03); B, product from incubation with myricetin (3′-methyl myricetin, RT =8.04); C, 3′,5′-dimethyl myricetin authentic standard (RT =8.73); D, product from incubation with 3′-methyl myricetin (3′,5′-dimethyl myricetin, RT =8.71).

S3.4

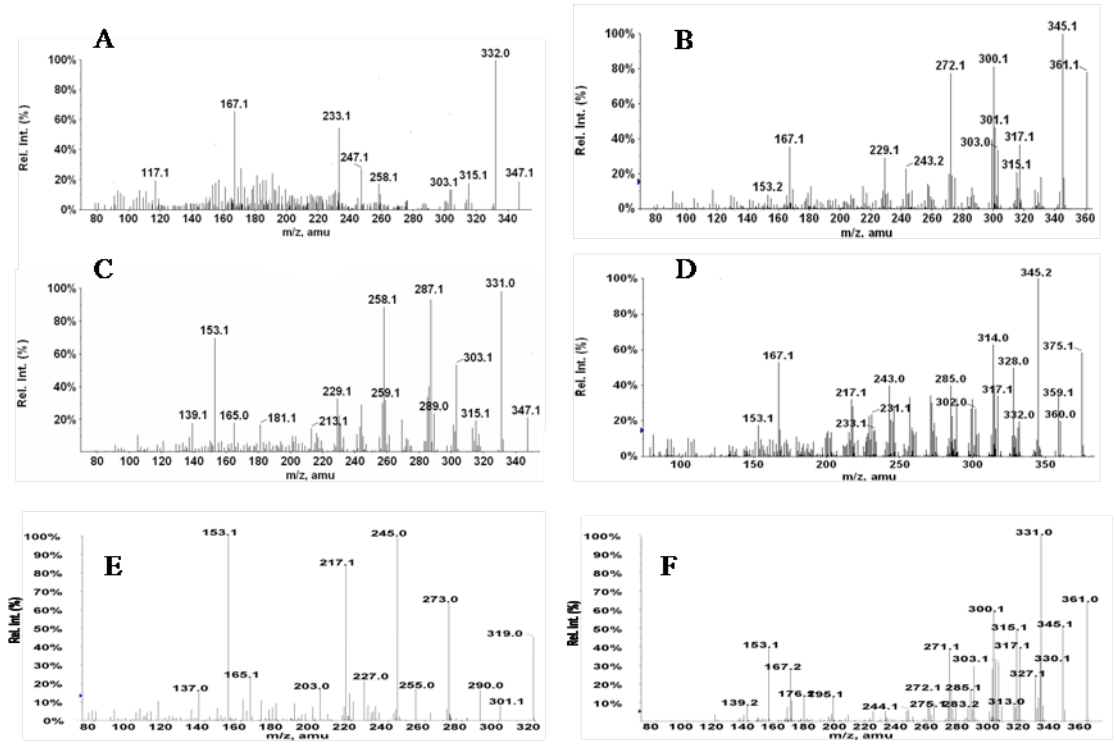

Supplemental Figure S3.4. Mass fragmentation patterns of products extracted from enzyme assays of ShMOMT2. A, product from incubation with myricetin (7,4′-dimethyl myricetin, RT =9.34); B, product from incubation with 3′-methyl myricetin (3′,4′-dimethyl myricetin, RT =8.97); C, product from incubation with 3′,5′-dimethyl myricetin (7,3′,5′-trimethyl myricetin, RT =10.14); D, product from incubation with 3′,4′,5′-trimethyl myricetin (7,3′,4′,5′-tetramethyl myricetin, RT =10.31); E, myricetin authentic standard (RT=6.49); F, 3′,4′,5′-trimethyl myricetin authentic standard (RT =9.70).

S3.5

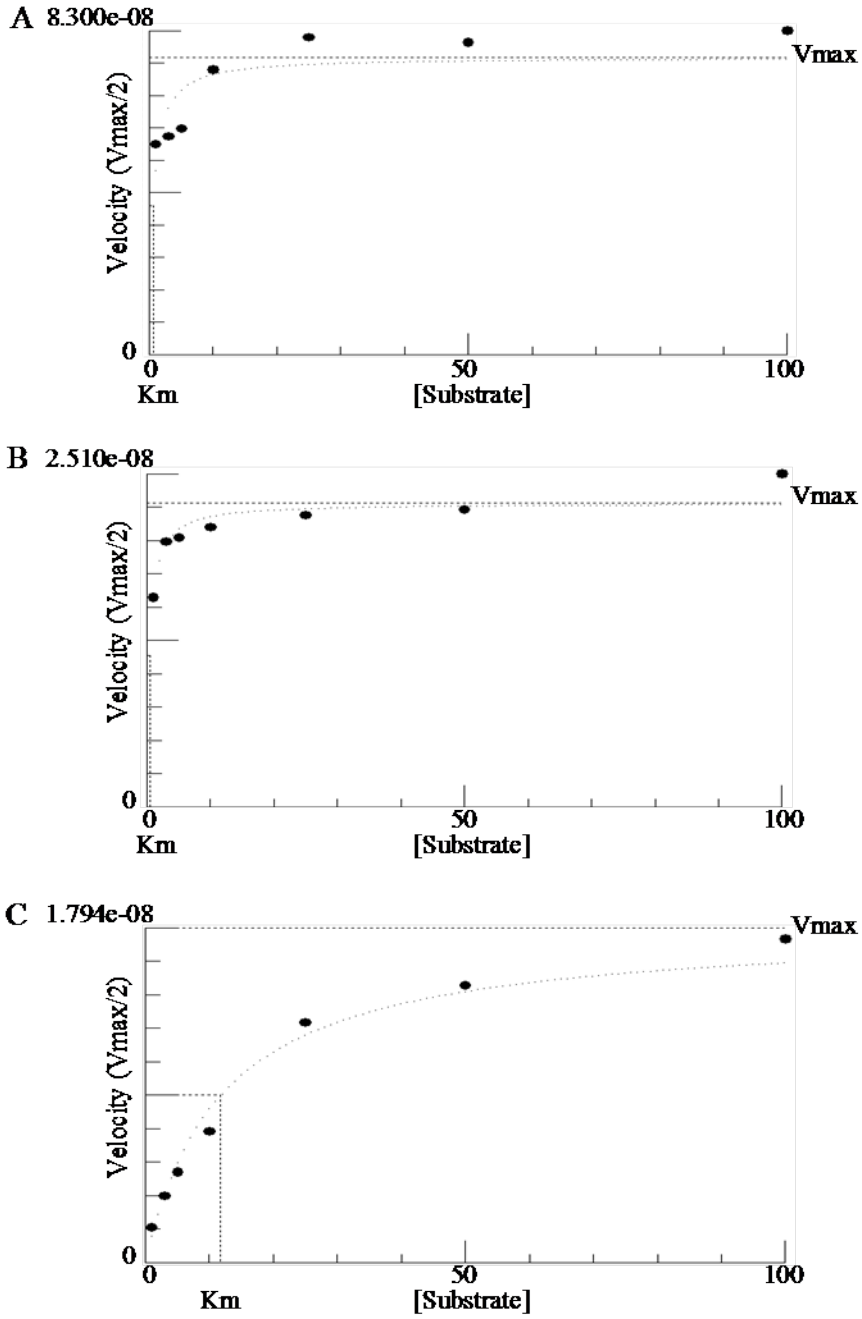

Supplemental Figure S3.5. Plots of velocity measurements for recombinant ShMOMT1 and one of the following substrates; A, myricetin, B, 3′-methyl myricetin (laricitrin), and C, [^{14}C]SAM.

S3.6

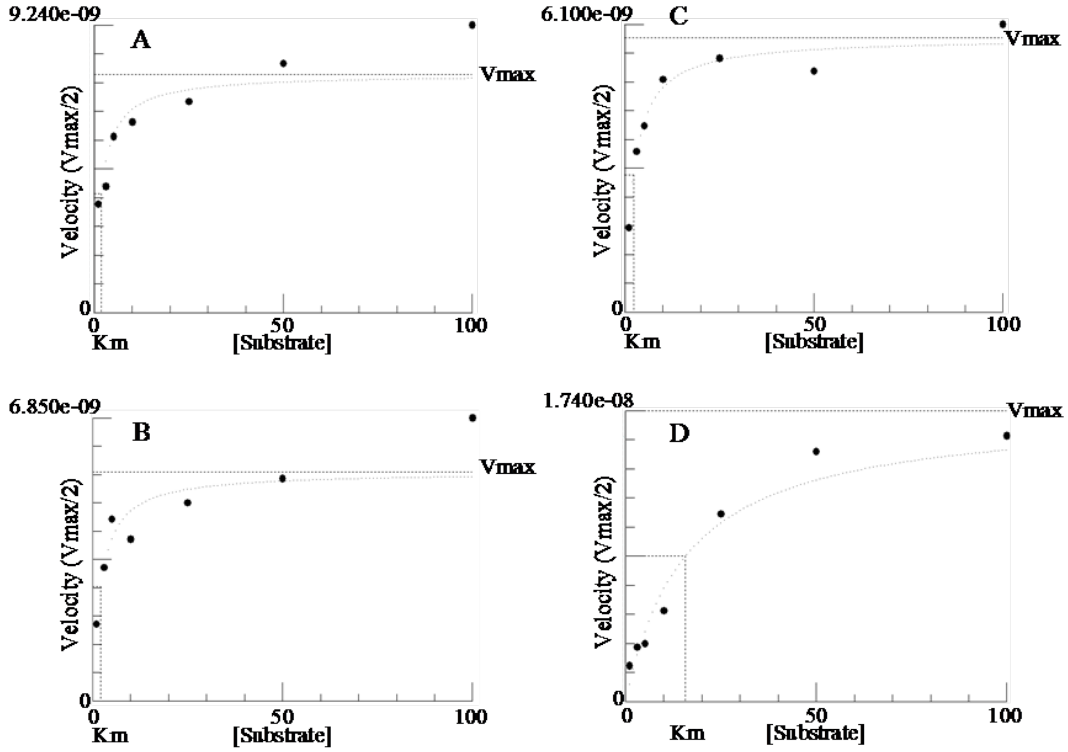

Supplemental Figure S3.6. Plots of velocity measurements for recombinant ShMOMT2 and one of the following substrates; A, myricetin, B, 4′-methyl kaempferol (kaempferide), C, 7-methyl quercetin (rhamnetin), and D, [^{14}C]SAM.

S3.7

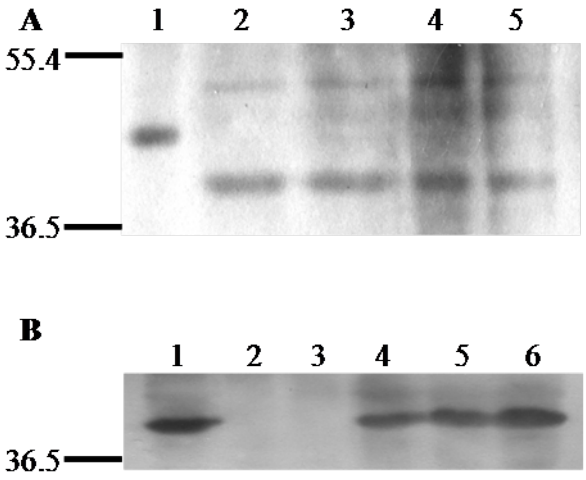

Supplemental Figure S3.7. Western Blot analysis using anti-ShMOMT1 (panel A) or anti-ShMOMT2 (panel B) to detect ShMOMT1 or ShMOMT2 in trichome and leaf extracts. Panel A, Lanes: 1, purified recombinant ShMOMT1 with 6 histidine residues at the C-terminus; 2, type 1 trichome extract; 3, type 4 trichome extract; 4, type 6 trichome extract; 5, leaf extract. Panel B, Lanes: 1, purified recombinant ShMOMT2; 2, *S. habrochaites* leaf extract; 3, *Solanum lycopersicum* leaf extract; 4, type 1 trichome extract; 5, type 4 trichome extract; 6, type 6 trichome extract.

Supplemental table

S3.I

Supplemental Figure S3.I. Representative cDNA sequences of flavonoid and flavonol biosynthetic enzymes detected in EST databases constructed from collections of individual gland types and leaf.

	Percent of total EST's			
Putative genes	Type 1	Type 4	Type 6	Whole leaf
Flavonoid pathway				
Chalcone synthase	0.10	0.07	0.20	0.05
Chalcone isomerase	nd[1]	nd	0.04	0.03
Naringenin 3 dioxygenase	nd	nd	nd	nd
Flavone 3 beta hydroxylase	nd	nd	nd	nd
Flavonol pathway				
Flavonol synthase	0.20	0.10	0.30	0.30
Flavonol 3' hydroxylase	0.03	0.16	nd	nd
Flavonol 3′, 5′ hydroxylase	0.50	nd	nd	nd

[1]nd, not detected

Literature Cited

Ambrsio SR, Oki Y, Heleno VCG, Chaves JS, Nascimento P, Lichston JE, Constantino MG, Varanda EM, Da Costa FB (2008) Constituents of glandular trichomes of *Tithonia diversifolia*: Relationships to herbivory and antifeedant activity. Phytochemistry **69:** 2052-2060

Ariyanathan S, Saraswathy A, Rajamanickam GV, Connolly JD (2010) Polyphenols from the roots of *Plumbago rosea*. Indian Journal of Chemistry Section B-Organic Chemistry Including Medicinal Chemistry **49:** 386-389

Braca A, Bilia AR, Mendez J, Morelli I (2001) Myricetin glycosides from *Licania densiflora*. Fitoterapia **72:** 182-185

Buer CS, Imin N, Djordjevic MA (2010) Flavonoids: New roles for old molecules. Journal of Integrative Plant Biology **52:** 98-111

Cacace S, Schroder G, Wehinger E, Strack D, Schmidt J, Schroder J (2003) A flavonol *O*-methyltransferase from *Catharanthus roseus* performing two sequential methylations. Phytochemistry **62:** 127-137

Croteau RB, Davis EM, Ringer KL, Wildung MR (2005) (-)-Menthol biosynthesis and molecular genetics. Naturwissenschaften **92:** 562-577

Cuyckens F, M Claeys (2005) Determination of the glycosylation site in flavonoid mono-*O*-glycosides by collision-induced dissociation of electrospray-generated deprotonated and sodiated molecules. J Mass Spectrom **40**: 364-372

Dachriyanus, Fahmi R, Sargent MV, Skelton BW, White AH (2004) 5-Hydroxy-3,3 ‘,4 ‘,5 ‘,7-pentamethoxyflavone (combretol). Acta Crystallographica Section E-Structure Reports Online **60:** O86-O88

D’ Auria JC, Chen F, Pichersky E (2002) Characterization of an acyltransferase capable of synthesizing benzylbenzoate and other volatile esters in flowers and damaged leaves of *Clarkia breweri*. Plant Physiology **130:** 466-476

De Luca V, Ibrahim RK (1985) Enzymatic synthesis of polymethylated flavonols in *Chrysosplenium Americanum*. 1. Partial purification and some properties of S-adenosyl-L-methionine flavonol 3-*O*-methyltransferases, 6-*O*-methyltransferases, 7-*O*-methyltransferases, and 4′-*O*-methyltransferases. Archives of Biochemistry

and Biophysics **238:** 596-605

Dudareva N, Cseke L, Blanc VM, Pichersky E (1996) Evolution of floral scent in *Clarkia*: Novel patterns of S-linalool synthase gene expression in the *C. breweri* flower. Plant Cell **8:** 1137-1148

Felsenstein J (1985) Confidence limits on phylogenies: An approach using the bootstrap. Evolution **39**:783-791.

Gerats AGM, Wallroth M, Donkerkoopman W, Groot SPC, Schram AW (1983) The genetic control of the enzyme UDP-glucose - 3-*O*-flavonoid-glucosyltransferase in flowers of *Petunia hybrida*. Theoretical and Applied Genetics **65:** 349-352

Gorbatsova J, Lougas T, Vokk R, Kalijurand M (2007) Comparison of the contents of various antioxidants of sea buckthorn berries using CE. Electrophoresis **28:** 4136-4142

Huang TS, Anzellotti D, Dedaldechamp F, Ibrahim RK (2004) Partial purification, kinetic analysis, and amino acid sequence information of a flavonol 3-*O*-methyltransferase from *Serratula tinctoria*. Plant Physiology **134:** 1366-1376

Ibrahim RK (1997) Plant *O*-methyltransferase signatures. Trends in Plant Science **2:** 249-250

Ibrahim RK (2005) A forty-year journey in plant research: Original contributions to flavonoid biochemistry. Canadian Journal of Botany-Revue Canadienne De Botanique **83:** 433-450

Ibrahim RK, De Luca V, Khouri H, Latchinian L, Brisson L, Charest PM (1987) Enzymology and compartmentation of polymethylated flavonol glucosides in *Chrysosplenium americanum*. Phytochemistry **26:** 1237-1245

Iijima Y, Gang DR, Fridman E, Lewinsohn E, Pichersky E (2004) Characterization of geraniol synthase from the peltate glands of sweet basil. Plant Physiology **134:** 370-379

Jay M, Voirin B, Hasan A, Gonnet JF, Viricel MR (1980) Chemotaxonomic study of vascular plants. 43. Chemosystematic experiment on tribe *Loteae*. Biochemical Systematics and Ecology **8:** 127-132

Joshi CP, Chiang VL (1998) Conserved sequence motifs in plant S-adenosyl-L-methionine-dependent methyltransferases. Plant Molecular Biology **37:** 663-674

Jung HA, Kim JE, Chung HY, Choi JS (2003) Antioxidant principles of *Nelumbo nucifera* stamens. Archives of Pharmacal Research **26:** 279-285

Kumar A, Malik AK, Tewary DK (2009) A new method for determination of myricetin and quercetin using solid phase microextraction-high performance liquid chromatography-ultra violet/visible system in grapes, vegetables and red wine samples. Analytica Chimica Acta **631:** 177-181

Kumar N, Bhandari P, Singh B, Gupta AP, Kaul VK (2008) Reversed phase-HPLC for rapid determination of polyphenols in flowers of rose species. Journal of Separation Science **31:** 262-267

Kumari GNK, Rao LJM, Rao NSP (1984) Myricetin methyl ethers from *Solanum Pubescens*. Phytochemistry **23:** 2701-2702

Lako J, Trenerry VC, Wahlqvist M, Wattanapenpaiboon N, Sotheeswaran S, Premier R (2007) Phytochemical flavonols, carotenoids and the antioxidant properties of a wide selection of Fijian fruit, vegetables and other readily available foods. Food Chemistry **101:** 1727-1741

Le K, Chiu F, Ng K (2007) Identification and quantification of antioxidants in *Fructus lycii*. Food Chemistry **105:** 353-363

Lee TH, Liu DZ, Hsu FL, Wu WC, Hou WC (2006) Structure-activity relationships of five myricetin galloylglycosides from leaves of *Acacia 97onfuse*. Botanical Studies: An International Journal **47:** 37-43

Lee YJ, Kim BG, Chong Y, Lim Y, Ahn JH (2008) Cation dependent *O*-methyltransferases from rice. Planta **227:** 641-647

Liu Y, Li WJ, Ling XM, Lai XY, Li YZ, Zhang QY, Zhao YY (2008) Simultaneous determination of the active ingredients in *Abelmoschus manihot* (L.) *Medicus* by CZE. Chromatographia **67:** 819-823

Luckwill, L. (1943) The genus *Lycopersicon*: An historical, biological, and taxonomic survey of the wild and cultivated tomatoes. PhD thesis. Aberdeen University, Aberdeen.

Mattivi F, Guzzon R, Vrhovsek U, Stefanini M, Velasco R (2006) Metabolite profiling of grape: Flavonols and anthocyanins. Journal of Agricultural and Food Chemistry **54:** 7692-7702

McDowell ET, Kapteyn J, Schmidt A, Li C, Kang J, Descour A, Shi F, Larson M, Schilmiller A, An L, Jones AD, Pichersky E, Soderlund CA and Gang DR (2011) Comparative functional genomic analysis of *Solanum* glandular trichome types. Plant Physiology (DOI:10.1104/pp.110.167114).

Michodjehoun-Mestres L, Souquet JM, Fulcrand H, Bouchut C, Reynes M, Brillouet JM (2009) Monomeric phenols of cashew apple (*Anacardium occidentale* L.). Food Chemistry **112:** 851-857

Min BS, Lee SY, Kim JH, Lee JK, Kim TJ, Kim DH, Kim YH, Joung H, Lee HK, Nakamura N, Miyashiro H, Hattori M (2003) Anti-complement activity of constituents from the stem-bark of *Juglans mandshurica*. Biological & Pharmaceutical Bulletin **26:** 1042-1044

Modolo LV, Li LN, Pan HY, Blount JW, Dixon RA, Wang XQ (2009) Crystal structures of glycosyltransferase UGT78G1 reveal the molecular basis for glycosylation and deglycosylation of (iso)flavonoids. Journal of Molecular Biology **392:** 1292-1302

Motta LB, Kraus JE, Salatino A, Salatino MLF (2005) Distribution of metabolites in galled and non-galled foliar tissues of *Tibouchina pulchra*. Biochemical Systematics and Ecology **33:** 971-981

Muzac I, Wang J, Auzellotti D, Zhang H, Ibrahim RK (2000) Functional expression of an *Arabidopsis* cDNA clone encoding a flavonol 3'-*O*-methyltransferase and characterization of the gene product. Archives of Biochemistry and Biophysics **375:** 385-388

Ojong PB, Njiti V, Guo ZB, Gao M, Besong S, Barnes SL (2008) Variation of flavonoid content among sweetpotato accessions. Journal of the American Society for Horticultural Science **133:** 819-824

Oliveira I, Sousa A, Valentao P, Andrade PB, Ferreira I, Ferreres F, Bento A, Seabra R, Estevinho L, Pereira JA (2007) Hazel (*Corylus avellana* L.) leaves as source of antimicrobial and antioxidative compounds. Food Chemistry **105:** 1018-1025

Owens DK and McIntosh CA (2009) Identification, recombinant expression, and biochemical characterization of a flavonol 3-O-glucosyltransferase clone from

Citrus paradise. Phytochemistry **70:** 1382-1391

Rausher MD (2008) The evolution of flavonoids and their genes. In E Grotewold, ed, Science of Flavonoids, Springer, New York, pp 175-211.

Reynertson KA, Yang H, Jiang B, Basile MJ, Kennelly EJ (2008) Quantitative analysis of antiradical phenolic constituents from fourteen edible *Myrtaceae* fruits. Food Chemistry **109:** 883-890

Riihinen K, Jaakola L, Karenlampi S, Hohtola A (2008) Organ-specific distribution of phenolic compounds in bilberry (*Vaccinium myrtillus*) and 'northblue' blueberry (*Vaccinium corymbosum* x *V. angustifolium*). Food Chemistry **110:** 156-160

Saitou N and Nei M (1987) The neighbor-joining method: A new method for reconstructing phylogenetic trees. Molecular Biology and Evolution **4**:406-425.

Schilmiller A, Shi F, Kim J, Charbonneau AL, Holmes D, Jones AD, Last RL (2010) Mass spectrometry screening reveals widespread diversity in trichome specialized metabolites of tomato chromosomal substitution lines. Plant Journal **62:** 391-403

Schilmiller AL, Last RL, Pichersky E (2008) Harnessing plant trichome biochemistry for the production of useful compounds. Plant Journal **54:** 702-711

Schmittgen TD, Livak KJ (2008) Analyzing real-time PCR data by the comparative CT method. Nature Protocols **3:** 1101-1108

Schröder G, Wehinger E, Lukacin R, Wellmann F, Seefelder W, Schwab W, Schröder J (2004) Flavonoid methylation: a novel 4′-*O*-methyltransferase from *Catharanthus roseus*, and evidence that partially methylated flavanones are substrates of four different flavonoid dioxygenases. Phytochemistry **65:** 1085-1094

Singh AP, Luthria D, Wilson T, Vorsa N, Singh V, Banuelos GS, Pasakdee S (2009) Polyphenols content and antioxidant capacity of eggplant pulp. Food Chemistry **114:** 955-961

Stevens JF, Hart H, Elema ET, Bolck A (1996) Flavonoid variation in *Eurasian sedum* and *Sempervivum*. Phytochemistry **41:** 503-512

Stevens JF, Hart HT, Wollenweber E (1995) The Systematic and evolutionary significance of exudate flavonoids in *Aeonium*. Phytochemistry **39:** 805-813

Tabart J, Kevers C, Pincemail J, Defraigne JO, Dommes J (2006) Antioxidant

capacity of black currant varies with organ, season, and cultivar. Journal of Agricultural and Food Chemistry **54:** 6271-6276

Tamura K, Dudley J, Nei M & Kumar S (2007) MEGA4: Molecular Evolutionary Genetics Analysis (MEGA) software version 4.0. Molecular Biology and Evolution **24**:1596-1599.

Taylor LP, Grotewold E (2005) Flavonoids as developmental regulators. Current Opinion in Plant Biology **8:** 317-323

Thresh K, Ibrahim RK (1985) Are Spinach chloroplasts involved in flavonoid *O*-methylation. Zeitschrift Fur Naturforschung C-A Journal of Biosciences **40:** 331-335

Vogt T (2004) Regiospecificity and kinetic properties of a plant natural product *O*-methyltransferase are determined by its N-terminal domain. FEBS Letters **561:** 159-162

Vogt T, Jones P (2000) Glycosyltransferases in plant natural product synthesis: Characterization of a supergene family. Trends in Plant Science **5:** 380-386

Wagner GJ (1991) Secreting glandular trichomes - More than just hairs. Plant Physiology **96:** 675-679

Wu JH, Huang CY, Tung YT, Chang ST (2008) Online RP-HPLC-DPPH screening method for detection of radical-scavenging phytochemicals from flowers of *Acacia 100onfuse*. Journal of Agricultural and Food Chemistry **56:** 328-332

Zhou JM, Gold ND, Martin VJJ, Wollenweber E, Ibrahim RK (2006) Sequential *O*-methylation of tricetin by a single gene product in wheat. Biochimica Et Biophysica Acta-General Subjects **1760:** 1115-1124

Zuckerkandl E & Pauling L (1965) Evolutionary divergence and convergence in proteins. In V Bryson, HJ Vogel, eds, Evolving Genes and Proteins, Academic Press, New York, pp. 97-166.

Chapter 4

Conclusion

A common theme emanating from historical accounts of crop evolution is the interdependence of crop improvement and utilization. There is no doubt that humans have been a major source of selective pressures driving the evolution of desirable traits characterizing our major crop species. However, the vast majority of this selection occurred unconsciously during the very early stages of cultivation and crop development. Thus, selection for traits such as seed non-shattering, determinant growth, increased seed production, regularity of germination, seedling vigor, and self-pollination, among others, were the result of planting and harvesting practices rather than targeting these specific traits (Heiser, 1988). This informal selection process was very effective at shaping emerging crop species for our usage and profit for thousands of years. It has only been relatively recently, within the past 200 years, that people have begun systematic breeding of crops with the sole intention of crop improvement. But lately, such intensive breeding techniques seem to have reached their limit. The fading effectiveness of informal selection stems from the gradual reduction in genetic variability and subsequent reductions in rates of natural improvement of cultivated species. Through the process of developing our crops we have inadvertently made them increasingly homogeneous, to the point that chance variants are few and far between. This reduces the rate of natural improvement and becomes a burden on the future success of the species by reducing its natural ability to adapt to changes in the environment.

The realization that future crop improvements will rely on non-traditional breeding approaches, which include interspecific crosses as well as molecular techniques, is commonly accepted today. This is especially evident in advancements made to improve the cultivated tomato. Examples of improved fruit organoleptic properties and fruit solids content, pest and disease resistance, and tolerance of abiotic stresses are

mostly the result of systematic breeding of different wild tomato species with the cultivated species. These efforts have gone a long way in making the tomato crop more nutritious, amenable to production technologies, more popular among the public, and more profitable for the producers. However, a major hurdle that still exists is our inability to reintroduce a robust dose of pest resistance. The wild species *Solanum habrochaites* and *Solanum pennellii* exhibit broad insect resistance and deterrence attributes that are associated with different glandular trichome types and trichome densities. Breeding this broad spectrum resistance into the cultivated tomato will require the concomitant reintroduction of the genetic loci controlling the development of specific types of glandular trichomes in densities similar to that of the wild species. This latter point is of considerable importance because the cultivated tomato has much lower densities of the type 1/4 and type 6 glandular trichomes that synthesize and store the biologically active metabolites linked to herbivore resistance, such as acyl-sugars and terpenoids.

Our investigation of the gland cells from different types of glandular trichomes has revealed metabolic and genetic differences among trichome types and between species (Chapter 2). This information could be put to use in the introduction of herbivore resistance in the cultivated tomato. Investigating gland cells from the different types of glandular trichomes has provided unequivocal evidence that the apical gland cells are a major site of synthesis and storage of biologically active metabolites linked to herbivore resistance. Comparisons among trichome types and between species revealed specific gene transcripts in the gland cells required for the synthesis of major classes of specialized metabolites that accumulate in them, and those required for photosynthesis and carbon fixation. However, the distinct chemical profiles of different trichome types within and between species could not be entirely discerned by differences in their gene transcript profiles. This brings to focus the importance of combining metabolite and gene transcript data in comparative genomic studies, and suggests that there are other regulatory mechanisms, in addition to those regulating gene expression, that are affecting metabolic outcomes in different types of glandular trichomes.

Focusing on accumulations of several methylated derivatives of the flavonol myricetin in glandular trichomes of *S. habrochaites*, we have shown that investigating a select portion of a specialized metabolic pathway is feasible using collections of apical

gland cells (Chapter 3). We characterized the distributions of methylated myricetins, gene transcripts associated with their synthesis, and the protein products of these transcripts in the different types of glandular trichomes. In the process, we showed that the biosynthesis of methylated myricetins is localized to the trichomes and does not appear to occur in other non-trichome leaf tissues. Myricetin and its methylated derivatives have been shown to accumulate in tissues of other plants, but these compounds have never before been reported in trichomes. The fact that they accumulate and are synthesized in glandular trichomes, and are most prevalent in the tallest type of glandular trichome, suggest that these compounds may serve in defense-related roles. Relatively low levels of accumulations combined with the difficulties associated with isolating these compounds make testing biological functions not feasible at this time. Nevertheless our findings have made a significant contribution by localizing their biosynthesis in specialized tissues regarded as a first line of defense against herbivores.

As we continue to isolate and characterize biosynthetic enzymes from glandular trichomes, the possibility of producing select metabolites *in vitro* may be realized. This would benefit investigations aimed at defining biological functions of trichome-derived metabolites that require a level of metabolite purity and concentration not normally attainable from plant sources. Studies of this type would help to further define the biological functions of such metabolites and may provide evidence linking certain metabolites to specific functions in herbivore and pathogen resistance. Future efforts to dissect the complex features defining specialized metabolism in glandular trichomes should strive to characterize the regulatory mechanisms controlling metabolic outcomes of the different gland types, and those responsible for determining trichome types and relative densities. Contributions to these areas would provide additional tools for systematic breeding efforts and may serve significant roles in overcoming some of the barriers preventing the transfer of broad-spectrum herbivore resistance into the cultivated tomato. The research summarized here represents a significant step towards characterizing the biological functions of *Solanum* glandular trichomes and it reveals significant gaps in our knowledge of these amazing structures. As with any scientific endeavor, success may be best measured by the number of questions our data enable us to pose rather than by the number of answers we obtain.

Literature Cited

Heiser CB (1988) Aspects of unconscious selection and the evolution of domesticated plants. Euphytica **37:** 77-81